Investigations in Cell Sorting Techniques

by

Bryan A. Sutermaster

M.S. Pennsylvania State University, University Park, PA 2012

B.S. Cornell University, Ithaca, NY 2010

Submitted in partial fulfillment of the requirements for the degree of Doctor of Philosophy in Biomedical Engineering, a joint program in the Division of Biology and Medicine and the School of Engineering at Brown University

Department of Molecular Pharmacology, Physiology, and Biotechnology
and
Center for Biomedical Engineering

PROVIDENCE, RHODE ISLAND
MAY 2019

This dissertation by Bryan A. Sutermaster is accepted in its present form by the School of Engineering and the Division of Biology and Medicine as satisfying the dissertation requirements for the degree of Doctor of Philosophy

Date	Eric Darling, Ph.D., Advisor

Recommended to the Graduate Council

Date	Dr. Braden Fleming, Ph.D., Reader
Date	Dr. Anita Shukla, Ph.D., Reader
Date	Dr. Anubhav Tripathi, Ph.D., Reader

Approved by the Graduate Council

Date	Andrew Campbell, Ph.D., Dean of the Graduate School

Curriculum Vitae

NAME, DATE, and PLACE OF BIRTH

Bryan A. Sutermaster
July 19, 1987, Pittsburgh, PA

EDUCATION

Brown University, Providence, RI
Ph.D., Biomedical Engineering
Advisor: Eric Darling, Ph.D.
Title of Dissertation: Investigations in Cell Sorting Techniques
Expected: December 2018

Pennsylvania State University, University Park, PA
M.S., Bioengineering,
Advisor: Peter Butler, Ph.D.
Title of Thesis: Development of Novel Ultra-Deformable Cationic Liposomes for siRNA Delivery to Fibrous Tumors
Completed: May 2012

Cornell University, Ithaca, NY
B.S., Biological Engineering
Completed: January 2010

PUBLICATIONS

Sutermaster, BA, and Darling, EM. (2018) *Considerations for high-yield, high-throughput cell enrichment: fluorescence versus magnetic sorting.* Scientific Reports, (in press)

Marble, HD, **Sutermaster, BA**, Kanthilal, M, Fonseca, VC, and Darling, EM. (2014) *Gene expression-based enrichment of live cells from adipose tissue produces subpopulations with improved osteogenic potential.* Stem Cell Research and Therapy, 5:145. doi: 10.1186/scrt502

Cross, VL, Zheng, Y, Choi, NW, Verbridge, SS, **Sutermaster, BA**, Bonassar, LJ, Fischbach, C, and Stroock, AD. (2010) *Dense type I collagen matrices that support cellular remodeling and microfabrication for studies of tumor angiogenesis and vasculogenesis in vitro*. Biomaterials 32(33):8596-8607. doi: 10.1016/j.biomaterials.2010.07.072

Huang, P, Misra, G, Vaish, A, Flanagan, J, **Sutermaster, BA**, and Lowe, T. (2008) *Novel nanogels with both thermoresponsive and hydrolytically degradable properties.* Macromolecules 41(22):8339-8345. doi: 10.1021/ma800081g

CONFERENCE ABSTRACTS

Sutermaster, B.A., and Darling, E.M. *Cell yields and sorting times: Investigating FACS vs. MACS.* (2018) Poster Presentation, Biomedical Engineering Society Advanced Bio-Manufacturing Special Interest Conference, Worcester, MA.

Sutermaster, B.A., and Darling, E. M. *Magnetic sorting offers efficient isolation of osteogenic cells from stromal vascular fraction of fat.* (2017) Poster Presentation, Orthopaedic Research Society Conference, San Diego, CA.

Sutermaster, B.A., and Darling, E. M. *Magnetic sorting offers rapid, high-throughput isolation of ALPL+ cells from lipoaspirate.* (2016) Oral Presentation, Biomedical Engineering Society Conference, Minneapolis, MN.

Sutermaster, B.A., Cross, V.L., Zheng, Y., Bowles, R. and Stroock, A.D. *Characterization of Fiber Morphology and Alignment in Collagen Hydrogels.* (2009) Poster Presentation, Biomedical Engineering Society Conference, Pittsburgh, PA.

Sutermaster, B.A., Misra, G., Siedlecki, C., Weiss, W., and Lowe, T. *Engineering of Cross-Linked Biomaterials for Controlled-Release of Therapeutics.* (2008) Poster Presentation, Biomedical Engineering Society Conference, St. Louis, MO.

Sutermaster, B.A., Misra, G., Siedlecki, C., and Lowe, T. *Anti-thrombogenic Polyurethaneurea Biomaterials: Pseudo-Intimal Layer Formation via Hydrogel Grafting, and Heparin-Nanogel Embedding.* (2007) Poster Presentation, Biomedical Engineering Society Conference, Hollywood, CA.

AWARDS AND LEADERSHIP

2012-2013	Sidney Frank Fellowship, Brown University
2014-2015	President, Graduate Biomedical Engineering Society, Brown University
2013-2014	Vice President, Graduate Biomedical Engineering Society, Brown University
2012	Tau Beta Pi Engineering Honor Society Inductee, Pennsylvania Beta Chapter
2010-2012	Graham Fellowship, Penn State University

TEACHING EXPERIENCE

2015 Primary Instructor, Engineering Biomedical Systems, Summer@Brown Program, Brown University

2014 Teaching Assistant, BIOL 1150: Stem Cell Engineering, Brown University

2013-2014 Teaching Assistant, Engineering Biomedical Systems, Summer@Brown Program, Brown University

TRAINING

Laboratory: Mammalian cell culture, PCR and qPCR, NanoDrop, gel electrophoresis, epifluorescence microscopy, confocal microscopy, scanning electron microscopy (SEM), immunofluorescence, spectrophotometry, flow cytometry, magnetic-activated cell sorting (MACS), fluorescence-activate cell sorting (FACS), ultra-centrifugation, density gradient centrifugation, characterization of stem cell differentiation (adipogenic and osteogenic).

Software: ImageJ, Cell Profiler, SigmaPlot, Statistica, Microsoft Office Suite, Adobe Illustrator and Photoshop

ADDITIONAL RESEARCH EXPERIENCE

2010-2012 Butler Lab, Pennsylvania State University, University Park, PA
Advisor: Peter Butler, Ph.D.

2007-2009 Stroock Lab, Cornell University, Ithaca, NY
Advisor: Abraham Stroock, Ph.D.

2007-2008 Lowe Lab, Pennsylvania State University College of Medicine, Hershey, PA
Advisor: Tao Lu Lowe, Ph.D.

Acknowledgements

First, I must thank my wonderful advisor, Dr. Eric Darling, It has been a wild ride, these last 6 and ½ years, and I am truly privileged to have been mentored by you. You took a chance on me, and have made me a better scientist, writer, and mentor in the process. The lab that you have assembled is like a second family, and is a testament to your judgement of character. Thank you for your patience, your steadfast belief, your encouragement, and your friendship. Thank you, thank you, thank you.

Secondly, I would like to thank the members of my thesis committee: Drs. Braden Fleming, Anita Shukla, and Anubhav Tripathi. Your critiques and suggestions throughout the completion of my thesis have positively impacted both my research and me.

In the anatomy of the Darling Lab, Dr. Darling is the brain, but Vera Fonseca is the heart. Vera, you have been a wonderful colleague and friend over the last 6 and ½ years. The positivity and kind-heartedness you display on a daily basis is a major reason why the Darling Lab is such a fantastic place to work. Your encyclopedia knowledge of peoples' birthdays and tenuous grasp on phonetics ("New-awr-eh," "Fwah-zi bear," etc… ☺) never cease to amaze me. In addition to all these great qualities, you're also a fantastic scientist. Thank you for your mentorship, willingness to always answer a question, loyalty, and friendship.

To the rest of the Darling Lab family, thank you for making my time at Brown a truly enjoyable one. Even on the most difficult experimental days, you make it a pleasure to come to work. Thank you all for slowing my inevitable descent into "crotchety old manhood." I'd especially like to thank Drs. Raf Gonzalez-Cruz and Nick Labriola for being the best darn desk-mates, period. I'd also like to thank Corey Holman, my former

undergraduate mentee. Your exuberance and enthusiasm for science was truly refreshing contagious. I wish you luck as you complete your own Ph.D.! Finally, Dr. Jess Sadick, thank you for your fantastic thesis-formatting template. I have retained significantly more hair through the writing process than I would have otherwise.

To the Molecular Pharmacology, Physiology, and Biotechnology administrative staff, thank you for all you do! A special thanks to Jess Bello, Tim Durning, Kris McCutcheon, Crystal Miller, Elly Peimer, Brian Quinn, and Melodie Vincenty.

As a 25-year student, I'd also like to thank all of the teachers, professors, and mentors I've had throughout my educational journey: From my time at Brown, I'd like to specifically acknowledge Drs. Edith Mathiowitz and Christoph Schorl. Dr. Mathiowitz, thank you for your mentorship and good nature. Despite not being one of your own students, you have never hesitated to assist me with my career development questions, and I truly appreciate it. Dr. Schorl, thank you for your unfailing positivity. I spent many a soul-crushing day at the Genomics Core performing day-long, unsuccessful experiments (a research rite-of-passage!), but chatting with you always brightened my day. Thank you for your encouragement; it meant more to me than you likely knew.

From my time at Penn State University during my Master's degree, I'd like to thank my mentor, Dr. Peter Butler. Thank you for giving me a chance in your lab, as the drummer of your band, and for your guidance and encouragement. I look forward to catching up when I next visit State College! From my undergraduate research experience at Penn State's Hershey Medical Center, I'd like to thank Drs. Tao Lu Lowe and Gauri Misra. You made my first research experience a positive one, and set me off on my current career path. For that, I will be forever grateful.

From my time during my undergraduate degree at Cornell University, I'd like to thank Drs. Larry Bonassar, Kevin Ernste, and Abe Stroock. Dr. Bonassar, thank you for your mentorship, career advice, and fantastic teaching. Your willingness to help during my graduate application process was, and is, truly appreciated! Dr. Kevin Ernste, the fearlessness and determination with which you approach musical expression and exploration is something that has profoundly influenced my own musical and scientific approaches. You are a truly wonderful educator, and I hope to catch up with you soon! Dr. Abe Stroock, thank you for being a fantastic undergraduate research mentor. My experience in your lab provided a fantastic foundation with which to build my career. Profusely, thank you.

From the days of my primary education, I'd like to thank Mr. Ron Andrasko, Mrs. Christy Brennan, Mr. Mark Flaherty, Mrs. Judy Fratto, and Mrs. Karen Ullman. Mr. Andrasko, thank you for fostering a well-rounded love of learning in me. Your passion for any manner of subject, from chemistry, to music, to college football, was something that truly I truly resonated with. Thank you. Mrs. Brennan, your tenacity and passionate teaching has resonated with me since I was a student in your Statistics class. I've always felt that you had an uncanny ability to draw the best in your students, and certainly did so with me. For that I thank you. Mr. Flaherty, you armed me with the debate skills that I have today, much to the benefit of my scientific career and civic life, and I thank you. Mrs. Fratto, you instilled a drive to push myself academically, which has stuck with me throughout my academic career. You sacrificed your lunch periods to teach advanced math, providing your students the opportunity to challenge themselves. I have never stopped doing so, and for that I am eternally grateful. Finally, Mrs. Ullman, you are,

without question, the most outstanding English teacher I have ever had. I still use your lessons daily. Any level of coherence I have achieved in the construction of this thesis is thanks to you. I wholeheartedly appreciate it.

Finally, I must thank my family. Heather, I love you and am eternally indebted to your patience, unfailing belief in me, and encouragement. I would not have completed this thesis, or (hopefully ☺) this degree, without your love and support. Mom and Dad, you have instilled the drive for excellence in me, and I thank you for your patience, love, and support for the last 31 years. Staci, you inspire me daily with your passion and drive for your own studies and career. Thanks for tolerating your older brother for all these years! Mr and Mrs. H., thank you for your support during these last few years. The visits to your house provided mini-vacations that enabled me to keep my sanity through some very stressful times. Justin and Lauren, thank you for being fellow nerds. I look forward to continuing to "nerd out" with you over recently performed surgeries, winter sports-related knee injury statistics, and free-market Monopoly in the coming years. To my aunts, uncles, cousins, and adopted second parents Pam and Vince Gaudio, thank you for for keeping me motivated with your sustained interest in my academic pursuits! Lastly, B and Greg, thank you for being my brothers for the last 28 years.

In closing, I'd like to dedicate this thesis to the memories of my grandparents: Joe and Katherine Jessloski, and Charles and Rae Sutermaster. Grandpa Joe, while we never had the opportunity to meet, you and Grandma Kay instilled the drive to academic excellence in your daughter that was passed to me. Grandmas Kay and Rae, if I managed to inherit a fraction of your grit and determination, I will be more than equipped to tackle any of life's future challenges. Finally, Grandpa Sutermaster, you were, and are, my

academic hero. Your memory helped carry me through the completion of this thesis, and I share this achievement with you.

Table of Contents

Curriculum Vitae iv
Acknowledgements vii
Table of Contents xii
List of Figures 1
1 Introduction 3
1.1 Motivation/ Chapter Overview 3
1.2 Background 5
1.2.1 Cell Sorting 5
1.2.2 Adipose-Derived Stem Cells (ASCs) 14
1.3 Closing Remarks 15
1.4 References 17
2 Considerations for high-yield, high-throughput cell enrichment: fluorescence versus magnetic sorting 34
2.1 Abstract 34
2.2 Introduction 35
2.3 Materials and Methods 37
2.3.1 SVF Isolation and Culture 37
2.3.2 Fluorescence-Activated Cell Sorting (FACS) 38
2.3.3 Magnetic-Activated Cell Sorting (MACS) (Manufacturer's Protocol) 40
2.3.4 Magnetic-Activated Cell Sorting Optimization 41
2.3.5 Magnetic-Activated Cell Sorting (MACS) (Optimized Protocol) 42
2.3.6 Statistical Analysis 42
2.4 Results 43
2.4.1 MACS Optimization 43
2.4.2 Cell Yield, Viability, and Sorting Time for Sorting Experiments 48
2.5 Discussion 49
2.6 Major Takeaways 55
2.7 Acknowledgements 56
2.8 Author Contributions 56

2.9 Additional Information 56
2.9.1 Competing Interests 56
2.10 References 57
2.11 Supplemental Information 63
2.11.1 Preliminary FACS and MACS Sorts 63
3 Mass-Added Density Centrifugation (MADC): A novel, particle-based, non-binary cell sorting method 65
3.1 Introduction 65
3.2 Materials and Methods 68
3.2.1 MADC Theory 68
3.2.2 Cell Culture and Fixation 69
3.2.3 Wheat Germ Agglutinin Staining 70
3.2.4 InnovaCoat® Gold CD51/61 Antibody Functionalization 71
3.2.5 Pre-Sera-Mag™ MADC Antibody Treatment 72
3.2.6 Anti-CD51/61-Functionalized InnovaCoat® Bead Treatment 72
3.2.7 Sera-Mag™ Bead Treatment 73
3.2.8 Density Gradient Centrifugation, Post-MADC Fractionation 74
3.2.9 Cellular Density Estimation 79
3.2.10 Flow Cytometry 80
3.2.11 Cell Lysis and Western Blot 81
3.2.12 Statistical Analysis 82
3.3 Results 83
3.3.1 Cell Density, Maximum Particles Per Cell, and Simulated Composite Density 83
3.3.2 MeWo Expression of CD271 in Response to 0 μM, 15 μM, and 30 μM Cisplatin 84
3.3.3 Continuous Gradient MADC using InnovaCoat® and Sera-Mag™ Beads 86
3.3.4 Discontinuous Gradient MADC using Sera-Mag™ Beads 93
3.4 Discussion 94
3.5 Acknowledgements 101
3.6 References 102
3.7 Supplemental Information 107

3.7.1 Determination of Percoll Gradient Parameters 107
4 Conclusions and Future Work 109
4.1 Chapter 2 109
4.2 Chapter 3 112
4.3 Closing Remarks 114
4.4 References 115

List of Figures

Figure 1-1. Schematic representations of fluorescence-activated cell sorting (FACS) and magnetic activated cell sorting (MACS). 7
Figure 1-2. Schematic of density gradient centrifugation modes. 12
Figure 2-1. Normalized output fraction of osteogenically primed SVF and A375 controlled-ratio sorts using FACS, manufacturer's protocol MACS, and optimized protocol MACS. 44
Figure 2-2. Cell yield and fraction analyses for MACS optimization trials of varying antibody and microbead concentrations. 45
Figure 2-3. Cell yield and flow cytometric analysis for high concentration antibody and microbead MACS optimization trials. 46
Figure 2-4. Post-MACS flow cytometric analysis of retained and flow-through fractions isolated using either manufacturer's or optimized protocols. 47
Figure 2-5. Total, live, and dead cell yields and post-sort viabilities for FACS, manufacturer's protocol MACS, and optimized protocol MACS sorts. 49
Figure 3-1. Schematic of MADC-separation of 1:1 mixtures of untreated, green-fluorescent cells and antibody/bead-treated, non- or red-fluorescent cells using pre-established continuous gradients. 75
Figure 3-2. Schematics of MADC separation and density gradient centrifugation using continuous gradients. 77
Figure 3-3. Schematics of MADC separation and density gradient centrifugation using discontinuous gradients. 79
Figure 3-4. Simulated density of cell/particle composites as a function of the number of particles added. 84
Figure 3-5. Flow cytometry and Western blot evaluation of MeWo cells exposed to 24 hr treatments of 0 μM, 15 μM, and 30 μM cisplatin ($MeWo_{NT}$, $MeWo_{15}$, $MeWo_{30}$, respectively). 85
Figure 3-6. Pictures of continuous MADC gradients after secondary centrifugation and before fractionation. 87
Figure 3-7. Flow cytometry evaluation of post-continuous MADC fractions using anti-CD271-functionalized InnovaCoat® beads and A375 cells. 88
Figure 3-8. Flow cytometry evaluation of post-continuous MADC fractions using anti-CD271-biotin antibodies, Sera-Mag™ beads, and $MeWo_{30}$ cells. 90
Figure 3-9. Per-fraction quantification of CD271/β-tubulin relative expression post continuous gradient MADC and density gradient centrifugation. 92
Figure 3-10. Per-fraction quantification of CD271/β-tubulin relative expression post discontinuous gradient MADC and density gradient centrifugation. 93

Figure S 2-1. Initial FACS and MACS post-sort yield and differentiation results. 64
Figure S 3-1. Preliminary experiments to determine candidate Percoll gradient parameters. 108

Chapter 1

Introduction

1.1 Motivation/ Chapter Overview

Cellular heterogeneity is a defining characteristic of multicellular organisms. Tissues are made of heterogeneous mixtures of cell types that each play unique, specialized roles. Interestingly, even these single cell types can display heterogeneity. Cell sorting is used to isolate unique cell types, or subpopulations within cell types, based on defining characteristics like gene or protein expression,[1,2] cellular density,[3] or cellular size,[4,5] for further study or translational therapies. Cell sorting methods can be characterized by their specificity (i.e. the effectiveness at isolating pure subpopulations), throughput (i.e. the number of cells that can be processed in a certain time), and yield (i.e. the number of cells that can be isolated from a certain input population). Though the specificity of any given sorting method is often discussed, cell yields and throughputs are vastly underreported. The goal of this thesis was to investigate these underappreciated sorting characteristics for common sorting methods, and subsequently to develop a novel sorting method designed to address common sorting pitfalls.

The remainder of Chapter 1 will focus on essential background information on sorting methods and cell sources. Brief overview descriptions will be presented for three common sorting methods: fluorescence-activated cell sorting (FACS), magnetic sorting, and density gradient centrifugation. Finally, adipose-derived stem cells (ASCs), an

attractive, heterogeneous cell source often investigated for both basic science and translational applications, will be overviewed.

Chapter 2 features a study designed to characterize the sorting efficiencies of two common sorting methods, FACS and magnetic-activated cell sorting (MACS). In a previous study in the Darling lab, we observed ~86% cell loss when using FACS to sort subpopulations of osteogenically primed stromal vascular fraction (SVF) cells.[1] After examining the relevant literature, it became apparent that cell yields and throughputs of common sorting methods are underreported. Thus, we set out to test the efficiencies of two common sorting methods, FACS and MACS. To test efficiencies, we used each method to sort known mixtures of osteogenically primed SVF cells and A375 human melanoma cells based on the expression of an osteogenic marker protein, alkaline phosphatase liver/bone/kidney, and compared resultant cell yields, viabilities, and processing times. Additionally, this study presented a detailed optimization procedure for MACS antibody and microbead treatment concentrations to ensure accurate subpopulation discrimination. The results of this study provide researchers with both a MACS optimization method and quantitative comparison between FACS and MACS, thus enabling more informed sorting method decisions.

Chapter 3 details progress on the development of mass-added density centrifugation (MADC): a novel, non-binary, particle-based sorting method that leverages small, massive nano/microparticles to alter cell density prior to density gradient centrifugation. While our previous study, presented in Chapter 2, indicated the suitability of MACS for high-yield and –throughput cell isolations, the separations were binary (i.e. based on whether a protein was expressed rather than the level of expression). We thus

set out to develop a particle-based sorting method that combined the gentle, bulk processing of MACS with the non-binary separations of FACS. We hypothesized that we could alter the mass of cells proportionally to their expression of a surface marker of interest by labeling them with either an antibody-functionalized nanoparticle or by a primary antibody and secondary microbead, followed by continuous or discontinuous density gradient centrifugation. After centrifugation, gradients were fractionated and subjected to either flow cytometry or Western blot to verify successful separation. This study indicates MADC may be a useful tool the binary separation of large numbers of cells, and suggests future refinements of the technique to achieve non-binary separation.

Chapter 4 summarizes and contextualizes the work presented within this thesis. Special attention is given to future directions that build upon the results presented herein.

1.2 Background

1.2.1 Cell Sorting

Traditional population level molecular biology assessments like Western blot, quantitative polymerase chain reaction (qPCR), and DNA microarray, can obscure cell-to-cell differences. In fact, cellular heterogeneity exists in many forms, including gene expression,[1] protein expression,[2] and mechanophenotype,[6] among others, which can have functional consequences.[7-10] Cell sorting provides a mechanism to isolate subpopulations for basic scientific investigations, diagnostic purposes,[11,12] or therapeutic applications.[13,14] While the gold standard of cell sorting is FACS,[15] alternative methods including magnetic-activated cell sorting,[16] microfluidic cell sorting,[17] or density gradient centrifugation,[18] each provide their own unique strengths and weaknesses (reviewed in

Tomlinson *et al.*[19]). As such, while all of these sorting methods are capable of being used by themselves, they are often used in combination.[20-22]

1.2.1.1 Fluorescence-Activated Cell Sorting (FACS)

Invented in the late 1960s, FACS can sort cells based on a number of parameters including size, granularity, and the color and intensity of fluorescence.[15,23,24] Despite many advancements in the design and construction of commercial FACS machines in the last 40-plus years, the fundamental sorting steps remain the same in the present day (**Figure 1-1a**). First, a heterogeneous input population containing fluorescent cells is input into the sorter as a single-cell suspension. The cells are then passed one-by-one through an assessment volume in individual droplets where they are exposed to an excitation laser. Detectors measure both the forward and side scattered light (FSC and SSC, corresponding to cell size and granularity/complexity, respectively), and the fluorescence intensity of the cell in the assessment volume. Based on user-defined size, granularity, and fluorescence gates, a charge is ascribed to the cell droplet, and deflected by charged plates into respective collection tubes.

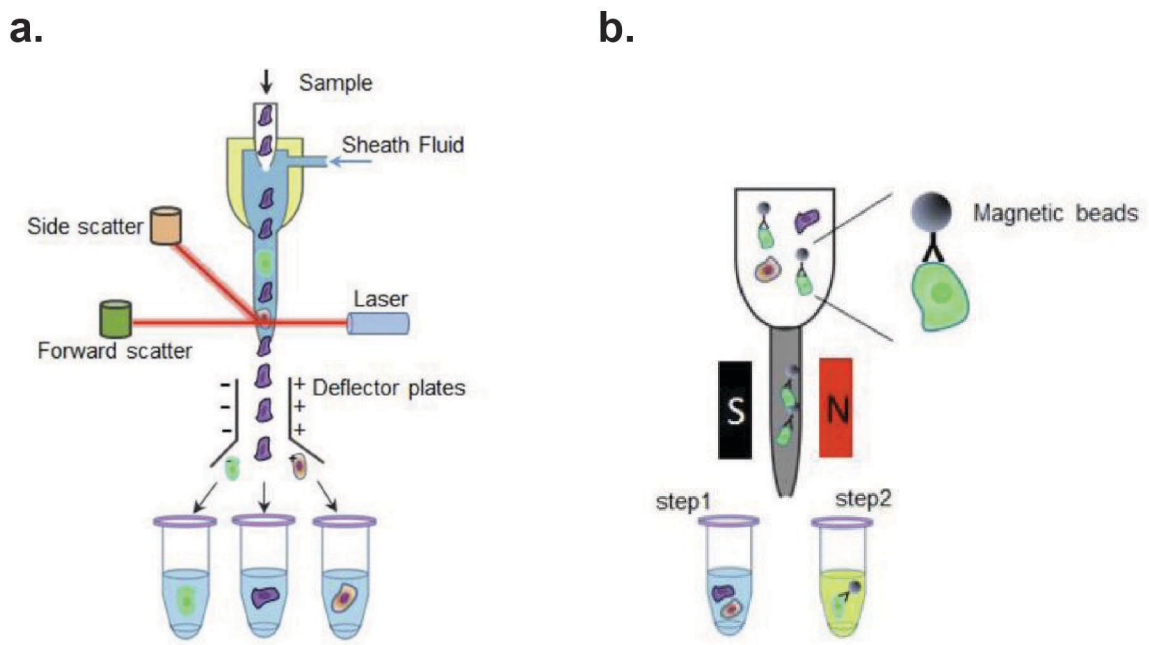

Figure 1-1. Schematic representations of fluorescence-activated cell sorting (FACS) and magnetic activated cell sorting (MACS). a.) FACS: Single cells contained in fluid droplets are assayed for size, granularity, and fluorescence in an assessment volume. Based on size, granularity, and fluorescence, the droplets are charged and deflected into specific collection tubes. b.) MACS: Cells are magnetically treated with antibody-labeled beads, and placed into a magnetic field. Unlabeled cells pass through and are collected in a tube (labeled "step 1"). Subsequently, the magnet is removed, allowing elution of the retained, labeled cells into a separate tube (labeled "step 2"). Figure modified from Hu *et al.*[25]

Fluorescent staining of cells is achieved in many and varied ways, and is the primary characteristic by which cells are sorted in FACS. Cellular fluorescence treatments can be split into two distinct categories: extra- and intra-cellular. The most common extracellular method for fluorescently staining cells is using antibodies targeting specific surface marker proteins. FACS sorting based on single or multi-surface marker panels is routinely performed to isolate subpopulations of heterogeneously differentiating cells,[26-28] and cancer and stem cell subpopulations, [29-32] among many others. Alternatively, cells can be labeled extracellularly with

fluorescent, folded oligonucleotide probes called aptamers that target surface proteins. [33-35] Researchers have used fluorescently labeled aptamers to isolate bone marrow-derived stem cells (BMSCs)[36] and putative cancer stem cells.[37,38] While extracellular labeling, especially by antibodies, is the most common fluorescent cell staining method, several intracellular alternatives also exist.

One method of rendering cells intracellularly fluorescent is the use of cell-permeant dyes. These dyes function either by binding specific intracellular locations (i.e. the mitochondrial membrane) or molecules (i.e. DNA), or act as substrates for intracellular enzymes like aldehyde dehydrogenase (ALDH).[39] Researchers have coupled a DNA dye, Hoechst 33342, with FACS to isolate subpopulations of mouse and trout testicular cells,[40-42] hematopoietic stem cells,[43] and cells in the various phases of the cell cycle.[44] Others have used mitochondrial membrane dyes rhodamine 123 (Rh123) and JC-1 to isolate subpopulations of mouse and rat testicular cells,[45,46] as well as mouse and human hematopoietic stem cells.[47-49] Aldehyde dehydrogenase (ALDH) substrates BODIPY-aminoacetaldehyde (BAAA) and N-dansyl aminoacetaldehyde (DAAA), have been used to isolate human kidney progenitors,[50] hematopoietic stem cells,[51,52] and subpopulations of mouse spermatogonial cells.[53] Finally, a newly developed, putatively stem-cell specific dye, CDy1, has been used to isolate induced pluripotent stem cells (iPSCs) and embryonic stem cells (ESCs),[54,55] mouse spermatogonial stem cells,[56] and even subpopulations of multiple myelomas.[57]

Molecular beacons can fluorescently label messenger RNA (mRNA) molecules, and provide an intracellular alternative to simple, cell permeant dyes. Invented by Tyagi and colleagues in the mid-1990s, molecular beacons are small, hairpin ribo- or

deoxyribo-nucleic acid (RNA and DNA, respectively) molecules that can be used to detect gene expression at the transcription level.[58] In their most basic form, they consist of a 5′ fluorophore and 3′ quencher, 5+ base-pair stem, and 15-35 base loop that can be made complementary to oligonucleotide molecules of interest.[59] In their unbound state, the 5′ fluorophore and 3′ quencher are kept in close proximity due to the self-complementary stem, but unwind upon hybridization with a target mRNA molecule. While simple DNA molecular beacons work incredibly well acellularly, they suffer from low signal-to-noise ratios *in vitro,* likely due to enzymatic degradation within the cell.[60,61] As such, new iterations of molecular beacons have been synthesized in an effort to avoid enzymatic degradation, including 2′-O-metyl and 2′-deoxy beacons,[62] locked nucleic acid (LNA) and LNA/DNA-hybrid beacons,[63,64] and peptide nucleic acid (PNA) beacons.[65-68] However, care must be exercised in the design of modified nucleic acid beacon constructs as their tight binding with endogenous mRNA may induce gene silencing.[69]Additionally, conventional beacons have been paired with other beacons to exhibit additional signal specificity,[70,71] or otherwise modified to ensure true-positive detection.[72-76] Various researchers have utilized molecular beacons or their derivatives with FACS to isolate human and mouse embryonic and neural stem cells,[77,78] cardiomyocytes from heterogeneously differentiating pluripotent stem cell populations,[79-81] and subpopulations of osteogenically primed SVF cells.[1]

With its many uses, and unparalleled specificity, FACS continues to be the most flexible cell sorting method. The abilities to use multiple markers to define extremely specific subpopulations and to separate cells based on differences in

fluorescence intensity make FACS an incredibly powerful tool. However, it is characterized by relatively low-throughput, and high cell losses, which will be discussed more in Chapter 2.

1.2.1.2 Magnetic-Activated Cell Sorting (MACS)

MACS* is performed much in the same way as FACS, but relies on targeted magnetic nanoparticles and an externally applied magnetic field to achieve cell separation (**Figure 1-1**).[16] Magnetic labeling can be performed directly, with an antibody-labeled magnetic bead, or indirectly, using a fluorescent or biotinylated primary antibody coupled with a secondary magnetic bead targeting the fluorophore/biotin of the primary antibody. Magnetically treated, heterogeneous cell populations are first pipetted into a column placed in a strong magnetic field. Cells that have bound sufficient magnetic beads are retained on the column, while unlabeled cells pass through into a collection tube. Subsequently, the column can be removed from the magnetic field, and the labeled cells eluted into a separate collection tube.

MACS is capable of performing analogous isolations to FACS, but is limited to binary separations using extracellular labeling. Like FACS, MACS has been used to isolate many different cell types, including lymphocytes,[16] spermatogonial and prostatic epithelial stem cells,[82,83] and various cancer stem cells,[2,84] among many others. Additionally, magnetic sorting is used clinically in certain leukemia treatment

*"MACS" is technically a trade name for the magnetic cell separation system commercially produced by Miltenyi Biotec, however it often used to reference magnetic cell sorting, generally.[16]

protocols.[13,14] Due to its bulk processing nature, MACS is very rapid and high throughput. As it is gravity-driven, it does not exert high cellular shear stresses like FACS, potentially resulting in higher post-sort viabilities.[85] MACS does not require expensive machinery, and can be performed by novice users with little training. However, it is insensitive to clumps of cells and can suffer from false-negatives, resulting in lower purity isolations.[26,86] Furthermore, MACS separates cells in a binary manner, isolating all cells based on whether or not they are labeled as opposed to the degree to which they are labeled. While concerns do exist as to whether the magnetic bead binding negatively affects cellular survival or post-sort phenotype, most studies indicate little to no effect.[16,87-93] The relative merits of FACS and MACS are discussed in further detail in Chapter 2.

1.2.1.3 Density Gradient Centrifugation

Density gradient centrifugation can be performed in two distinct modes, rate-zonal and isopycnic centrifugation, which enable the separation of different cell types on the basis of size and density, respectively (**Figure 1-2**). In either method, cell movements can be described by their sedimentation rates. The sedimentation rate, v_{cell}, of a spherical cell in a fluid under constant centrifugation is a function of the cell's size and density, and the density and viscosity of the surrounding fluid (**Equation 1-1**).[94]

$$v_{cell} = \frac{d_{cell}^2 \cdot (\rho_{cell} - \rho_{fluid})}{18 * \eta_{fluid}} * f_{centrifugal} \qquad \textbf{Equation 1-1}$$

where d_{cell} = diameter of the cell, ρ_{cell} = density of the cell, ρ_{fluid} = density of the fluid, η_{fluid} = viscosity of the fluid, and $f_{centrifugal}$ = the applied centrifugal force.

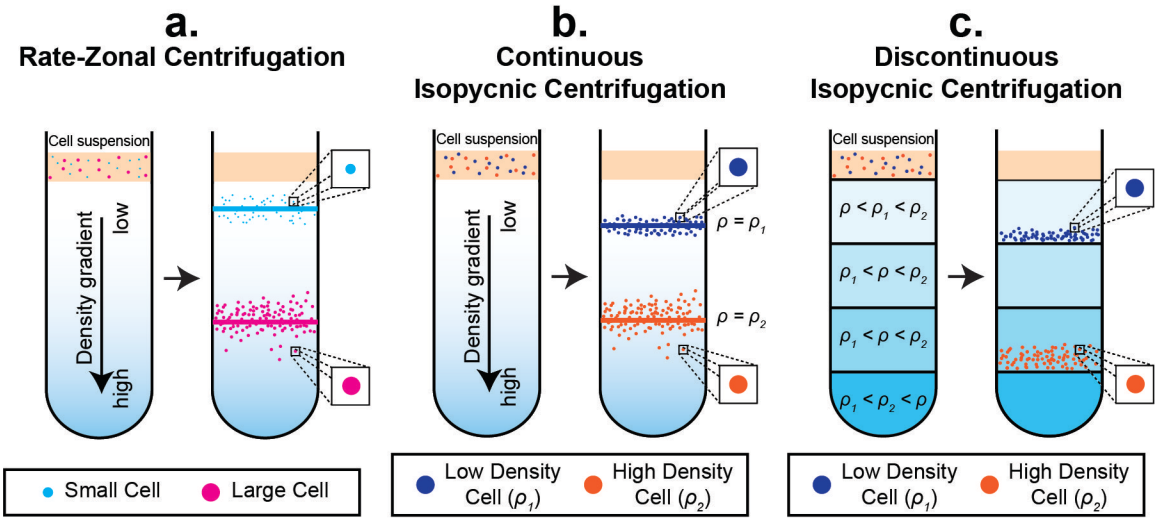

Figure 1-2. Schematic of density gradient centrifugation modes. a.) Rate-zonal centrifugation separates cells solely based on size. b.) Continuous and c.) discontinuous isopycnic centrifugations separate cells solely based on density.

In rate-zonal centrifugation, heterogeneous mixtures of cells of different sizes are layered on a pre-formed, continuous density gradient which is less dense than the cells at all points, and centrifuged. During centrifugation, the larger cells will exhibit faster sedimentation rates than the smaller cells (**Figure 1-2a**). If the centrifugation process is stopped prior to when cells of the denser cell type pellet, these gradients can be fractionated to isolate the individual cell types.

Isopycnic centrifugation can be performed with either continuous or discontinuous density gradients. In continuous isopycnic centrifugation, mixtures of cell types of differing density are layered on top of a pre-formed continuous gradient with a maximum density that is greater than that of the cells. Upon centrifugation, each cell type moves down the gradient at their characteristic sedimentation rates

until they reach the gradient position that matches their density (**Figure 1-2b**). In discontinuous isopycnic centrifugation, a density gradient medium is diluted to make solutions of varied densities, which are carefully layered from most to least dense. Heterogeneous mixtures of cell types of varied density are then layered on top of the discontinuous gradient, which is subsequently centrifuged. Cells progress through the gradient steps until they reach an interface with a step of greater density than their own (**Figure 1-2**). After continuous or discontinuous isopycnic centrifugation, gradients can be fractionated to isolate the individual cell types.

Density gradient centrifugation has been performed with a variety of different density gradient media to separate a myriad of cell types. While Ficoll[95] and Percoll[18,96] are two of the most common density gradient media compatible with cell use, many others exist, including Metrizamide,[97] Nycodenz,[98] and Iodixanol/Optiprep,[99] among others. Since the late-1960s, polysaccharide Ficoll has been routinely used to perform discontinuous isopycnic separations of whole blood to isolate various cell types.[100,101] Percoll, developed in the late-1970s, is composed of colloidal silica particles coated in polyvinylpyrrolidone (PVP).[96] In addition to being used for discontinuous isopycnic centrifugation, Percoll can be centrifuged at high-g to make self-forming, continuous gradients due to its colloidal nature. As such, it has been used to separate many different cell types including spermatozoa,[102] cardiomyocytes,[103] and various blood cells.[104-106] A novel application of Percoll density centrifugation is presented in Chapter 3.

1.2.2 Adipose-Derived Stem Cells (ASCs)

Adipose-derived stem cells (ASCs) are a multipotent cell population found in the vascular-associated cellular component, or stromal vascular fraction (SVF), of fat tissue. Discovered by Zuk and colleagues, ASCs possess both self-renewal and differentiation capacities, and lack the risk of teratoma formation posed by iPSCs or ESCs.[107,108] ASCs are derived from the mesoderm, and can be differentiated down various mesodermal lineages including adipo-,[109] chrondro-,[110] myo-,[111] and osteo-genic.[112] Additionally, ASCs have even been reported to offer immunomodulatory effects.[113] Though ASCs share many of these interesting qualities with other mesenchymal stem cells (MSCs), like bone marrow stem cells (BMSCs) and muscle-derived stem cells (MDSCs), ASCs possess distinct advantages over MSCs from other stem cell niches.

Adipose tissue is an attractive stem cell source for both basic science and therapeutic applications due to its accessibility and the relative abundance of resident differentiable cells compared to other stem cell niches. Adipose tissue has been reported to contain a higher percentage of adult stem cells (ASCs: 1% - 40%)[114,115] compared to bone marrow (BMSCs: 0.001% – 0.1%).[116] ASCs can be easily procured from lipoaspirate waste, a byproduct of routinely performed liposuction surgeries (~250,000 performed in U.S. in 2017).[117] Prolonged passaging or active sorting processes are used to isolate ASCs from the SVF.

Prolonged passaging leverages ASCs' plastic adherence and self-renewal capacities to separate them from the rest of the cells of the SVF.[118] First, lipoaspirate waste is processed by a combination of mechanical agitation and collagenase digestion to liberate the SVF. The SVF is then plated onto tissue culture plastic, allowing the adherent

cell types to attach and spread. Cells are then allowed to multiply in an expansion medium that maintains the proliferative and differentiation capabilities of the ASCs. Over the course of expansion and passaging, the proliferative ASCs overtake the remaining terminally differentiated cell types. While effective at isolation and purification of ASCs, prolonged passaging is not without its drawbacks. It is time-consuming and, despite the use of specialized expansion medium designed to maintain cell stemness, has been shown to affect ASC gene expression and differentiation potential due to sustained exposure to stiff cell culture plastic.[119-121]

Cell sorting of ASCs is complicated by their dynamic surface marker profile.[122] The International Federation of Adipose Therapeutics and Science (IFATS) and the International Society for Cellular Therapy (ISCT) suggests a minimum surface marker definition of ASCs to include four markers (CD34+/CD31-/CD45-/CD235a-), with an additional four for increased specificity (CD13+/CD73+/CD90+/CD105+).[114] These strict surface marker definitions can adversely affect cell yields, impairing thorough study or isolation of therapeutically relevant cell numbers. In the Darling Lab, we have conducted a study using a less stringent, gene expression-based sorting approach in an effort to increase functional cell yields.[1] The large cell losses we observed during FACS separations in that study motivated the comparison of sorting efficiencies presented in Chapter 2.

1.3 Closing Remarks

This thesis serves to emphasize the importance of cell yields, throughputs, and resultant viabilities in cell sorting procedures. To this point, sorting purity has been the

primary characteristic by which sorting methods have been judged. However, as the personalized medicine revolution gains momentum and numerous new cell-based therapies are proposed, sorting parameters including yields, viabilities, and throughputs will have be afforded additional emphasis. Our rigorous characterization of these parameters for common sorting methods FACS and MACS (presented in Chapter 2) will serve both as a valuable decision-making tool as well as a template for others to conduct their own evaluations of sorting methods. Finally, with further development, our novel, particle-based sorting technology, MADC (presented in Chapter 3), will provide a much needed alternative for high-throughput, non-binary separations.

1.4 References

1 Marble, H. D., Sutermaster, B. A., Kanthilal, M., Fonseca, V. C. & Darling, E. M. Gene expression-based enrichment of live cells from adipose tissue produces subpopulations with improved osteogenic potential. *Stem Cell Res Ther* **5**, 145, doi:10.1186/scrt502 (2014).

2 Singh, S. K. *et al.* Identification of a cancer stem cell in human brain tumors. *Cancer research* **63**, 5821-5828 (2003).

3 Pertoft, H. Fractionation of cells and subcellular particles with Percoll. *J Biochem Biophys Methods* **44**, 1-30 (2000).

4 Gossett, D. R. *et al.* Label-free cell separation and sorting in microfluidic systems. *Anal Bioanal Chem* **397**, 3249-3267, doi:10.1007/s00216-010-3721-9 (2010).

5 Yamada, M. *et al.* Microfluidic devices for size-dependent separation of liver cells. *Biomed Microdevices* **9**, 637-645, doi:10.1007/s10544-007-9055-5 (2007).

6 Gonzalez-Cruz, R. D., Fonseca, V. C. & Darling, E. M. Cellular mechanical properties reflect the differentiation potential of adipose-derived mesenchymal stem cells. *Proceedings of the National Academy of Sciences of the United States of America* **109**, E1523-1529, doi:10.1073/pnas.1120349109 (2012).

7 Altschuler, S. J. & Wu, L. F. Cellular heterogeneity: do differences make a difference? *Cell* **141**, 559-563, doi:10.1016/j.cell.2010.04.033 (2010).

8 Almendro, V., Marusyk, A. & Polyak, K. Cellular heterogeneity and molecular evolution in cancer. *Annu Rev Pathol* **8**, 277-302, doi:10.1146/annurev-pathol-020712-163923 (2013).

9 Fisher, R., Pusztai, L. & Swanton, C. Cancer heterogeneity: implications for targeted therapeutics. *Br J Cancer* **108**, 479-485, doi:10.1038/bjc.2012.581 (2013).

10 McLeod, C. M. & Mauck, R. L. On the origin and impact of mesenchymal stem cell heterogeneity: new insights and emerging tools for single cell analysis. *Eur Cell Mater* **34**, 217-231, doi:10.22203/eCM.v034a14 (2017).

11 Yu, Z. T., Aw Yong, K. M. & Fu, J. Microfluidic blood cell sorting: now and beyond. *Small* **10**, 1687-1703, doi:10.1002/smll.201302907 (2014).

12 Nagrath, S. *et al.* Isolation of rare circulating tumour cells in cancer patients by microchip technology. *Nature* **450**, 1235-1239, doi:10.1038/nature06385 (2007).

13 Devine, S. M. *et al.* Low Risk of Chronic Graft-versus-Host Disease and Relapse Associated with T Cell-Depleted Peripheral Blood Stem Cell Transplantation for Acute Myelogenous Leukemia in First Remission: Results of the Blood and Marrow Transplant Clinical Trials Network Protocol 0303. *Biol Blood Marrow Tr* **17**, 1343-1351, doi:10.1016/j.bbmt.2011.02.002 (2011).

14 Pasquini, M. C. *et al.* Comparative Outcomes of Donor Graft CD34(+) Selection and Immune Suppressive Therapy As Graft-Versus-Host Disease Prophylaxis for Patients With Acute Myeloid Leukemia in Complete Remission Undergoing HLA-Matched Sibling Allogeneic Hematopoietic Cell Transplantation. *J Clin Oncol* **30**, 3194-3201, doi:10.1200/Jco.2012.41.7071 (2012).

15 Bonner, W. A., Hulett, H. R., Sweet, R. G. & Herzenberg, L. A. Fluorescence activated cell sorting. *Rev Sci Instrum* **43**, 404-409 (1972).

16 Miltenyi, S., Muller, W., Weichel, W. & Radbruch, A. High gradient magnetic cell separation with MACS. *Cytometry* **11**, 231-238, doi:10.1002/cyto.990110203 (1990).

17 Shields, C. W., Reyes, C. D. & Lopez, G. P. Microfluidic cell sorting: a review of the advances in the separation of cells from debulking to rare cell isolation. *Lab on a Chip* **15**, 1230-1249, doi:10.1039/c4lc01246a (2015).

18 Pertoft, H., Rubin, K., Kjellen, L., Laurent, T. C. & Klingeborn, B. The viability of cells grown or centrifuged in a new density gradient medium, Percoll(TM). *Exp Cell Res* **110**, 449-457 (1977).

19 Tomlinson, M. J., Tomlinson, S., Yang, X. B. & Kirkham, J. Cell separation: Terminology and practical considerations. *J Tissue Eng* **4**, 2041731412472690, doi:10.1177/2041731412472690 (2013).

20 Fischer, K. *et al.* Isolation and characterization of human antigen-specific TCR alpha beta+ CD4(-)CD8- double-negative regulatory T cells. *Blood* **105**, 2828-2835, doi:10.1182/blood-2004-07-2583 (2005).

21 Schweitzer, C. M. *et al.* Isolation and culture of human bone marrow endothelial cells. *Exp Hematol* **23**, 41-48 (1995).

22 Sullivan, S., Bergstresser, P. R., Tigelaar, R. E. & Streilein, J. W. FACS purification of bone marrow-derived epidermal populations in mice: Langerhans cells and Thy-1+ dendritic cells. *The Journal of investigative dermatology* **84**, 491-495 (1985).

23 Hulett, H. R., Bonner, W. A., Barrett, J. & Herzenbe.La. Cell Sorting - Automated Separation of Mammalian Cells as a Function of Intracellular Fluorescence. *Science* **166**, 747-&, doi:DOI 10.1126/science.166.3906.747 (1969).

24 Herzenberg, L. A. *et al.* The history and future of the fluorescence activated cell sorter and flow cytometry: a view from Stanford. *Clin Chem* **48**, 1819-1827 (2002).

25 Hu, P., Zhang, W., Xin, H. & Deng, G. Single Cell Isolation and Analysis. *Front Cell Dev Biol* **4**, 116, doi:10.3389/fcell.2016.00116 (2016).

26 Pruszak, J., Sonntag, K. C., Aung, M. H., Sanchez-Pernaute, R. & Isacson, O. Markers and methods for cell sorting of human embryonic stem cell-derived neural cell populations. *Stem Cells* **25**, 2257-2268, doi:10.1634/stemcells.2006-0744 (2007).

27 Doi, D. *et al.* Isolation of human induced pluripotent stem cell-derived dopaminergic progenitors by cell sorting for successful transplantation. *Stem Cell Reports* **2**, 337-350, doi:10.1016/j.stemcr.2014.01.013 (2014).

28 Dubois, N. C. *et al.* SIRPA is a specific cell-surface marker for isolating cardiomyocytes derived from human pluripotent stem cells. *Nat Biotechnol* **29**, 1011-U1082, doi:10.1038/nbt.2005 (2011).

29 Prince, M. E. *et al.* Identification of a subpopulation of cells with cancer stem cell properties in head and neck squamous cell carcinoma. *Proceedings of the National Academy of Sciences of the United States of America* **104**, 973-978, doi:10.1073/pnas.0610117104 (2007).

30 Dalerba, P. *et al.* Phenotypic characterization of human colorectal cancer stem cells. *Proceedings of the National Academy of Sciences of the United States of America* **104**, 10158-10163, doi:10.1073/pnas.0703478104 (2007).

31 Li, C. *et al.* Identification of pancreatic cancer stem cells. *Cancer research* **67**, 1030-1037, doi:10.1158/0008-5472.CAN-06-2030 (2007).

32 Shackleton, M. *et al.* Generation of a functional mammary gland from a single stem cell. *Nature* **439**, 84-88, doi:10.1038/nature04372 (2006).

33 Ellington, A. D. & Szostak, J. W. In vitro selection of RNA molecules that bind specific ligands. *Nature* **346**, 818-822, doi:10.1038/346818a0 (1990).

34 Jayasena, S. D. Aptamers: an emerging class of molecules that rival antibodies in diagnostics. *Clin Chem* **45**, 1628-1650 (1999).

35 Tuerk, C. & Gold, L. Systematic evolution of ligands by exponential enrichment: RNA ligands to bacteriophage T4 DNA polymerase. *Science* **249**, 505-510 (1990).

36 Guo, K. T. *et al.* A new technique for the isolation and surface immobilization of mesenchymal stem cells from whole bone marrow using high-specific DNA aptamers. *Stem Cells* **24**, 2220-2231, doi:10.1634/stemcells.2006-0015 (2006).

37 Sefah, K. *et al.* Cell-based selection provides novel molecular probes for cancer stem cells. *Int J Cancer* **132**, 2578-2588, doi:10.1002/ijc.27936 (2013).

38 Kim, Y. *et al.* Aptamer identification of brain tumor-initiating cells. *Cancer research* **73**, 4923-4936, doi:10.1158/0008-5472.CAN-12-4556 (2013).

39 Balber, A. E. Concise review: aldehyde dehydrogenase bright stem and progenitor cell populations from normal tissues: characteristics, activities, and emerging uses in regenerative medicine. *Stem Cells* **29**, 570-575, doi:10.1002/stem.613 (2011).

40 Falciatori, I. *et al.* Identification and enrichment of spermatogonial stem cells displaying side-population phenotype in immature mouse testis. *FASEB J* **18**, 376-378, doi:10.1096/fj.03-0744fje (2004).

41 Hayashi, M. *et al.* Enrichment of spermatogonial stem cells using side population in teleost. *Biol Reprod* **91**, 23, doi:10.1095/biolreprod.113.114140 (2014).

42 Lassalle, B. *et al.* 'Side Population' cells in adult mouse testis express Bcrp1 gene and are enriched in spermatogonia and germinal stem cells. *Development* **131**, 479-487, doi:10.1242/dev.00918 (2004).

43 Goodell, M. A., Brose, K., Paradis, G., Conner, A. S. & Mulligan, R. C. Isolation and functional properties of murine hematopoietic stem cells that are replicating in vivo. *J Exp Med* **183**, 1797-1806 (1996).

44 Juan, G., Hernando, E. & Cordon-Cardo, C. Separation of live cells in different phases of the cell cycle for gene expression analysis. *Cytometry* **49**, 170-175, doi:10.1002/cyto.10173 (2002).

45 Lo, K. C., Brugh, V. M., 3rd, Parker, M. & Lamb, D. J. Isolation and enrichment of murine spermatogonial stem cells using rhodamine 123 mitochondrial dye. *Biol Reprod* **72**, 767-771, doi:10.1095/biolreprod.104.033464 (2005).

46 Ryu, B. Y., Orwig, K. E., Kubota, H., Avarbock, M. R. & Brinster, R. L. Phenotypic and functional characteristics of spermatogonial stem cells in rats. *Dev Biol* **274**, 158-170, doi:10.1016/j.ydbio.2004.07.004 (2004).

47 Chaudhary, P. M. & Roninson, I. B. Expression and activity of P-glycoprotein, a multidrug efflux pump, in human hematopoietic stem cells. *Cell* **66**, 85-94 (1991).

48 Ploemacher, R. E. & Brons, N. H. Cells with marrow and spleen repopulating ability and forming spleen colonies on day 16, 12, and 8 are sequentially ordered on the basis of increasing rhodamine 123 retention. *Journal of cellular physiology* **136**, 531-536, doi:10.1002/jcp.1041360320 (1988).

49 Spangrude, G. J. & Johnson, G. R. Resting and activated subsets of mouse multipotent hematopoietic stem cells. *Proceedings of the National Academy of Sciences of the United States of America* **87**, 7433-7437 (1990).

50 Lindgren, D. *et al.* Isolation and characterization of progenitor-like cells from human renal proximal tubules. *Am J Pathol* **178**, 828-837, doi:10.1016/j.ajpath.2010.10.026 (2011).

51 Storms, R. W. *et al.* Isolation of primitive human hematopoietic progenitors on the basis of aldehyde dehydrogenase activity. *Proceedings of the National Academy of Sciences of the United States of America* **96**, 9118-9123 (1999).

52 Jones, R. J. *et al.* Assessment of aldehyde dehydrogenase in viable cells. *Blood* **85**, 2742-2746 (1995).

53 Kanatsu-Shinohara, M., Mori, Y. & Shinohara, T. Enrichment of mouse spermatogonial stem cells based on aldehyde dehydrogenase activity. *Biol Reprod* **89**, 140, doi:10.1095/biolreprod.113.114629 (2013).

54 Im, C. N. *et al.* A fluorescent rosamine compound selectively stains pluripotent stem cells. *Angew Chem Int Ed Engl* **49**, 7497-7500, doi:10.1002/anie.201002463 (2010).

55 Kang, N. Y., Yun, S. W., Ha, H. H., Park, S. J. & Chang, Y. T. Embryonic and induced pluripotent stem cell staining and sorting with the live-cell fluorescence imaging probe CDy1. *Nat Protoc* **6**, 1044-1052, doi:10.1038/nprot.2011.350 (2011).

56 Kanatsu-Shinohara, M., Morimoto, H. & Shinohara, T. Enrichment of Mouse Spermatogonial Stem Cells by the Stem Cell Dye CDy1. *Biol Reprod* **94**, 13, doi:10.1095/biolreprod.115.135707 (2016).

57 Hawley, T. S. *et al.* Identification of an ABCB1 (P-glycoprotein)-positive carfilzomib-resistant myeloma subpopulation by the pluripotent stem cell fluorescent dye CDy1. *Am J Hematol* **88**, 265-272, doi:10.1002/ajh.23387 (2013).

58 Tyagi, S. & Kramer, F. R. Molecular beacons: probes that fluoresce upon hybridization. *Nat Biotechnol* **14**, 303-308, doi:10.1038/nbt0396-303 (1996).

59 Tyagi, S., Bratu, D. P. & Kramer, F. R. Multicolor molecular beacons for allele discrimination. *Nat Biotechnol* **16**, 49-53, doi:10.1038/nbt0198-49 (1998).

60 Chen, A. K., Behlke, M. A. & Tsourkas, A. Avoiding false-positive signals with nuclease-vulnerable molecular beacons in single living cells. *Nucleic acids research* **35**, e105, doi:10.1093/nar/gkm593 (2007).

61 Molenaar, C. *et al.* Linear 2' O-Methyl RNA probes for the visualization of RNA in living cells. *Nucleic acids research* **29**, E89-89 (2001).

62 Tsourkas, A., Behlke, M. A. & Bao, G. Hybridization of 2'-O-methyl and 2'-deoxy molecular beacons to RNA and DNA targets. *Nucleic acids research* **30**, 5168-5174 (2002).

63 Wang, L., Yang, C. J., Medley, C. D., Benner, S. A. & Tan, W. Locked nucleic acid molecular beacons. *J Am Chem Soc* **127**, 15664-15665, doi:10.1021/ja052498g (2005).

64 Yang, C. J. *et al.* Synthesis and investigation of deoxyribonucleic acid/locked nucleic acid chimeric molecular beacons. *Nucleic acids research* **35**, 4030-4041, doi:10.1093/nar/gkm358 (2007).

65 Egholm, M. *et al.* PNA hybridizes to complementary oligonucleotides obeying the Watson-Crick hydrogen-bonding rules. *Nature* **365**, 566-568, doi:10.1038/365566a0 (1993).

66 Kam, Y., Rubinstein, A., Nissan, A., Halle, D. & Yavin, E. Detection of endogenous K-ras mRNA in living cells at a single base resolution by a PNA molecular beacon. *Mol Pharm* **9**, 685-693, doi:10.1021/mp200505k (2012).

67 Nielsen, P. E., Egholm, M., Berg, R. H. & Buchardt, O. Sequence-selective recognition of DNA by strand displacement with a thymine-substituted polyamide. *Science* **254**, 1497-1500 (1991).

68 Ortiz, E., Estrada, G. & Lizardi, P. M. PNA molecular beacons for rapid detection of PCR amplicons. *Mol Cell Probes* **12**, 219-226, doi:10.1006/mcpr.1998.0175 (1998).

69 Stein, C. A. *et al.* Efficient gene silencing by delivery of locked nucleic acid antisense oligonucleotides, unassisted by transfection reagents. *Nucleic acids research* **38**, e3, doi:10.1093/nar/gkp841 (2010).

70 Santangelo, P. J., Nix, B., Tsourkas, A. & Bao, G. Dual FRET molecular beacons for mRNA detection in living cells. *Nucleic acids research* **32**, e57, doi:10.1093/nar/gnh062 (2004).

71 Tsourkas, A., Behlke, M. A., Xu, Y. & Bao, G. Spectroscopic features of dual fluorescence/luminescence resonance energy-transfer molecular beacons. *Analytical chemistry* **75**, 3697-3703 (2003).

72 Yang, Y., Chen, M., Krueger, C. J., Tsourkas, A. & Chen, A. K. Quantifying Gene Expression in Living Cells with Ratiometric Bimolecular Beacons. *Methods in molecular biology* **1649**, 231-242, doi:10.1007/978-1-4939-7213-5_15 (2018).

73 Song, Y., Zhang, X., Huang, L., Behlke, M. A. & Tsourkas, A. Real-time imaging of single engineered RNA transcripts in living cells using ratiometric bimolecular beacons. *J Vis Exp*, e51544, doi:10.3791/51544 (2014).

74 Zhang, X., Zajac, A. L., Huang, L., Behlke, M. A. & Tsourkas, A. Imaging the directed transport of single engineered RNA transcripts in real-time using ratiometric bimolecular beacons. *Plos One* **9**, e85813, doi:10.1371/journal.pone.0085813 (2014).

75 Zhang, X. *et al.* Quantitative assessment of ratiometric bimolecular beacons as a tool for imaging single engineered RNA transcripts and measuring gene expression in living cells. *Nucleic acids research* **41**, e152, doi:10.1093/nar/gkt561 (2013).

76 Chen, A. K., Davydenko, O., Behlke, M. A. & Tsourkas, A. Ratiometric bimolecular beacons for the sensitive detection of RNA in single living cells. *Nucleic acids research* **38**, e148, doi:10.1093/nar/gkq436 (2010).

77 King, F. W., Liszewski, W., Ritner, C. & Bernstein, H. S. High-Throughput Tracking of Pluripotent Human Embryonic Stem Cells with Dual Fluorescence Resonance Energy Transfer Molecular Beacons. *Stem Cells Dev* **20**, 475-484, doi:10.1089/scd.2010.0219 (2011).

78 Larsson, H. M. *et al.* Sorting live stem cells based on Sox2 mRNA expression. *Plos One* **7**, e49874, doi:10.1371/journal.pone.0049874 (2012).

79 Ban, K. *et al.* Purification of cardiomyocytes from differentiating pluripotent stem cells using molecular beacons that target cardiomyocyte-specific mRNA. *Circulation* **128**, 1897-1909, doi:10.1161/CIRCULATIONAHA.113.004228 (2013).

80 Jha, R. *et al.* Molecular beacon-based detection and isolation of working-type cardiomyocytes derived from human pluripotent stem cells. *Biomaterials* **50**, 176-185, doi:10.1016/j.biomaterials.2015.01.043 (2015).

81 Ban, K. *et al.* Non-genetic Purification of Ventricular Cardiomyocytes from Differentiating Embryonic Stem Cells through Molecular Beacons Targeting IRX-4. *Stem Cell Reports* **5**, 1239-1249, doi:10.1016/j.stemcr.2015.10.021 (2015).

82 von Schonfedt, V., Krishnamurthy, H., Foppiani, L. & Schlatt, S. Magnetic cell sorting is a fast and effective method of enriching viable spermatogonia from djungarian hamster, mouse, and marmoset monkey testes. *Biology of Reproduction* **61**, 582-589, doi:DOI 10.1095/biolreprod61.3.582 (1999).

83 Richardson, G. D. *et al.* CD133, a novel marker for human prostatic epithelial stem cells. *J Cell Sci* **117**, 3539-3545, doi:10.1242/jcs.01222 (2004).

84 Collins, A. T., Berry, P. A., Hyde, C., Stower, M. J. & Maitland, N. J. Prospective identification of tumorigenic prostate cancer stem cells. *Cancer research* **65**, 10946-10951, doi:10.1158/0008-5472.CAN-05-2018 (2005).

85 Geens, M. *et al.* The efficiency of magnetic-activated cell sorting and fluorescence-activated cell sorting in the decontamination of testicular cell suspensions in cancer patients. *Hum Reprod* **22**, 733-742, doi:10.1093/humrep/del418 (2007).

86 Fong, C. Y., Peh, G. S., Gauthaman, K. & Bongso, A. Separation of SSEA-4 and TRA-1-60 labelled undifferentiated human embryonic stem cells from a heterogeneous cell population using magnetic-activated cell sorting (MACS) and fluorescence-activated cell sorting (FACS). *Stem Cell Rev* **5**, 72-80, doi:10.1007/s12015-009-9054-4 (2009).

87 Schmitz, B. *et al.* Magnetic activated cell sorting (MACS)--a new immunomagnetic method for megakaryocytic cell isolation: comparison of different separation techniques. *Eur J Haematol* **52**, 267-275 (1994).

88 Handgretinger, R. *et al.* Isolation and transplantation of autologous peripheral CD34+ progenitor cells highly purified by magnetic-activated cell sorting. *Bone Marrow Transplant* **21**, 987-993, doi:10.1038/sj.bmt.1701228 (1998).

89 Schumm, M. *et al.* Isolation of highly purified autologous and allogeneic peripheral CD34+ cells using the CliniMACS device. *J Hematother* **8**, 209-218, doi:10.1089/106161299320488 (1999).

90 Lang, P. *et al.* Clinical scale isolation of highly purified peripheral CD34+progenitors for autologous and allogeneic transplantation in children. *Bone Marrow Transplant* **24**, 583-589, doi:10.1038/sj.bmt.1701961 (1999).

91 Stanciu, L. A., Shute, J., Holgate, S. T. & Djukanovic, R. Production of IL-8 and IL-4 by positively and negatively selected CD4+ and CD8+ human T cells following a four-step cell separation method including magnetic cell sorting (MACS). *J Immunol Methods* **189**, 107-115 (1996).

92 Servida, F. *et al.* Functional and morphological characterization of immunomagnetically selected CD34+ hematopoietic progenitor cells. *Stem Cells* **14**, 430-438, doi:10.1002/stem.140430 (1996).

93 Zahler, S. *et al.* The function of neutrophils isolated by a magnetic antibody cell separation technique is not altered in comparison to a density gradient centrifugation method. *J Immunol Methods* **200**, 173-179 (1997).

94 in *Cell Separation Media: Methodology and Applications* (GE Healthcare Bio-Sciences AB, Uppsala, Sweden, 1985).

95 Holter, H. & Moller, K. M. A substance for aqueous density gradients. *Exp Cell Res* **15**, 631-632 (1958).

96 Pertoft, H., Laurent, T. C., Laas, T. & Kagedal, L. Density gradients prepared from colloidal silica particles coated by polyvinylpyrrolidone (Percoll). *Anal Biochem* **88**, 271-282 (1978).

97 Rickwood, D. & Birnie, G. D. Metrizamide, a new density-gradient medium. *FEBS Lett* **50**, 102-110 (1975).

98 Rickwood, D., Ford, T. & Graham, J. Nycodenz: a new nonionic iodinated gradient medium. *Anal Biochem* **123**, 23-31 (1982).

99 Ford, T., Graham, J. & Rickwood, D. Iodixanol: a nonionic iso-osmotic centrifugation medium for the formation of self-generated gradients. *Anal Biochem* **220**, 360-366, doi:10.1006/abio.1994.1350 (1994).

100 Noble, P. B. & Cutts, J. H. Separation of blood leukocytes by Ficoll gradient. *Can Vet J* **8**, 110-111 (1967).

101 Noble, P. B., Cutts, J. H. & Carroll, K. K. Ficoll flotation for the separation of blood leukocyte types. *Blood* **31**, 66-73 (1968).

102 Parrish, J. J., Krogenaes, A. & Susko-Parrish, J. L. Effect of bovine sperm separation by either swim-up or Percoll method on success of in vitro fertilization and early embryonic development. *Theriogenology* **44**, 859-869 (1995).

103 Xu, C., Police, S., Rao, N. & Carpenter, M. K. Characterization and enrichment of cardiomyocytes derived from human embryonic stem cells. *Circ Res* **91**, 501-508 (2002).

104 Gartner, I. Separation of human eosinophils in density gradients of polyvinylpyrrolidone-coated silica gel (Percoll). *Immunology* **40**, 133-136 (1980).

105 Gmelig-Meyling, F. & Waldmann, T. A. Separation of human blood monocytes and lymphocytes on a continuous Percoll gradient. *J Immunol Methods* **33**, 1-9 (1980).

106 Kurnick, J. T. *et al.* A rapid method for the separation of functional lymphoid cell populations of human and animal origin on PVP-silica (Percoll) density gradients. *Scand J Immunol* **10**, 563-573 (1979).

107 Zuk, P. A. *et al.* Human adipose tissue is a source of multipotent stem cells. *Mol Biol Cell* **13**, 4279-4295, doi:10.1091/mbc.E02-02-0105 (2002).

108 Zuk, P. A. *et al.* Multilineage cells from human adipose tissue: Implications for cell-based therapies. *Tissue engineering* **7**, 211-228, doi:Doi 10.1089/107632701300062859 (2001).

109 Li, H. *et al.* Adipogenic potential of adipose stem cell subpopulations. *Plast Reconstr Surg* **128**, 663-672, doi:10.1097/PRS.0b013e318221db33 (2011).

110 Diekman, B. O., Rowland, C. R., Lennon, D. P., Caplan, A. I. & Guilak, F. Chondrogenesis of adult stem cells from adipose tissue and bone marrow: induction by growth factors and cartilage-derived matrix. *Tissue engineering. Part A* **16**, 523-533, doi:10.1089/ten.TEA.2009.0398 (2010).

111 Mizuno, H. *et al.* Myogenic differentiation by human processed lipoaspirate cells. *Plast Reconstr Surg* **109**, 199-209; discussion 210-191 (2002).

112 Halvorsen, Y. D. *et al.* Extracellular matrix mineralization and osteoblast gene expression by human adipose tissue-derived stromal cells. *Tissue engineering* **7**, 729-741, doi:10.1089/107632701753337681 (2001).

113 Melief, S. M., Zwaginga, J. J., Fibbe, W. E. & Roelofs, H. Adipose tissue-derived multipotent stromal cells have a higher immunomodulatory capacity than their bone marrow-derived counterparts. *Stem Cells Transl Med* **2**, 455-463, doi:10.5966/sctm.2012-0184 (2013).

114 Bourin, P. *et al.* Stromal cells from the adipose tissue-derived stromal vascular fraction and culture expanded adipose tissue-derived stromal/stem cells: a joint statement of the International Federation for Adipose Therapeutics and Science

(IFATS) and the International Society for Cellular Therapy (ISCT). *Cytotherapy* **15**, 641-648, doi:10.1016/j.jcyt.2013.02.006 (2013).

115 Suga, H. *et al.* Numerical measurement of viable and nonviable adipocytes and other cellular components in aspirated fat tissue. *Plastic and Reconstructive Surgery* **122**, 103-113, doi:10.1097/PRS.0b013e31817742ed (2008).

116 Pittenger, M. F. *et al.* Multilineage potential of adult human mesenchymal stem cells. *Science* **284**, 143-147, doi:DOI 10.1126/science.284.5411.143 (1999).

117 in *2017 Plastic Surgery Statistics Report* (ed American Society of Plastic Surgeons) (2017).

118 Estes, B. T., Diekman, B. O., Gimble, J. M. & Guilak, F. Isolation of adipose-derived stem cells and their induction to a chondrogenic phenotype. *Nat Protoc* **5**, 1294-1311, doi:10.1038/nprot.2010.81 (2010).

119 Safwani, W. K. Z. W., Makpol, S., Sathapan, S. & Chua, K. H. The changes of stemness biomarkers expression in human adipose-derived stem cells during long-term manipulation. *Biotechnol Appl Bioc* **58**, 261-270, doi:10.1002/bab.38 (2011).

120 Izadpanah, R. *et al.* Long-term in vitro expansion alters the biology of adult mesenchymal stem cells. *Cancer research* **68**, 4229-4238, doi:10.1158/0008-5472.Can-07-5272 (2008).

121 Zhao, Y. M., Waldman, S. D. & Flynn, L. E. The Effect of Serial Passaging on the Proliferation and Differentiation of Bovine Adipose-Derived Stem Cells. *Cells Tissues Organs* **195**, 414-427, doi:10.1159/000329254 (2012).

122 Mitchell, J. B. *et al.* Immunophenotype of human adipose-derived cells: temporal changes in stromal-associated and stem cell-associated markers. *Stem Cells* **24**, 376-385, doi:10.1634/stemcells.2005-0234 (2006).

Chapter 2

Considerations for high-yield, high-throughput cell enrichment: fluorescence versus magnetic sorting

Bryan A. Sutermaster, M.S. and Eric M. Darling, Ph.D.

Sutermaster, B.A. and Darling, E.M. *Scientific Reports* XX (2018) Article Number: XXXX

2.1 Abstract

Efficient sorting methods are required for the isolation of cellular subpopulations in basic science and translational applications. Despite this, throughputs, yields, viabilities, and processing times of common sorting methods like fluorescence-activated cell sorting (FACS) and magnetic-activated cell sorting (MACS) are underreported. In the current study, we set out to quantify the ability of these sorting methods to separate defined mixtures of alkaline phosphatase liver/bone/kidney (ALPL)-expressing and non-expressing cell types. Results showed that initial MACS runs performed using manufacturer's recommended antibody and microbead concentrations produced inaccurate ALPL+ vs. ALPL- cell splits compared to FACS when ALPL+ cells were present in larger proportions (>~25%). Accuracy at all proportions could be achieved by using substantially higher concentrations of labeling reagents. Importantly, MACS sorts resulted in only 7-9% cell loss compared to ~70% cell loss for FACS. Additionally, MACS processing was 4-6 times faster than FACS for low proportion samples but took

similar time for high-proportion samples. Average cell viability for all groups remained high (>83%), regardless of sorting method. Despite requiring substantial optimization, the ability of MACS to isolate increased cell numbers in less time than FACS may prove valuable in both basic science and translational, cell-based applications.

2.2 Introduction

Cell sorting, enrichment, and purification methods are powerful tools enabling the isolation of cellular subpopulations for basic science and clinical applications. The stromal vascular fraction (SVF), or vascular-associated cellular component, of lipoaspirate has been identified as an attractive cell source for both basic science and translational study as it contains subpopulations of adipose-derived stem cells (ASCs) and other progenitors.[1,2] Compared to other stem cell niches like bone marrow and muscle, adipose tissue contains higher percentages of differentiable cells, and can be isolated with ease and little donor site morbidity.[3] As the SVF is comprised of a heterogeneous cell population, *in vitro* plating/expansion or cell separation techniques are required to isolate ASCs from non-stem cell types.[4-6] Plating and expansion is a time consuming process not compatible with single-surgery procedures. More rapid cell separation techniques are needed for time-sensitive applications.

Subpopulations of ASCs and other progenitors can be fluorescently tagged based on biochemical markers and subsequently isolated from other cell types in the SVF by cell sorting techniques.[7-12] The gold standard for cell separation is fluorescence-activated cell sorting (FACS). While FACS is capable of processing millions of cells and isolating multiple, high purity subpopulations, it is also relatively time consuming for very large

cell numbers and requires expensive machinery. A related technology, magnetic-activated cell sorting (MACS), relies on direct (primary antibody-conjugated microbead) or indirect (primary antibody plus secondary antibody-conjugated microbead) magnetic labeling of cells prior to separation in a magnetic field.[13] MACS is also used to select for cell populations using surface markers but is less time consuming and requires less expensive equipment than FACS. However, it lacks the sensitivity and cell-specific data provided by a fluorescence-based system and is not easily compatible with multiple-marker profiles. Surprisingly, measures of cell throughput and yield, viabilities, and processing time between FACS and MACS are largely unreported, making it difficult to compare the practicality of the two techniques for a given application.

Cell separation techniques for ASCs often employ multiple surface markers to specifically define the cell type, as a single, definitive marker has yet to be identified.[14,15] A general ASC definition proposed by the International Federation of Adipose Therapeutics and Science (IFATS) includes positive/negative expression for four surface markers (CD34+/CD31-/CD45-/CD235a-), with an additional four markers for increased specificity (CD13, CD73, CD90, and CD105).[15] These restrictive definitions result in very small numbers of enriched, yet still heterogeneous, cells such that the population input to FACS must be extremely large to acquire therapeutically relevant numbers ($\sim 10^6$-10^8) as output.[16-22] Less restrictive surface marker profiles may enable isolation of larger cell populations and prove advantageous for regenerative medicine applications. One such marker, alkaline phosphatase liver/bone/kidney (ALPL), is a membrane bound protein involved in early matrix mineralization during osteogenesis and may be a useful target for identifying stem cell subpopulations, particularly for end applications of bone

regeneration.[23-28] Previously, groups have isolated subpopulations of induced pluripotent stem cells and jaw periosteal cells based on ALPL expression that were capable of increased osteogenesis, though this has not yet been demonstrated with primary SVF cells.[29,30]

The objective of this study was to quantify the processing times, cell yields and viabilities of MACS and FACS separations using defined mixtures of osteogenically primed SVF cells and A375 human melanoma cells based on their expression of ALPL. To accomplish this, primary SVF cells were first expanded and osteogenically stimulated to upregulate expression of the ALPL marker in responsive cell types. After priming, SVF cells were mixed in defined ratios with A375 cells (0:1, 1:3, 1:1, 3:1, 1:0) and separated based on ALPL expression using FACS or MACS. Processing time and cell throughput, yield, and viability for ALPL+ and ALPL- groups were quantified and compared between the two sorting methods. Effort was made to identify and reconcile discrepancies between the two approaches to better inform researchers using these techniques for cell enrichment/purification studies.

2.3 Materials and Methods

2.3.1 SVF Isolation and Culture

For all FACS and MACS sorts, freshly thawed, passage 0 (P0) SVF cells were maintained in expansion medium with medium changes every other day until > 90% confluent in T182 tissue culture flasks (Genesee Scientific, San Diego, CA). Expansion medium maintained cells in a proliferative, multipotent state and consisted of Dulbecco's modified Eagle's medium: nutrient mixture F-12 (DMEM-F12) (GE Healthcare

HyClone, Pittsburgh, PA), 10% fetal bovine serum (FBS, ZenBio, Research Triangle Park, NC), 5 ng/mL epidermal growth factor, 1 ng/mL fibroblast growth factor, 0.25 ng/mL transforming growth factor-β1 (R&D Systems, Minneapolis, MN), and 1X antibiotic/antimycotic (anti/anti, GE Healthcare HyClone).[31] Once at near confluence, cells were primed with osteogenic medium for four days prior to sorting procedures. Osteogenic medium consisted of DMEM with high glucose (DMEM-hg, GE Healthcare HyClone), 10% FBS (ZenBio), 10 mM β-glycerophosphate, 150 μM ascorbate-2-phosphate, 10 nM dexamethasone, 9.1 nM vitamin-D3 (Sigma-Aldrich, St. Louis, MO), and 1X anti/anti (GE Healthcare HyClone). Concurrently, freshly thawed A375 human melanoma cells were maintained in growth medium, with medium changes every other day for twelve days prior to sorting procedures. A375 growth medium consisted of DMEM-F12 (GE Healthcare HyClone) with 10% FBS (ZenBio) and 1X anti/anti (GE Healthcare HyClone).

2.3.2 Fluorescence-Activated Cell Sorting (FACS)

Four-day, osteogenically primed, P0, ALPL+ SVF cells and ALPL- A375 cells were detached from flasks using Accutase cell detachment solution (Corning Life Sciences, Tewksbury, MA) and filtered through 40 μm cell strainers (Fisher Scientific, Hampton, NH). Viability and cell numbers were determined using a trypan blue exclusion method. 8 x 10^6 cell mixtures were made according to the following ALPL+:ALPL- cell ratios: 0:1, 1:3, 1:1, 3:1, and 1:0. Cell mixtures were pelleted, and resuspended in 110 μL of 1:11 dilutions of anti-ALPL-allophycocyanin (APC) stock antibody solution for 10 min at 4°C, according to manufacturer's protocol (Clone: W8B2,

Catalogue Number: 130-093-589, Miltenyi Biotec GmbH, Bergisch Gladbach, Germany). After labeling, cells were maintained on ice until sorted.

To lessen the impact of user variability, a single, expert operator with over 20 years of fluorescence sorting experience performed all FACS sorts using a stream-in-air BD Influx cell sorter fitted with a 100 μm nozzle and 488 nm trigger and 633 nm fluorescence excitation lasers (Becton Dickinson, Franklin Lakes, NJ). Sorts were performed using a 20.1 psi driving pressure and a droplet frequency of 38.15 kHz. Though droplet delay was set independently for each sort, a typical value from a representative experiment was 28.9967 ms (1/droplet frequency). FSC and SSC gates and laser gains were established using two, 8 x 10^6 cell, unlabeled (A375 and osteo-primed SVF, respectively) and two, 8 x 10^6 cell, anti-ALPL-APC-labeled (A375 and osteo-primed SVF, respectively) samples in 500 μL autoMACS rinsing solution (Miltenyi Biotec) with 0.5% BSA (Sigma-Aldrich, St. Louis, MO) after filtering through 40 μm cell strainers. Subsequently, 8 x 10^6 ALPL+:ALPL- cell mixtures of the ratios described above were passed through 40 μm cell strainers and sorted into ALPL+ and ALPL- fractions. 50 mL conical collection tubes (Genesee Scientific) containing 5 mL of cold, DMEM-hg base medium were used to preserve post-sort viability. After sorting, cells were maintained on ice until counted. Total cell yields were defined as the sum of live and dead cells counted at the output. Output fractions were calculated for both ALPL+ and ALPL- subpopulations by dividing the post-sort total cell count for each subpopulation by the sum of ALPL+ and ALPL- post-sort total cell counts. Viability was defined as the number of live output cells divided by the sum of live and dead output

cells, multiplied by 100. Each five-condition run (0:1, 1:3, 1:1, 3:1, 1:0) was repeated three times.

2.3.3 Magnetic-Activated Cell Sorting (MACS) (Manufacturer's Protocol)

For experimental sorting runs, four-day, osteogenically primed, P0, ALPL+ SVF and ALPL- A375 cells were uplifted, filtered, and combined into mixtures of defined ratios as described above. Four unlabeled and anti-ALPL-APC-labeled control conditions were prepared as described previously. The remaining 8 x 10^6 cell experimental conditions (0:1, 1:3, 1:1, 3:1, and 1:0 ALPL+:ALPL-) were antibody-labeled as previously described, pelleted, and subsequently labeled with 100 µL of 1:5 dilution, anti-APC microbeads (Catalogue Number: 130-090-855, Miltenyi Biotec) for 15 minutes at 4°C. Each 8 x 10^6 antibody- and microbead-labeled condition was magnetically sorted at room temperature using "MS" columns, inserted into a Miltenyi OctoMACS separator (Catalogue Numbers: 130-042-201 and 130-042-109, respectively, Miltenyi Biotec). Post-sort retained and flow-through fractions from each experimental condition were counted, and viabilities determined as described previously. After sorting, cells were maintained on ice until counted. Output fractions, retained and flow-through yield, and viability were calculated as described above. After counting, all retained and flow-through fractions for each experimental condition were further analyzed by flow cytometry to quantify the distribution of ALPL+ and ALPL- cells within each fraction/condition. FSC and SSC gates and laser gains were established using the four, labeled and unlabeled control conditions, as described previously. Each five-condition run (0:1, 1:3, 1:1, 3:1, 1:0) was repeated three times.

2.3.4 Magnetic-Activated Cell Sorting Optimization

Optimization experiments were performed to reconcile discrepancies between MACS-isolated retained and flow-through fractions and the defined ALPL+ and ALPL- cell splits. Antibody and microbead labeling concentrations were varied to determine their effect on retained and flow-through output fractions and percent cell yield using only fixed, ALPL+ SVF cells. Primary SVF cells were expanded and osteogenically primed as described previously. After four days of priming, cells were detached from flasks using Accutase, pelleted, and fixed in suspension for 15 min in 10% formalin phosphate (Fisher Scientific) at room temperature. To determine the influence of microbead concentration, five aliquots of 8 x 10^6 fixed, ALPL+ SVF cells were labeled with 1:11 antibody dilutions, followed by 1:16, 1:8, 1:5, 1:2, or pure anti-APC microbead solutions prior to magnetic sorting using MS columns fitted with 70 μm filters (Miltenyi Biotec). Similarly, to determine the influence of antibody concentration, four aliquots of 8 x 10^6 fixed, ALPL+ SVF cells were labeled with 1:11, 1:7.5, 1:5, or 1:2.5 anti-ALP-APC antibody dilutions prior to labeling with 1:5 microbead dilutions and MACS processing using MS columns fitted with 70 μm filters. Finally, to examine the effect of simultaneously varying antibody and microbead concentration, two 8 x 10^6 ALPL+ SVF aliquots were labeled with 1:2.5 antibody dilutions followed by a 1:5 dilution or pure microbead solution and processed by MACS using MS columns fitted with 70 μm filters. Following all magnetic sorts, cells were counted and calculations made for retained and flow-through output fractions and percent cell yield. Post-sort retained and flow-through fractions of antibody-varied and simultaneous antibody- and microbead-varied trials were

further analyzed by flow cytometry to determine distributions of ALPL+ and ALPL- cells within each sample.

2.3.5 Magnetic-Activated Cell Sorting (MACS) (Optimized Protocol)

Three separate, five-condition (0:1, 1:3, 1:1, 3:1, 1:0 ALPL+:ALPL-) runs were performed as described previously but with increased antibody and microbead labeling concentrations. For optimized MACS protocol runs, cells were labeled with 110 µL of a 1:2.5 dilution of anti-ALPL-APC antibodies for 10 min at 4°C, followed by 100 µL of undiluted anti-APC microbeads for 15 min at 4°C. All post-sort counting, viability, and flow cytometric assessment was performed as described previously.

2.3.6 Statistical Analysis

For MACS optimization, correlations between retained output fractions and either antibody or microbead dilution were determined by calculating Pearson's r values on log-transformed data. For FACS and manufacturer's and optimized protocol MACS, comparisons of total, live, and dead cell yields were made using a Kruskal-Wallis one-way analysis of variance (ANOVA) on ranks (factor: sorting method, $p < 0.05$). Comparisons of average viability for all ratio conditions were made using a Kruskal-Wallis one-way ANOVA on ranks (factor: sorting method, $p < 0.05$) to determine statistical differences between FACS ($n = 25$), manufacturer's protocol MACS ($n = 27$), and optimized MACS ($n = 27$).

2.4 Results

2.4.1 MACS Optimization

Manufacturer's protocol MACS runs displayed major differences in retained and flow-through output fractions compared to FACS-separated ALPL+ and ALPL- fractions (**Figure 2-1**). To determine whether antibody and microbead concentrations specified by the manufacturer's MACS protocol was responsible for the observed differences, MACS antibody- and microbead- treatment concentrations were varied in a series of optimization trials to determine their effect on isolation of fixed, ALPL+ SVF cells. Data showed that when antibody labeling concentration was held constant (1:11) and microbead concentration varied (1:16, 1:8, 1:5, 1:2, and no dilution), a very strong positive correlation existed between microbead concentration and retained cell yields for MACS optimization tests (**Figure 2-2a**, $r = 0.95$). Similarly, in MACS optimization runs performed with varied antibody concentrations (1:11, 1:7.5, 1:5, and 1:2.5) and fixed microbead concentration (1:5), a very strong positive correlation existed between antibody concentration and retained fraction yields (**Figure 2-2b**, $r = 0.99$). Regardless of antibody concentration, flow cytometric analysis showed that the retained and flow-through fractions all exhibited high fluorescence and large overlaps in their fluorescence histograms (**Figure 2-2c**). This overlap suggested manufacturer's protocol MACS-isolated flow-through subpopulations were comprised largely of false-negatives. To address this complication, MACS optimization runs were performed with high antibody concentration (1:2.5) coupled with high microbead concentration (1:5 or no dilution). When performing MACS with these increased antibody and microbead concentrations,

false-negative rates were minimized as evidenced by low flow-through cell percentages and little fluorescence overlap between retained and flow-through fractions (**Figure 2-3**).

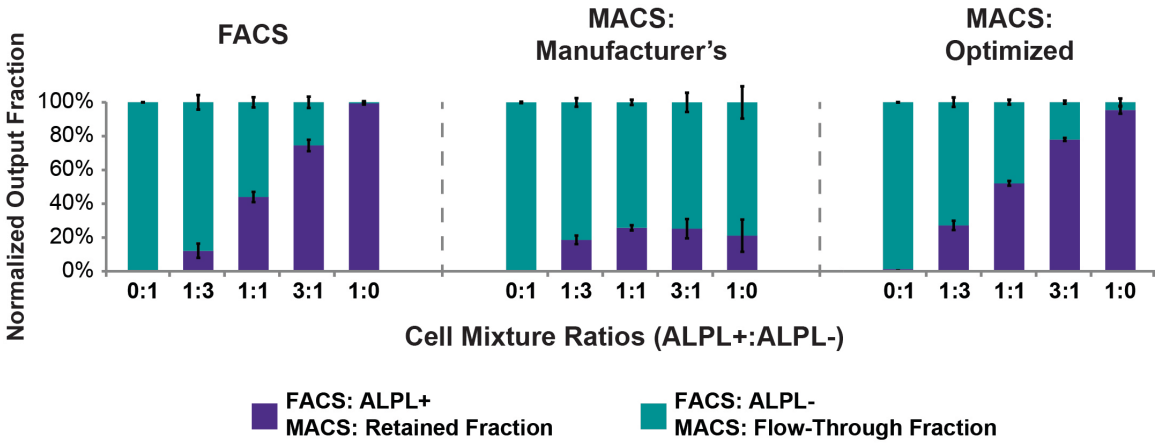

Figure 2-1. Normalized output fraction of osteogenically primed SVF and A375 controlled-ratio sorts using FACS, manufacturer's protocol MACS, and optimized protocol MACS. Defined mixtures of osteogenically primed SVF and A375 cells were labeled with anti-ALPL-APC antibodies (and anti-APC microbeads for MACS) prior to cell sorting. After separation, ALPL+/retained and ALPL-/flow-through fractions were counted and normalized output fractions computed. For ALPL+:ALPL- cell ratios > 1:3, manufacturer's protocol MACS sorts were not able to accurately separate ALPL+ and ALPL- cells. Error bars indicate standard deviation.

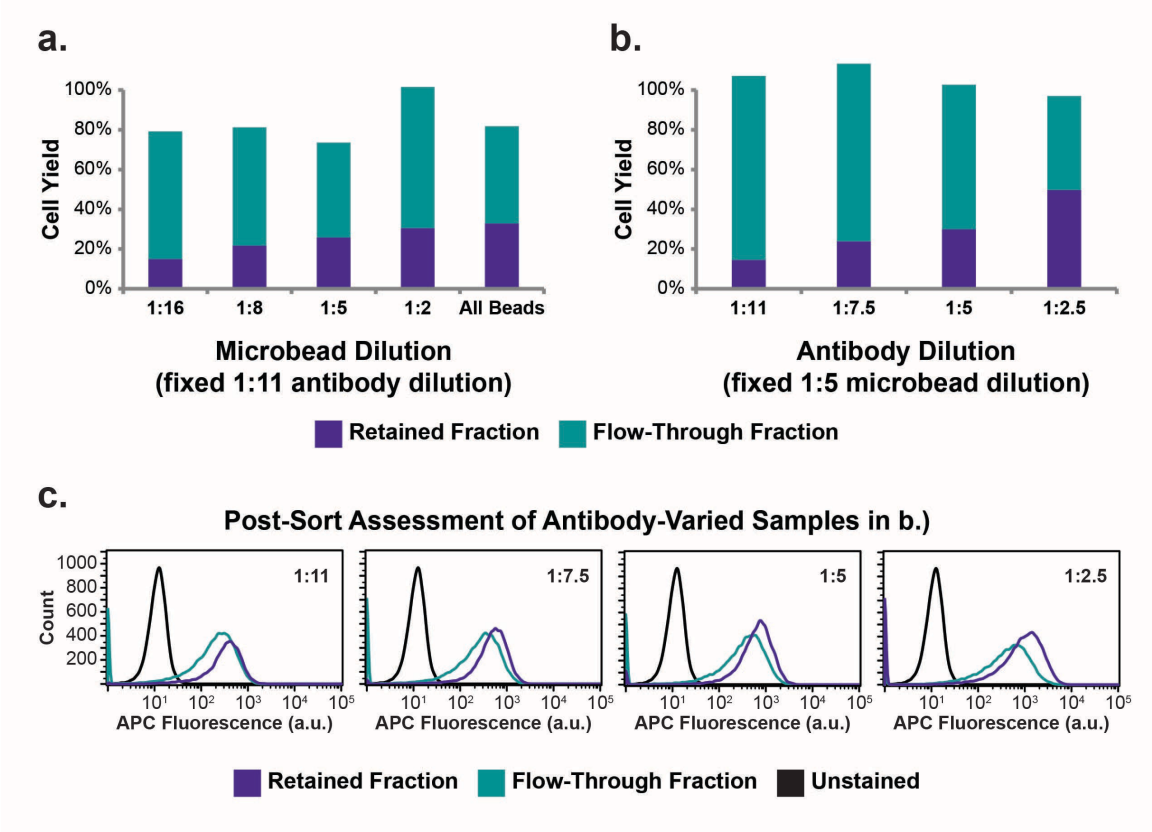

Figure 2-2. Cell yield and fraction analyses for MACS optimization trials of varying antibody and microbead concentrations. MACS cell yields of retained and flow-through fractions for pure ALPL+ optimization sorts when a) microbead dilution was varied with a fixed (1:11) antibody dilution and b) antibody dilution was varied with a fixed (1:5) microbead dilution. c) Distributions of ALPL+ cells within retained and flow-through fractions of antibody-varied trials displayed in b) were assessed via flow cytometry and confirmed a high false-negative rate in flow-through fractions. (APC fluorescence corresponds to APC dye on anti-ALPL antibody).

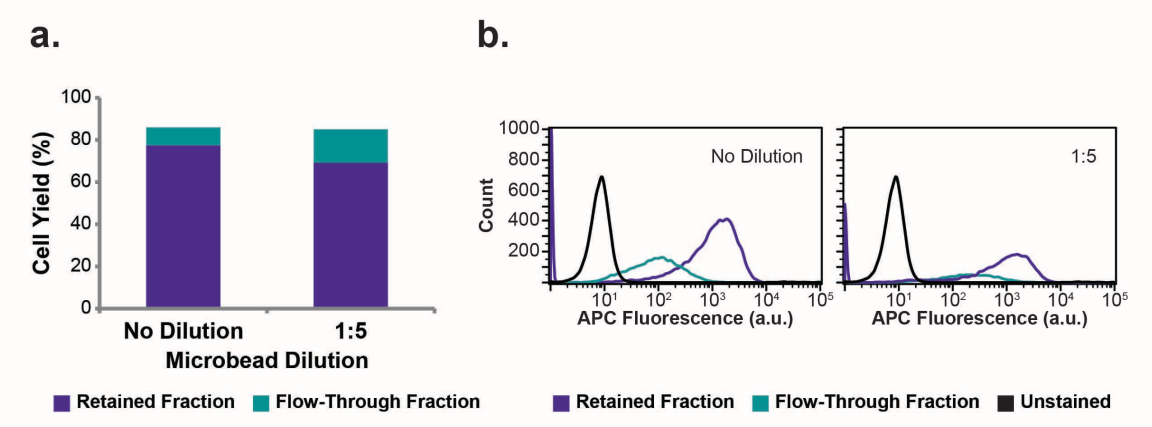

Figure 2-3. Cell yield and flow cytometric analysis for high concentration antibody and microbead MACS optimization trials. Fixed SVF cells were labeled with 1:2.5 antibody dilutions prior to 1:5 or no dilution microbead labeling and then magnetically sorted. Retained and flow-through fractions were counted and percent cell yields calculated prior to flow cytometric analysis. a) Percent cell yields, b) flow cytometry fluorescence histograms of post-sort fractions (APC fluorescence corresponds to APC dye on anti-ALPL antibody).

A complete set of MACS runs was performed using the optimized antibody (1:2.5 dilution) and microbead (no dilution) concentrations. Retained and flow-through fractions collected with the optimized protocol mirrored both the ALPL+/ALPL- fractions observed with FACS, and the defined input fractions (**Figure 2-1**). Flow cytometry of the retained and flow-through fractions indicated low fluorescence overlap, and thus accurate ALPL+/ALPL- subpopulation separation, compared to results using the manufacturer's MACS protocol (**Figure 2-4**).

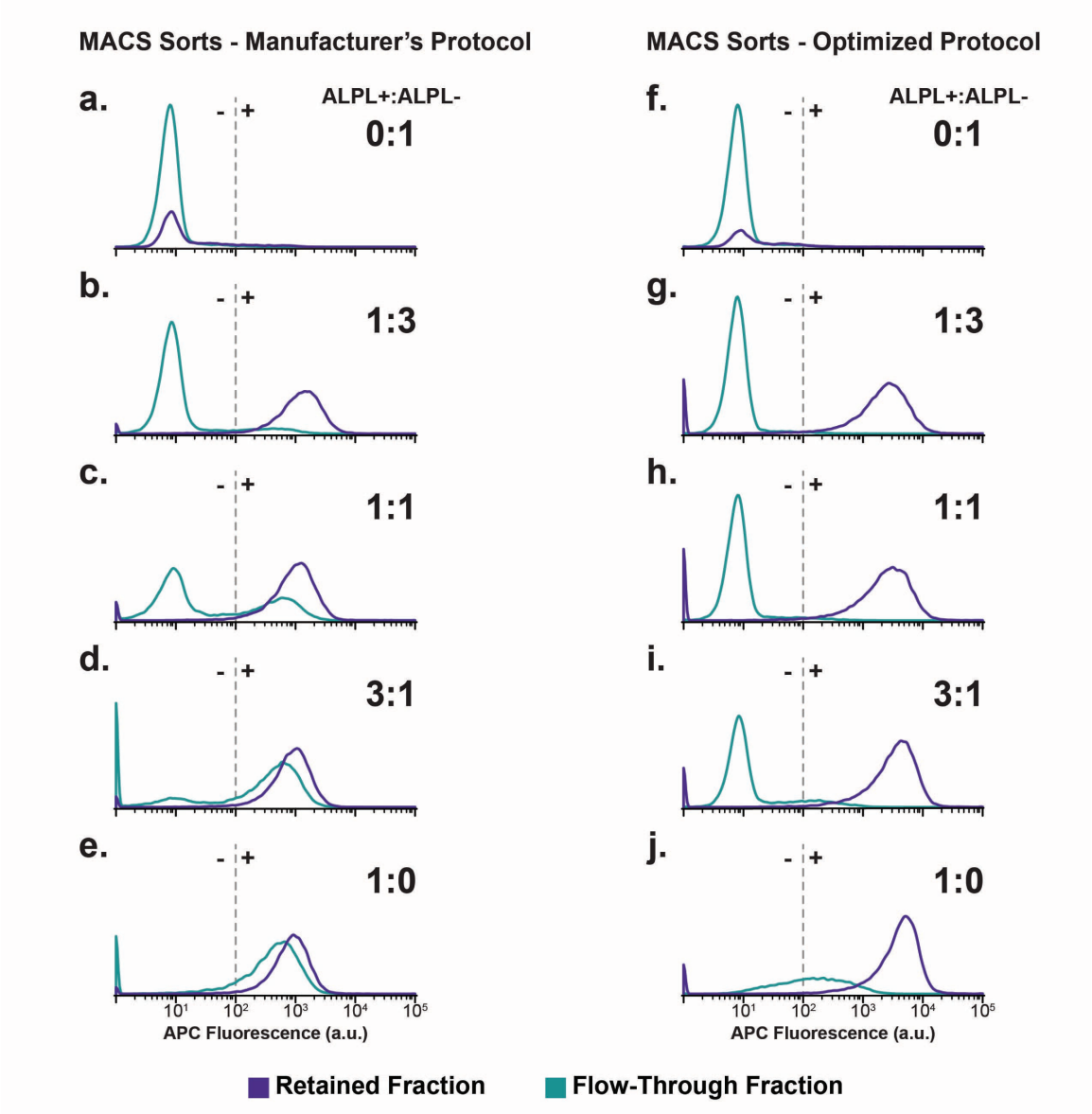

Figure 2-4. Post-MACS flow cytometric analysis of retained and flow-through fractions isolated using either manufacturer's or optimized protocols. After MACS separation of defined mixtures of ALPL+ and ALPL- cells (0:1, 1:3, 1:1, 3:1, 1:0) according to manufacturer's (a-e) or optimized protocols (f-j), post-sort subpopulations were assessed by flow cytometry. For input populations larger than 1:3, manufacturer's protocol sorts exhibited large false-negative rates.

2.4.2 Cell Yield, Viability, and Sorting Time for Sorting Experiments

The effectiveness of a cell sorting procedure depends substantially on the number of viable cells it can process. Comparisons were made between FACS and manufacturer's and optimized protocol MACS approaches, with special focus on cell yields (total, live, and dead) and viability. On average, FACS produced low total and live cell yields (**Figure 2-5a**). Comparatively, manufacturer's and optimized protocol MACS produced high cell yields, exhibiting only 10% and 14% of total FACS cell loss (**Figure 2-5a**). Dead cell yields were universally low (**Figure 2-5a**). Likewise, average cell viability was universally high among sorting methods, though both manufacturer's and optimized protocol MACS exhibited slightly higher viability than FACS ($p < 0.0001$ and $p<0.002$, respectively, **Figure 2-5b**). As a practical parameter, individual FACS procedures took 20-30 minutes, while individual manufacturer's protocol MACS procedures took approximately 5 minutes. Individual optimized protocol MACS sorting times scaled with increasing ALPL+:ALPL- input ratios, such that small ratios (0:1 and 1:3) took ~5 minutes while large ratios (3:1 and 1:0) took ~30 minutes to complete.

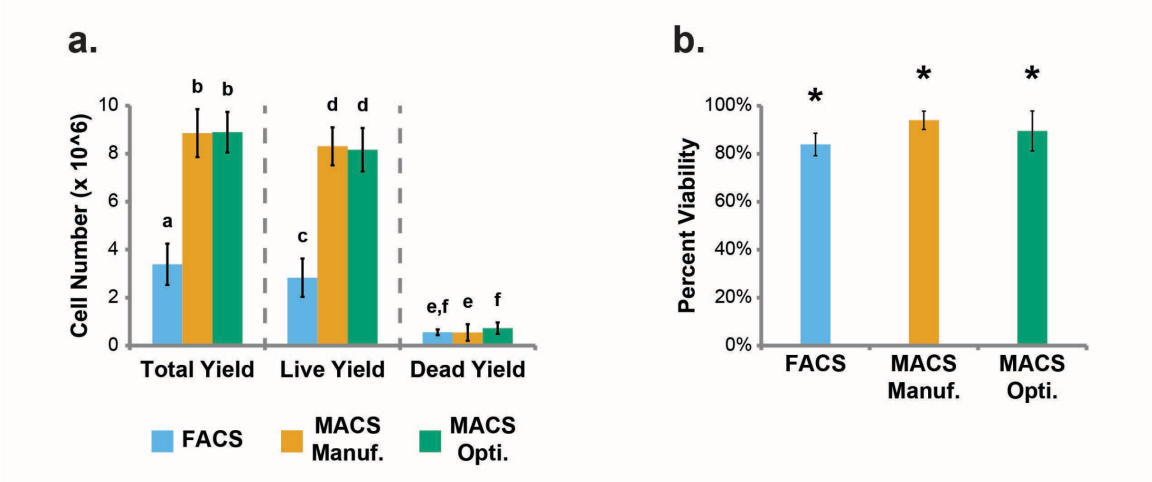

Figure 2-5. Total, live, and dead cell yields and post-sort viabilities for FACS, manufacturer's protocol MACS, and optimized protocol MACS sorts. Post-sort a) total, live, and dead cell yields and b) viabilities for FACS and manufacturer's and optimized protocol MACS (a. Unlike letters within total, live, and dead yield sections indicate statistical difference, $p < 0.05$; b. * Indicates significant difference in viability among sorting methods, $p < 0.05$). Error bars indicate standard deviation. Average live cell input cell number: $8x10^6$ for all sorting methods. Average total cell input number: $10.7\pm1.4x10^6$ for FACS, $9.5\pm0.8x10^6$ for manufacturer's protocol MACS, and $9.8\pm0.3x10^6$ for optimized protocol MACS.

2.5 Discussion

The overarching goal of this study was to enable researchers to make informed decisions about cell sorting methods by quantifying important, vastly underreported sorting parameters including cell throughputs, yields, and viabilities of FACS and MACS procedures. To do this we created a series of defined mixtures of osteogenically primed SVF (ALPL+) and A375 human melanoma (ALPL-) cells and separated them using FACS and MACS. We hypothesized that MACS would enable faster isolation of larger numbers of highly viable cells compared to FACS. Indeed, we found that manufacturer's protocol MACS sorts were considerably faster and lost fewer cells than FACS but were unable to accurately separate ALPL+ from ALPL- subpopulations. Optimization necessitated substantially increased MACS antibody and microbead labeling

concentrations, thereby enabling accurate separation of ALPL+ and ALPL- subpopulations, albeit at a higher cost-per-sort. Optimized protocol MACS procedures were completed 0-6 times faster than FACS per sort, with larger ALPL+:ALPL- mixtures taking progressively longer than smaller ratio mixtures.

While FACS runs confirmed our preconceptions of fluorescence-based sorting (i.e., high purity, low throughput and yield), comparative manufacturer's protocol MACS runs yielded contradictory results as flow-through fractions exhibited high false-negative rates.. Though manufacturer's protocol MACS provided a higher percent total cell yield (93% ± 8% versus 32% ± 11%, $p<0.0001$) and percent live cell yield (104% ± 10% versus 35% ± 10%, $p<0.0001$), its retained- and flow-through-normalized output fractions diverged from the defined input values for the higher, osteo-primed SVF:A375 ratios (1:1, 3:1, and 1:0, **Figure 2-1**). The larger than anticipated flow-through normalized output fractions suggested that manufacturer's protocol MACS-isolated flow-through groups were primarily composed of false-negative cells. These suspicions were confirmed upon flow cytometric analysis of the retained (nominally "ALPL+") and flow-through (nominally "ALPL-") fractions. The fluorescence histograms for these fractions exhibited overlapping, high fluorescence values, indicating inadequate separation of highly fluorescent, ALPL+ and non-fluorescent, ALPL- cells. These results are consistent with a previous study, which demonstrated high (16%-35%) false-negative rates with manufacturer's protocol MACS separations.[32] Our subsequent hypothesis was that the manufacturer-recommended MACS protocol provided insufficient antibodies and/or microbeads to sufficiently label a highly expressed surface protein like ALPL across large numbers of cells. Insufficient amounts of antibody could result in too few surface

ALPL proteins being antibody-labeled, thereby limiting the potential binding partners for magnetic microbeads that are required to hold cells in the MACS column. Similarly, insufficient numbers of microbeads could result in incomplete saturation of available antibody-labeled ALPL surface proteins, preventing cells from being retained in the column.

To determine whether the manufacturer's protocol MACS antibody and microbead treatment concentrations were responsible for inaccurate separation of ALPL+ and ALPL- cells, , antibody and microbead concentrations were varied systematically prior to sorting in a series of optimization experiments on pure, fixed, ALPL+ SVF cells. Solely increasing antibody or microbead labeling concentration was insufficient to isolate the pure, ALPL+ input cell population. However, by coupling increased antibody concentration (1:2.5) with increased microbead concentration (1:5 or no dilution), percent-retained cell yield could be brought within 10% of the defined, ~100% input population. As such, we concluded that the manufacturer's protocol antibody and microbead concentrations were indeed insufficient to adequately label, and isolate high-proportion ALPL+ populations. We subsequently hypothesized these optimized MACS antibody and microbead labeling concentrations would enable accurate separation of ALPL+ SVF and ALPL- A375 cells, in contrast to the manufacturer's protocol.

Optimized protocol MACS sorts were performed on live cells using the higher antibody (1:2.5) and microbead (no dilution) concentrations, yielding retained and flow-through splits that more closely matched the defined input. Post-sort flow cytometric analysis indicated appropriate separation of ALPL+ and ALPL- fractions, as the fluorescence histograms of highly fluorescent retained (ALPL+) and lowly fluorescent

flow-through (ALPL-) fractions displayed minimal overlap. Compared to FACS, optimized protocol MACS experiments displayed higher percent total cell yield (91% ± 8% versus 32% ± 11%, $p<0.0001$) and live cell yield (102% ± 11% versus 35% ± 10%, $p<0.0001$). The discrepancies in cell loss between manufacturer's and optimized protocol MACS and FACS is likely due to the FSC and SSC (size and granularity) gating required by FACS. To ensure purity of the isolated subpopulations, FACS imposes strict size and granularity constraints on the assessed populations. As a result, multi-cell aggregates and debris are rejected during sorting, lowering yield but maintaining the purity of the output streams. MACS does not impose size and granularity constraints, thereby increasing yield at the potential expense of purity. Discrepancies in cell yield were not the only differences exhibited by FACS and MACS, however.

FACS sorts took considerably longer (~20-30 min per sort) to complete than MACS manufacturer's protocol sorts (~5 min per sort). Processing time for MACS optimized protocol sorts varied with the proportion of ALPL+ cells in the sample; quick for lower proportions and slow for higher proportions (~5-30 minutes per sort). This characteristically slower processing time for FACS is due to the single-cell assessment approach inherent in the technology. While FACS systems can use higher fluid (air or liquid) flow rates to increase the speed of cell sorting, it is still a relatively slow process compared to MACS, which is accomplished as a bulk separation. While relatively modest cell numbers were sorted in this study (8×10^6 cells), accurately separating larger, clinically relevant cell numbers with FACS would take progressively longer. Additionally, FACS sorts must be performed serially, while MACS sorts can be performed in parallel. As a result, the total time required for five, serial FACS sorts

(~1.7-2.5 hrs) vastly exceeded the time required for the five, parallel MACS sorts (~5 min for manufacturer's protocol, ~30 min for optimized protocol). Furthermore, the ready parallelization afforded by MACS allows for vast increases in input cell numbers without appreciable increases in sorting time.

Longer sorting times were required for optimized protocol MACS sorts with larger ALPL+:ALPL- sorting ratios. As cells proceed through the MACS column, magnetically labeled cells are sequestered, and the void volume of the column is effectively reduced, requiring unlabeled cells and fluid to take a slower, more circuitous path to the outlet. Thus, as ALPL+:ALPL- ratios increased so did the sorting times. This knowledge may be useful, especially when separating cells without prior knowledge of the number of positive cells in the population. By measuring the approximate sorting time, a researcher can get an estimate of the percentage of positive cells in the population. Additionally, sorting times for populations containing high percentages of positive cells could likely be reduced by diluting the population and simultaneously sorting through multiple MACS columns.

In addition to the anticipated differences in throughputs, yields , and sorting times, manufacturer's and optimized protocol MACS displayed slightly higher, post-sort viability compared to FACS (94% ± 4% and 90% ± 8% versus 84% ± 5%, $p<0.0001$ and $p=0.002$, respectively), consistent with published reports.[32,33] In FACS, the high fluid flow rates coupled with small nozzle diameters have the potential to reduce cellular viability due to high shear stresses.[34] Conversely, MACS is a gravity-driven process that does not impart high shear stresses, which should help maintain good viability. In both

sorting methods, keeping the cells on ice both pre- and post-sort better maintained viability as it effectively lowered the metabolic rate of the cells.

The current study used single, representative FACS and MACS systems to investigate the general performance of these technologies as measured by cell throughput, yield, and viability. That said, results will likely vary for different device operators and equipment choices (i.e., alternative cell sorter models or magnetic bead suppliers). In the current study, user-to-user variability and equipment differences were controlled for by having a single, experienced operator use equipment from a single manufacturer (BD Influx for FACS sorts, Miltenyi Biotec MACS beads and OctoMACS magnet for MACS sorts). While not conducted as part of the current study, we have completed similar FACS runs with different operators and cell sorters (BD FACS Aria and BioRad S3) for general comparison purposes. Minor variations existed, but the overall trends related to cell throughput, yield, and viability were conserved. Many different options exist for immunolabeled, magnetic cell sorting beads, like Dynabeads (Thermo Fisher) or EasySep (Stem Cell Technologies), but direct comparisons of the technologies are complicated by the proprietary nature of their characteristics (e.g., particle size, antibody density, magnetic moment, etc.). However, each of these technologies is likely to have similar limitations to Miltenyi's MACS system, necessitating a rigorous optimization as presented in the current study to ensure sorting accuracy regardless of magnetic bead supplier. As such, though the specific throughputs, yields, and sorting times of different FACS and MACS equipment will likely vary, the relative comparison between fluorescence- and magnetic-based sorting observed in the current study is expected to remain consistent.

In conclusion, we demonstrated that MACS performed according to optimized protocols enabled a more rapid, higher-yield, and higher-viability isolation of osteo-primed, ALPL+ SVF cells in our stem cell isolation model compared to FACS. As such, MACS may be the more attractive option when selecting for low-abundance cell populations or time-sensitive clinical samples intended for cell therapy applications. In fact, this has been demonstrated by clinical trials using magnetic bead-based, FDA-approved CliniMACS and ISOLEX 300i CD34+ cell isolation systems for treatment of leukemia and other hematologic diseases.[35-37] Moving forward, it will be important to study the impact that parallelized, high-throughput sorting may have in a broader range of clinical applications. Increasing the efficiency of cell separation will enable isolation of larger cell numbers in less time than current methods, an asset for both basic science and cell-based therapies.

2.6 Major Takeaways

- MACS processes cells more quickly and with greater yields than FACS.
- Selecting for highly abundant subpopulations with MACS requires substantially more antibodies and magnetic microbeads than recommended by manufacturer protocols.
- The occurrence of false-negatives in MACS, a commonly noted limitation, can be lessened by antibody/microbead optimization.

2.7 Acknowledgements

The authors would like to thank Mark Dooner and the flow cytometry core facility of Rhode Island Hospital for performing the FACS runs. Financial support for this work was provided by National Institutes of Health (R01 AR063642) and National Science Foundation (EAGER CBET 1547819 and CAREER CBET 1253189). The content of this article is solely the responsibility of the authors and does not necessarily represent the official views of the National Institutes of Health or National Science Foundation.

2.8 Author Contributions

BAS and EMD designed the study, performed data analyses, and prepared the manuscript. BAS conducted all experiments.

2.9 Additional Information

2.9.1 Competing Interests

The authors declare no competing interests.

2.10 References

1 Zuk, P. A. *et al.* Human adipose tissue is a source of multipotent stem cells. *Mol Biol Cell* **13**, 4279-4295, doi:10.1091/mbc.E02-02-0105 (2002).

2 Zuk, P. A. *et al.* Multilineage cells from human adipose tissue: Implications for cell-based therapies. *Tissue engineering* **7**, 211-228, doi:Doi 10.1089/107632701300062859 (2001).

3 Fraser, J. K., Wulur, I., Alfonso, Z. & Hedrick, M. H. Fat tissue: an underappreciated source of stem cells for biotechnology. *Trends Biotechnol* **24**, 150-154, doi:10.1016/j.tibtech.2006.01.010 (2006).

4 Bjorntorp, P. *et al.* Isolation and characterization of cells from rat adipose tissue developing into adipocytes. *J Lipid Res* **19**, 316-324 (1978).

5 Van, R. L., Bayliss, C. E. & Roncari, D. A. Cytological and enzymological characterization of adult human adipocyte precursors in culture. *J Clin Invest* **58**, 699-704, doi:10.1172/JCI108516 (1976).

6 Estes, B. T., Diekman, B. O., Gimble, J. M. & Guilak, F. Isolation of adipose-derived stem cells and their induction to a chondrogenic phenotype. *Nat Protoc* **5**, 1294-1311, doi:10.1038/nprot.2010.81 (2010).

7 Marble, H. D., Sutermaster, B. A., Kanthilal, M., Fonseca, V. C. & Darling, E. M. Gene expression-based enrichment of live cells from adipose tissue produces subpopulations with improved osteogenic potential. *Stem Cell Res Ther* **5**, 145, doi:10.1186/scrt502 (2014).

8 Chung, M. T. *et al.* CD90 (Thy-1)-positive selection enhances osteogenic capacity of human adipose-derived stromal cells. *Tissue engineering. Part A* **19**, 989-997, doi:10.1089/ten.TEA.2012.0370 (2013).

9 Zimmerlin, L. *et al.* Stromal vascular progenitors in adult human adipose tissue. *Cytometry A* **77**, 22-30, doi:10.1002/cyto.a.20813 (2010).

10 Kanthilal, M. & Darling, E. M. Characterization of mechanical and regenerative properties of human, adipose stromal cells. *Cell Mol Bioeng* **7**, 585-597, doi:10.1007/s12195-014-0350-y (2014).

11 Hager, G. *et al.* Three specific antigens to isolate endothelial progenitor cells from human liposuction material. *Cytotherapy* **15**, 1426-1435, doi:10.1016/j.jcyt.2013.06.018 (2013).

12 Zielins, E. R. *et al.* Enrichment of Adipose-Derived Stromal Cells for BMPR1A Facilitates Enhanced Adipogenesis. *Tissue engineering. Part A* **22**, 214-221, doi:10.1089/ten.TEA.2015.0278 (2016).

13 Miltenyi, S., Muller, W., Weichel, W. & Radbruch, A. High-Gradient Magnetic Cell-Separation with Macs. *Cytometry* **11**, 231-238, doi:DOI 10.1002/cyto.990110203 (1990).

14 Yoshimura, K. *et al.* Characterization of freshly isolated and cultured cells derived from the fatty and fluid portions of liposuction aspirates. *Journal of cellular physiology* **208**, 64-76, doi:10.1002/jcp.20636 (2006).

15 Bourin, P. *et al.* Stromal cells from the adipose tissue-derived stromal vascular fraction and culture expanded adipose tissue-derived stromal/stem cells: a joint statement of the International Federation for Adipose Therapeutics and Science

(IFATS) and the International Society for Cellular Therapy (ISCT). *Cytotherapy* **15**, 641-648, doi:10.1016/j.jcyt.2013.02.006 (2013).

16 Garcia-Olmo, D. *et al.* A phase I clinical trial of the treatment of Crohn's fistula by adipose mesenchymal stem cell transplantation. *Dis Colon Rectum* **48**, 1416-1423, doi:10.1007/s10350-005-0052-6 (2005).

17 Garcia-Olmo, D. *et al.* Autologous stem cell transplantation for treatment of rectovaginal fistula in perianal Crohn's disease: a new cell-based therapy. *Int J Colorectal Dis* **18**, 451-454, doi:10.1007/s00384-003-0490-3 (2003).

18 Garcia-Olmo, D. *et al.* Expanded adipose-derived stem cells for the treatment of complex perianal fistula: a phase II clinical trial. *Dis Colon Rectum* **52**, 79-86, doi:10.1007/DCR.0b013e3181973487 (2009).

19 Garcia-Olmo, D. *et al.* Treatment of enterocutaneous fistula in Crohn's Disease with adipose-derived stem cells: a comparison of protocols with and without cell expansion. *Int J Colorectal Dis* **24**, 27-30, doi:10.1007/s00384-008-0559-0 (2009).

20 Garcia-Arranz, M. *et al.* Treatment of Crohn's-Related Rectovaginal Fistula With Allogeneic Expanded-Adipose Derived Stem Cells: A Phase I-IIa Clinical Trial. *Stem Cells Transl Med* **5**, 1441-1446, doi:10.5966/sctm.2015-0356 (2016).

21 Pers, Y. M. *et al.* Adipose Mesenchymal Stromal Cell-Based Therapy for Severe Osteoarthritis of the Knee: A Phase I Dose-Escalation Trial. *Stem Cells Transl Med* **5**, 847-856, doi:10.5966/sctm.2015-0245 (2016).

22 Bura, A. *et al.* Phase I trial: the use of autologous cultured adipose-derived stroma/stem cells to treat patients with non-revascularizable critical limb ischemia. *Cytotherapy* **16**, 245-257, doi:10.1016/j.jcyt.2013.11.011 (2014).

23 Boesze-Battaglia, E. E. G. a. K. The role of alkaline phosphatase in mineralization. *Current Opinion in Orthopaedics* **18**, 444-448 (2007).

24 Alexander, D., Rieger, M., Klein, C., Ardjomandi, N. & Reinert, S. Selection of osteoprogenitors from the jaw periosteum by a specific animal-free culture medium. *Plos One* **8**, e81674, doi:10.1371/journal.pone.0081674 (2013).

25 Battula, V. L. *et al.* Isolation of functionally distinct mesenchymal stem cell subsets using antibodies against CD56, CD271, and mesenchymal stem cell antigen-1. *Haematologica* **94**, 173-184, doi:10.3324/haematol.13740 (2009).

26 Devito, L. *et al.* Wharton's jelly mesenchymal stromal/stem cells derived under chemically defined animal product-free low oxygen conditions are rich in MSCA-1(+) subpopulation. *Regen Med* **9**, 723-732, doi:10.2217/Rme.14.60 (2014).

27 O'Connor, M. D. *et al.* Alkaline phosphatase-positive colony formation is a sensitive, specific, and quantitative indicator of undifferentiated human embryonic stem cells. *Stem Cells* **26**, 1109-1116, doi:10.1634/stemcells.2007-0801 (2008).

28 Sobiesiak, M. *et al.* The Mesenchymal Stem Cell Antigen MSCA-1 is Identical to Tissue Non-specific Alkaline Phosphatase. *Stem Cells Dev* **19**, 669-677, doi:10.1089/scd.2009.0290 (2010).

29 Ochiai-Shino, H. *et al.* A Novel Strategy for Enrichment and Isolation of Osteoprogenitor Cells from Induced Pluripotent Stem Cells Based on Surface

Marker Combination. *Plos One* **9**, doi:ARTN e9953410.1371/journal.pone.0099534 (2014).

30 Alexander, D. *et al.* MSCA-1/TNAP Selection of Human Jaw Periosteal Cells Improves their Mineralization Capacity. *Cell Physiol Biochem* **26**, 1073-1080, doi:10.1159/000323985 (2010).

31 Estes, B. T., Diekman, B. O. & Guilak, F. Monolayer cell expansion conditions affect the chondrogenic potential of adipose-derived stem cells. *Biotechnol Bioeng* **99**, 986-995, doi:10.1002/bit.21662 (2008).

32 Fong, C. Y., Peh, G. S., Gauthaman, K. & Bongso, A. Separation of SSEA-4 and TRA-1-60 labelled undifferentiated human embryonic stem cells from a heterogeneous cell population using magnetic-activated cell sorting (MACS) and fluorescence-activated cell sorting (FACS). *Stem Cell Rev* **5**, 72-80, doi:10.1007/s12015-009-9054-4 (2009).

33 Li, Q. *et al.* Comparison of the sorting efficiency and influence on cell function between the sterile flow cytometry and immunomagnetic bead purification methods. *Prep Biochem Biotechnol* **43**, 197-206, doi:10.1080/10826068.2012.719846 (2013).

34 Durack, G. & Robinson, J. P. *Emerging tools for single-cell analysis : advances in optical measurement technologies*. (Wiley-Liss, 2000).

35 Devine, S. M. *et al.* Low Risk of Chronic Graft-versus-Host Disease and Relapse Associated with T Cell-Depleted Peripheral Blood Stem Cell Transplantation for Acute Myelogenous Leukemia in First Remission: Results of the Blood and

Marrow Transplant Clinical Trials Network Protocol 0303. *Biol Blood Marrow Tr* **17**, 1343-1351, doi:10.1016/j.bbmt.2011.02.002 (2011).

36 Jakubowski, A. A. *et al.* T Cell-Depleted Unrelated Donor Stem Cell Transplantation Provides Favorable Disease-Free Survival for Adults with Hematologic Malignancies. *Biol Blood Marrow Tr* **17**, 1335-1342, doi:10.1016/j.bbmt.2011.01.005 (2011).

37 Pasquini, M. C. *et al.* Comparative Outcomes of Donor Graft CD34(+) Selection and Immune Suppressive Therapy As Graft-Versus-Host Disease Prophylaxis for Patients With Acute Myeloid Leukemia in Complete Remission Undergoing HLA-Matched Sibling Allogeneic Hematopoietic Cell Transplantation. *J Clin Oncol* **30**, 3194-3201, doi:10.1200/Jco.2012.41.7071 (2012).

2.11 Supplemental Information

2.11.1 Preliminary FACS and MACS Sorts

Initial FACS and MACS sorts were performed on live, osteogenically primed SVF cells. Post-sort ALPL+ and ALPL- fractions were subjected to a 21-day, post-sort osteogenic differentiation protocol prior to ALPL activity assessment. Unsorted cells and "mock sorted" cells, i.e. those only subjected to size and granularity gating (FACS) or passed through columns not placed in the magnetic field (MACS), were included as controls. Two-way analysis of variance (factors: condition and sorting method) with an unequal N, modified Tukey post hoc test ($p < 0.05$) was performed to determine statistical differences between FACS ($N = 3$, $n = 9 – 12$) and MACS ($N = 1$, $n = 4$).

Exceedingly small ALPL- fractions in FACS sorts indicated pre-sort expansion and osteogenic priming likely homogenized the cell population, selecting for ALPL+ cells (**Figure S 2-1a**). Stark differences in ALPL+/ALPL- splits between FACS and MACS indicated the possibility of MACS-isolated ALPL- subpopulations being composed primarily of false-negatives (**Figure S 2-1a**). This was confirmed by the lack of difference in ALPL+ and ALPL- groups' 21-day, post-sort ALPL activities (**Figure S 2-1b**).

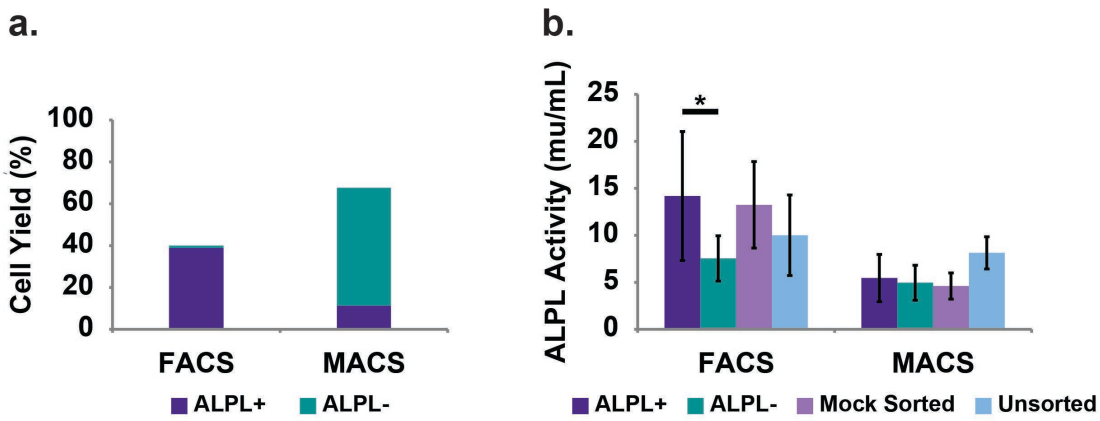

Figure S 2-1. Initial FACS and MACS post-sort yield and differentiation results. a.) Cell yields and b.) 21-day, post-sort ALPL activity for FACS and MACS isolated subpopulations. * indicates statistically different difference ($p < 0.05$).

Chapter 3

Mass-Added Density Centrifugation (MADC): A novel, particle-based, non-binary cell sorting method

Bryan Sutermaster, M.S.

3.1 Introduction

Cell sorting methods can be used to isolate subpopulations of cells from complex, heterogeneous cell mixtures for both basic science and clinical applications.[1-3] The two most common cell sorting methods, fluorescence-activated cell sorting (FACS) and magnetic-activated cell sorting (MACS), leverage fluorescent and magnetic labels, respectively, to separate cells.[4-6] FACS is characterized by ability to isolate highly pure subpopulations, but does so at the expense of throughput and resultant cell viability.[7] Additionally, FACS requires specialized, expensive equipment and a skilled operator capable of performing calibration and maintenance. In contrast, MACS is gentle and high-throughput, but cannot provide the specificity offered by FACS.[8] However, MACS can be performed with a simple magnet, and by novice users. While these are the most common and flexible sorting methods, other, more specialized sorting methods exist.

Isopycnic, or density gradient, centrifugation enables cell separation based on differences in density, and is a technique commonly used to separate various cell types

from whole blood or subcellular organelles from cell lysates.[9-13] Isopycnic centrifugation requires a density gradient medium and a centrifuge, and can be performed by novice users. Percoll, a common density gradient medium, is a colloidal suspension of polyvinylpyrrolidone (PVP)-coated silica particle which can be used to sort cells at their physiological densities.[14,15] Upon high-g centrifugation, the colloidal silica particles self-sort based on size, forming a continuous density gradient. Alternatively, Percoll solutions of defined density can be layered in a discontinuous gradient. In either method, cells are layered on top of the pre-formed continuous or discontinuous gradients and centrifuged at low-g. In continuous density gradient centrifugation, cells travel through the gradient until they reach the region of the gradient that matches their density (the isopycnic point). In discontinuous gradient centrifugation, cells travel through the gradient steps and ultimately stop when they reach the interface of a step that is greater than their own density. After centrifugation, either continuous or discontinuous gradients can be fractionated to isolate cells. While isopycnic centrifugation is incredibly useful for separating cells/subcellular organelles of varying density, it is by definition incapable of separating cells/particles of the same density.

Sorting technologies have been proposed to alter cell density prior to separation using a density gradient, but published studies have used density-altering particles larger than the cells, themselves. In a since-expired U.S. patent and book chapter, a method for altering the density of cells using 0.1 μm – 5 μm particles was proposed, however no studies using this method were ever published.[16,17] Additionally, a separate, recent study was published in which multiple fetal nucleated red blood cells were bound to anti-CD147-functionalized, 30 μm gelatin-coated silica microparticles to enable discontinuous

density gradient separation from normal blood cells.[18] As this technique utilized particles that are larger than that of the cell, it only enabled binary separations that obscure potentially important cellular heterogeneity. Thus, an opportunity exists for the development of a non-binary, particle-based sorting method capable of separation of cellular subpopulations exhibiting graded protein expressions.

For effective sorting, surface marker targets should be characteristically expressed by cellular subpopulations of interest. CD51/61 and CD271 are two important surface markers expressed in various human melanoma cells. CD51/61 is a heterodimeric integrin, also known as the vitronectin receptor, that is uniformly highly expressed in A375 cells.[19] Various reports have implicated either CD51/61 expression or that of its subunits in melanoma tumorigenicity/metastasis.[20-23] In MeWo cells, CD271, or nerve growth factor receptor, has been shown to be upregulated in a dose-dependent manner in response to treatment with common chemotherapeutic drug cisplatin.[24] CD271 has been implicated in metastasis and chemotherapeutic resistance, and has even been posited as a melanoma cancer stem cell marker.[25-31] These markers may be useful as targets in cell sorting of melanoma subpopulations.

In the study that follows, we set out to design a novel sorting method called mass-added density centrifugation (MADC), in which cellular density was altered by the binding of small, massive nano/microparticles prior to conventional density gradient centrifugation. To determine the feasibility of this novel separation method, we designed a three-pronged, proof-of-concept study. First, A375s and MeWo were labeled with massive micro- or nano-particles targeting CD51/61 and CD271, respectively, mixed with untreated cells, and subjected to density gradient centrifugation using continuous

gradients to determine the ability of MADC to perform binary separations. After centrifugation, the gradients were fractionated and subjected to flow cytometry to determine the relative per-fraction splits of treated and untreated cells. To test whether MADC was capable of non-binary separations, anti-CD271/microparticle-treated MeWo cells were subjected to density gradient centrifugation using continuous gradients, prior to fractionation and Western blot analysis for per-fraction CD271 expression. Finally, an analogous experiment was performed with anti-CD271/microparticle-treated MeWo cells using a discontinuous gradient, prior to fractionation and Western blot to quantify per-fraction CD271 expression. The objective of developing this novel, particle-based sorting method was to equip researchers with a versatile, accessible sorting technology combining the gentle, high-throughput nature of MACS with the non-binary separation capabilities of FACS. Furthermore, used in tandem with MACS, MADC could enable non-binary separation of magnetically sorted subpopulations, addressing one of the magnetic sorting modality's primary weaknesses.

3.2 Materials and Methods

3.2.1 MADC Theory

Cellular mass and volume is altered by binding of small, massive particles. The mass and volume of a cell-particle composite can be described as a function of their individual masses and volumes (**Equations 3-1,3-2**), where (m_{cell}, $m_{particle}$, $m_{cell+particles}$), (v_{cell}, $v_{particle}$, $v_{cell+particles}$), and (r_{cell}, $r_{cell+particles}$) are the masses, volumes, and radii, respectively, of the cell, particles, and cell/particle composites, and n is the number of bound particles. Hence, the density of the cell/particle composite, $\rho_{cell+particles}$, can be

described as a function of their individual masses and volumes (**Equation 3-3**). Provided that the radius of the mass-adding particles is much, much smaller than that of the cell, the cell/particle composite can be made more massive without precipitously changing volume.

$$m_{cell+particles} = m_{cell} + n \cdot m_{particle} \qquad \textbf{Equation 3-1}$$

$$v_{cell+particles} = \frac{4}{3} \cdot \pi \cdot {r_{cell}}^3 + n \cdot \left(\frac{4}{3} \cdot \pi \cdot {r_{particle}}^3\right) \qquad \textbf{Equation 3-2}$$

$$\rho_{cell+particles} = \frac{m_{cell}+n \cdot m_{particle}}{\frac{4}{3} \cdot \pi [{r_{cell}}^3 + n \cdot ({r_{particle}}^3)]} \qquad \textbf{Equation 3-3}$$

Estimates of the maximum possible number of particles added per cell were calculated for each particle type by dividing the surface area of a cell ($d_{cell} \approx 20$ μm) by the cross-sectional area of the particle.

3.2.2 Cell Culture and Fixation

A375 human melanoma cells were plated into T182 flasks (Genesee Scientific, San Diego, CA) and expanded to confluence in growth medium composed of Dulbecco's Modified Eagle's Medium with high glucose (DMEM-hg, GE Healthcare HyClone, Pittsburgh, PA), 10% fetal bovine serum (Genesee Scientific), and 1%

penicillin/streptomycin (GE Healthcare HyClone). Once confluent, cells were detached using Accutase Cell Detachment Solution (Innovative Cell Technologies, San Diego, CA) to preserve trypsin-vulnerable surface markers, and centrifuged for 5 min at 400 g to pellet. Cells were then fixed in 10% formalin phosphate (Fisher Scientific, Hampton, NH) for 30 min at room temperature. After fixation, the cells were washed twice in phosphate buffered saline (PBS, Fisher Scientific) and stored at 4°C prior to use.

MeWo human melanoma cells were similarly plated into T182 flasks and expanded to confluence in growth medium composed of Modified Eagle's Medium, 1% penicillin/streptomycin , 1% L-Glutamine, 1% non-essential amino acids (GE Hyclone), and 10% fetal bovine serum. Fresh stocks of 1.67 mM cisplatin (Sigma-Aldrich, St. Louis, MO) were made the day of treatment in 0.9% saline. 15 μM and 30 μM cisplatin stocks were made by diluting the 1.67 mM cisplatin stock solution with complete MeWo growth medium. Confluent T182 flasks of MeWo cells were treated with either 0 μM ($MeWo_{NT}$), 15 μM ($MeWo_{15}$), or 30 μM ($MeWo_{30}$) cisplatin in complete growth medium for 24 hrs at 37°C and 5% CO_2. After 24 hrs, cells were uplifted with Accutase and fixed as described previously.

3.2.3 Wheat Germ Agglutinin Staining

For trials using Sera-Mag™ beads, fixed $MeWo_{30}$ cells (20×10^6) were stained with either wheat germ agglutinin-AlexaFluor 488 or -AlexaFluor 647 (WGA488, WGA647, respectively, Thermo Fisher Scientific, Waltham, MA) according to manufacturer's protocols. Briefly, cell pellets were resuspended in 5 μg/mL WGA488 or WGA647 in Hank's buffered saline solution (HBSS, GE Healthcare HyClone) for 10 min

while rocking covered in foil at room temperature. After the 10 minute incubation, cells were washed once in HBSS prior to a second fixation in 10% formalin phosphate for 30 min at room temperature while covered in foil to prevent dye leaching. After secondary fixation, 10 x 10^6 WGA647-stained cells were pelleted prior to antibody treatment, while 10 x 10^6 WGA488-stained cells were resuspended in 500 µL autoMACS Rinsing Solution (Miltenyi Biotech, Bergisch Gladbach, Germany) + 0.5% bovine serum albumin (BSA, Millipore Sigma, Burlington, MA) and stored until density gradient centrifugation.

For trials using 80 nm InnovaCoat® gold beads (Expedeon, San Diego, CA), 2 x 10^6 A375 cells were stained with WGA488 according to manufacturer's protocols. Cells were incubated covered at room temperature without additional agitation for 10 min. After the 10 minute incubation period, cells were washed twice in PBS and stored prior to density gradient centrifugation.

3.2.4 InnovaCoat® Gold CD51/61 Antibody Functionalization

80 nm InnovaCoat® Gold nanoparticles were functionalized with anti-CD51/61 antibody (Catalogue Number: 16-0519-81, Clone: 23C6, Invitrogen, Carlsbad, CA) according to manufacturer's protocols with slight modifications. Briefly, anti-CD51/61 antibody was diluted to 0.05 mg/mL using the provided antibody diluent solution. The diluted antibody stock was further diluted to a final concentration of 0.01 mg/mL with provided reaction buffer. Using 450 µL of the 0.01 mg/mL antibody dilution, the dried InnovaCoat® beads were reconstituted, and incubated at room temperature for 15 min. After 15 min, 50 µL of the supplied quenching buffer was added, and the solution incubated for another 5 min. To wash out remaining unbound antibodies, the quenching

buffer was diluted 1:20 in water, and 5 mL was added to the antibody-functionalized gold beads. The solution was then centrifuged at 9,000 g for 10 min to pellet the beads. After centrifugation, the beads were resuspended in 500 µL PBS. Antibody functionalization was confirmed using Conjugate Check&Go! lateral flow assays according to manufacturer's protocols (Expedeon).

3.2.5 Pre-Sera-Mag™ MADC Antibody Treatment

10 x 10^6 WGA647-stained or unstained $MeWo_{30}$ cells subjected to 24hr cisplatin treatment as described previously were pelleted and resuspended in 200uL of anti-CD271-biotin antibody (Catalogue Number: 557195, Clone: C40-1457, BD Biosciences, San Jose, CA) and incubated for 15 min at room temperature. After 15 min, 1 mL of cold autoMACS Rinsing Solution + 0.5% BSA was added, and the cells pelleted. The cells were washed once more in cold autoMACS Rinsing Solution + 0.5% BSA, and pelleted prior to magnetic microbead treatment.

3.2.6 Anti-CD51/61-Functionalized InnovaCoat® Bead Treatment

2 x 10^6 unstained A375 cells were first blocked with 3% BSA for 1 hr at room temperature. After blocking, cells were pelleted and resuspended in 500 µL of anti-CD51/61-functionalized Innovacoat® beads in PBS + 1% BSA and incubated for 1 hr at RT. After the 1 hr incubation, the cells were pelleted and washed twice with PBS. Finally, the bead-treated cells were resuspended in 100 µL PBS.

3.2.7 Sera-Mag™ Bead Treatment

For continuous gradient MADC experiments designated for post-separation flow cytometry, 10 mg/mL magnetic, neutravidin coated particles (Sera-Mag™ SpeedBeads, diameter: ~1 μm, density: ~2.0 g/cm^3, GE Healthcare Life Sciences, Marlborough, MA) were diluted to a final concentration of 1 mg/mL using cold autoMACS Rinsing Solution + 0.5% BSA (10 μL 10 mg/mL Sera-Mag™ beads + 90 μL autoMACS Rinsing Solution + 0.5% BSA). 10 x 10^6 MeWo$_{30}$ (anti-CD271-biotin-treated, WGA647-stained) cells were resuspended in diluted Sera-Mag™ beads and incubated at room temperature for 15 min while covered in foil. After the incubation, 1 mL of cold autoMACS Rinsing Solution + 0.5% BSA was added to the cell/bead mixture and pelleted. The cell pellet was washed twice more in cold autoMACS Rinsing Solution + 0.5% BSA prior to cell counting using trypan blue exclusion. Antibody/bead-treated MeWo$_{30}$ cells were then resuspended at a concentration of 2 x 10^6 cells per 100 μL.

For continuous gradient MADC experiments designated for post-separation Western blot, unstained MeWo$_{30}$ cells were antibody- and bead-treated as above, and subjected to density gradient centrifugation alone (i.e. without mixing with WGA488-stained MeWo$_{30}$ cells). After separation, density gradients were fractionated, lysed, and subjected to Western blot.

For discontinuous gradient MADC experiments, 10 x 10^6 unstained MeWo$_{30}$ cells were antibody-treated as previously described. Subsequently, MeWo$_{30}$ cells were treated with 500 μL (50 μL of 10 mg/mL Sera-Mag™ beads + 450 μL autoMACS Rinsing Solution + 0.5% BSA) of 1 mg/mL Sera-Mag™ solution for 15 min at room temperature while gently rocking. After bead treatment, treated MeWo$_{30}$ cells were washed as above

before undergoing discontinuous density gradient centrifugation, fractionation, lysis, and Western blot.

10 μL or 50 μL of 10 mg/mL Sera-Mag™ particles were incubated with 10 x 10^6 untreated, A375 cells or 8 x 10^6 untreated, $MeWo_{30}$ cells, respectively, for 15 min at 4°C prior to attempted magnetic separation with a MagJET Separation Rack (Catalogue Number: MR01, Thermo Fisher Scientific) to determine approximate non-specific binding rate. After the attempted separation, the supernatant and cell pellet were collected separately, prior to cell counting via trypan blue exclusion assay. Non-specific binding rate was defined as the percentage of cells collected in the "pellet" on the magnetic stand divided by the total number of input cells.

3.2.8 Density Gradient Centrifugation, Post-MADC Fractionation

For the experiment using InnovaCoat® beads, Percoll (GE Healthcare Life Sciences) and 1.5 M NaCl were mixed to make an isotonic stock (SIP), prior to dilution with 0.15 M NaCl to a final density of 1.064 g/mL according to the manufacturer's protocol.[32] 3.5mL of the 1.064 g/mL Percoll solution was pipetted into a polypropylene OptiSeal™ centrifuge tube (13 x 48 mm, Beckman Coulter, Indianapolis, IN), and centrifuged at 45,000 g for 15 min at 4°C in an Optima Max ultracentrifuge fitted with TLA-110 rotor (Beckman Coulter) to make a continuous gradient. Then, 2 x 10^6 WGA488-stained A375 cells (no bead treatment) were mixed with 2 x 10^6 unstained A375 cells (treated with anti-CD51/61-functionalized beads) and pipetted on top of the pre-established gradient. The cell-containing gradient was then centrifuged for 5 min at 1043 g (5000 RPM) and 4°C. The tube was inspected for the presence of multiple cell

bands, and then subjected to an additional two 5 min/1043 g centrifugations. The gradient was fractionated by puncturing a hole in the bottom of the centrifuge tubes using an 18 gauge, 1 ½" needle (Becton Dickinson, Franklin Lakes, NJ) and draining into a 1.7 mL tube snap-cap tube (~275 µL per fraction, Genesee Scientific). All fractions were then analyzed by flow cytometry (**Figure 3-1**).

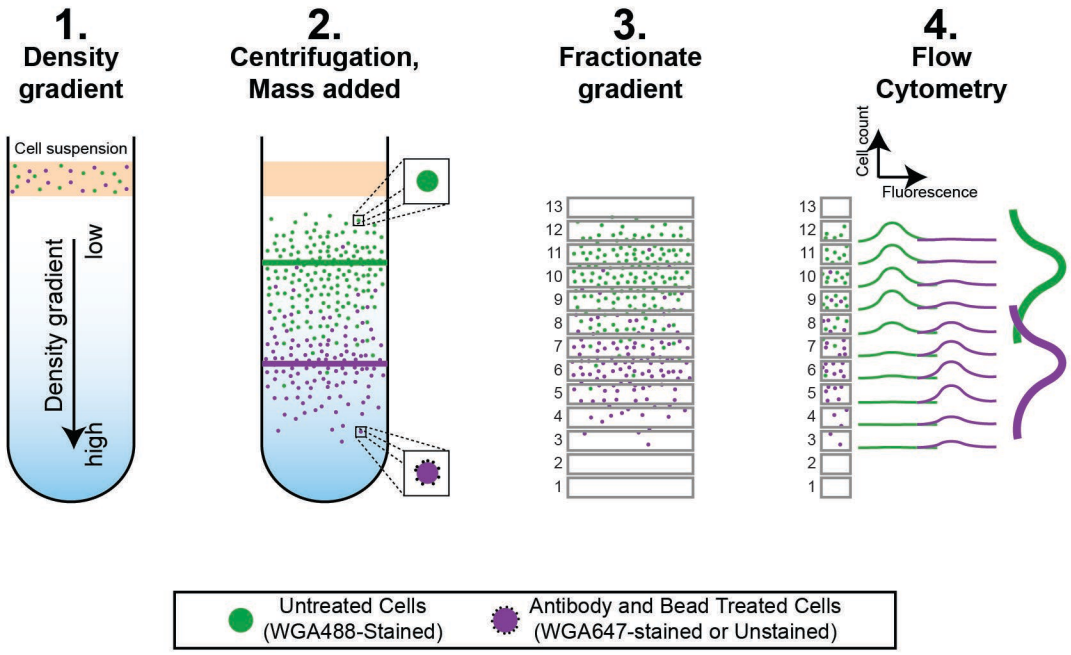

Figure 3-1. Schematic of MADC-separation of 1:1 mixtures of untreated, green-fluorescent cells and antibody/bead-treated, non- or red-fluorescent cells using pre-established continuous gradients. For anti-CD51/61-functionalized InnovaCoat® MADC separations of A375 cells, bead-treated cells were left unstained, while untreated cells were stained fluorescent green with WGA488. For anti-CD217-biotin/Sera-Mag MADC separations of $MeWo_{30}$ cells, antibody/bead-treated cells were stained fluorescent red with WGA647, while untreated cells were stained fluorescent green with WGA488.

For continuous gradient experiments using Sera-Mag™ beads, 3.5 mL of the 1.064 g/mL Percoll solution was pipetted into 4 - 6 polypropylene OptiSeal centrifuge tubes. To one of the tubes, density gradient marker beads (1.02 g/cm^3, 1.04 g/cm^3, 1.06

g/cm^3, and 1.09 g/cm^3, Cospheric, Santa Barbara, CA) were added to visualize the gradient distribution after each centrifugation. Tubes were then weighed and balanced, and gradients established as described previously. For experiments designated for flow cytometry evaluation, 2 x 10^6 WGA488-stained $MeWo_{30}$ cells (no antibody or microbead treatment) were mixed with 2 x 10^6 WGA647-stained $MeWo_{30}$ cells (treated with antibody and microbeads), gently pipetted on the top of three, pre-established, continuous gradients, and rebalanced. All gradients (3x experimental, cell-containing gradients, and 1x density marker bead gradient) were centrifuged a second time as described above. All cell-containing gradients were then fractionated (~ 275 µL/fraction) and subjected to flow cytometry (**Figure 3-1**). For experiments designated for Western blot evaluation, 4 x 10^6 $MeWo_{30}$ cells (treated with antibody and beads) or 4 x 10^6 $MeWo_{30}$ cells (without antibody or bead treatment) were pipetted on top of pre-established 1.064 g/mL Percoll gradients, centrifuged and fractionated as above. Fractions were then lysed, and proteins quantified using a BCA assay kit (Catalogue Number: 23225, Pierce, Thermo Fisher Scientific). Contiguous fractions possessing > 5 µg of protein were sequentially renumbered (from the bottommost fraction up) and subjected to Western blot (**Figure 3-2**).

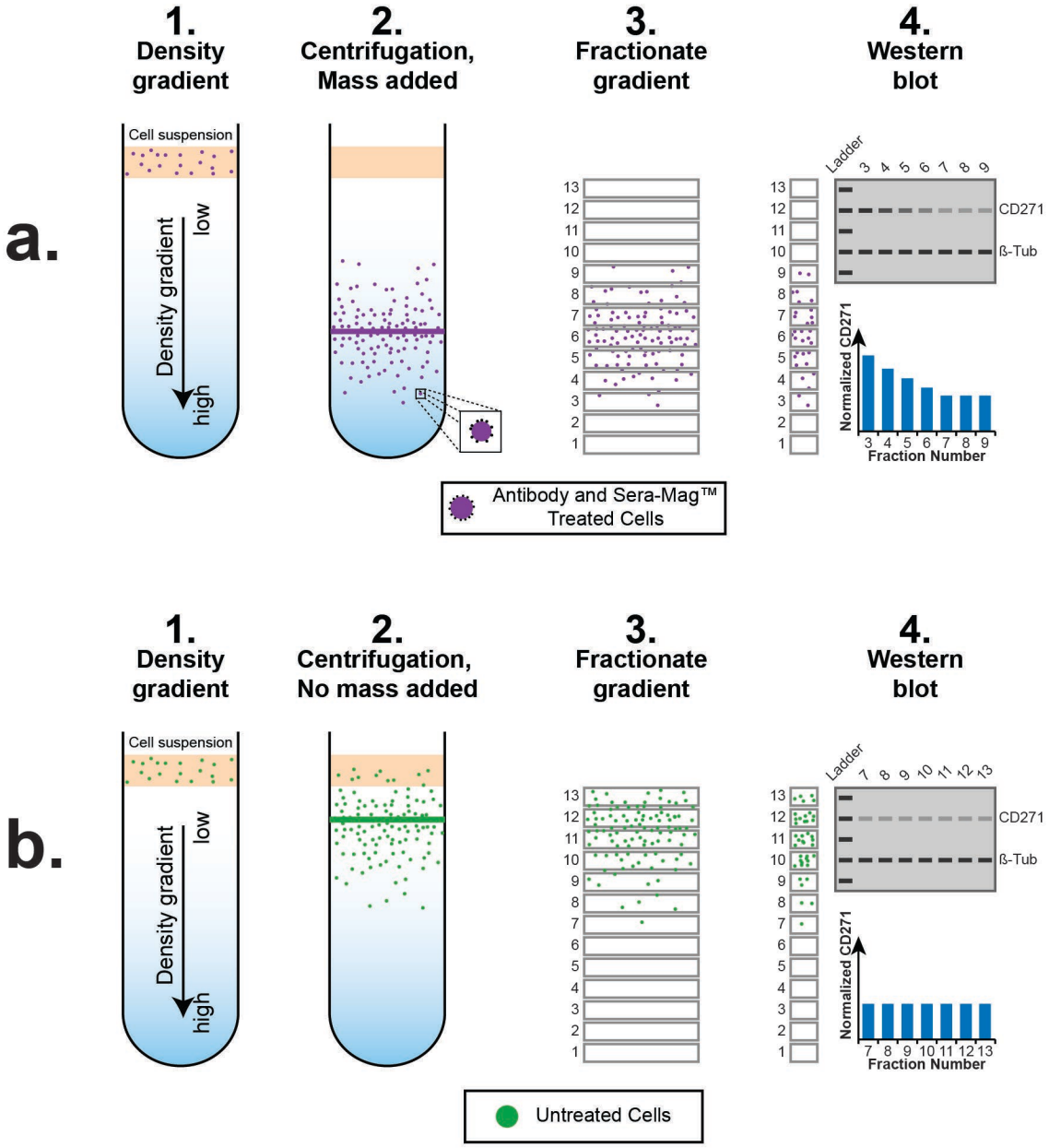

Figure 3-2. Schematics of MADC separation and density gradient centrifugation using continuous gradients. a.) MADC-separation of anti-CD271-biotin/Sera-Mag™-treated $MeWo_{30}$ cells. b.) density gradient centrifugation of untreated $MeWo_{30}$ cells.

For discontinuous gradient experiments using Sera-Mag™ beads, SIP was diluted with 0.15M NaCl to make Percoll solutions of 1.040 g/mL, 1.042 g/mL, 1.044 g/mL, 1.046 g/mL, 1.048 g/mL, and 1.050 g/mL per the manufacturer's protocol. In two 15 mL

centrifuge tubes (Genesee Scientific), 2 mL of each Percoll density was carefully layered from most to least dense. 10 x 10^6 antibody/bead-treated $MeWo_{30}$ cells were pipetted on to the top of one of the discontinuous gradients, while 10 x 10^6 untreated $MeWo_{30}$ cells were pipetted on top of the other. The gradients were then centrifuged for 15 min at 400 g in a Sorvall™ Legend™ X1R centrifuge fitted with a FIBERLite® F15-8x50C rotor (Thermo Fisher Scientific). After centrifugation, the gradients were split into four 3 mL fractions by carefully aspirating from the tops of the gradients. The fractions were then lysed and subjected to Western blot (**Figure 3-3**).

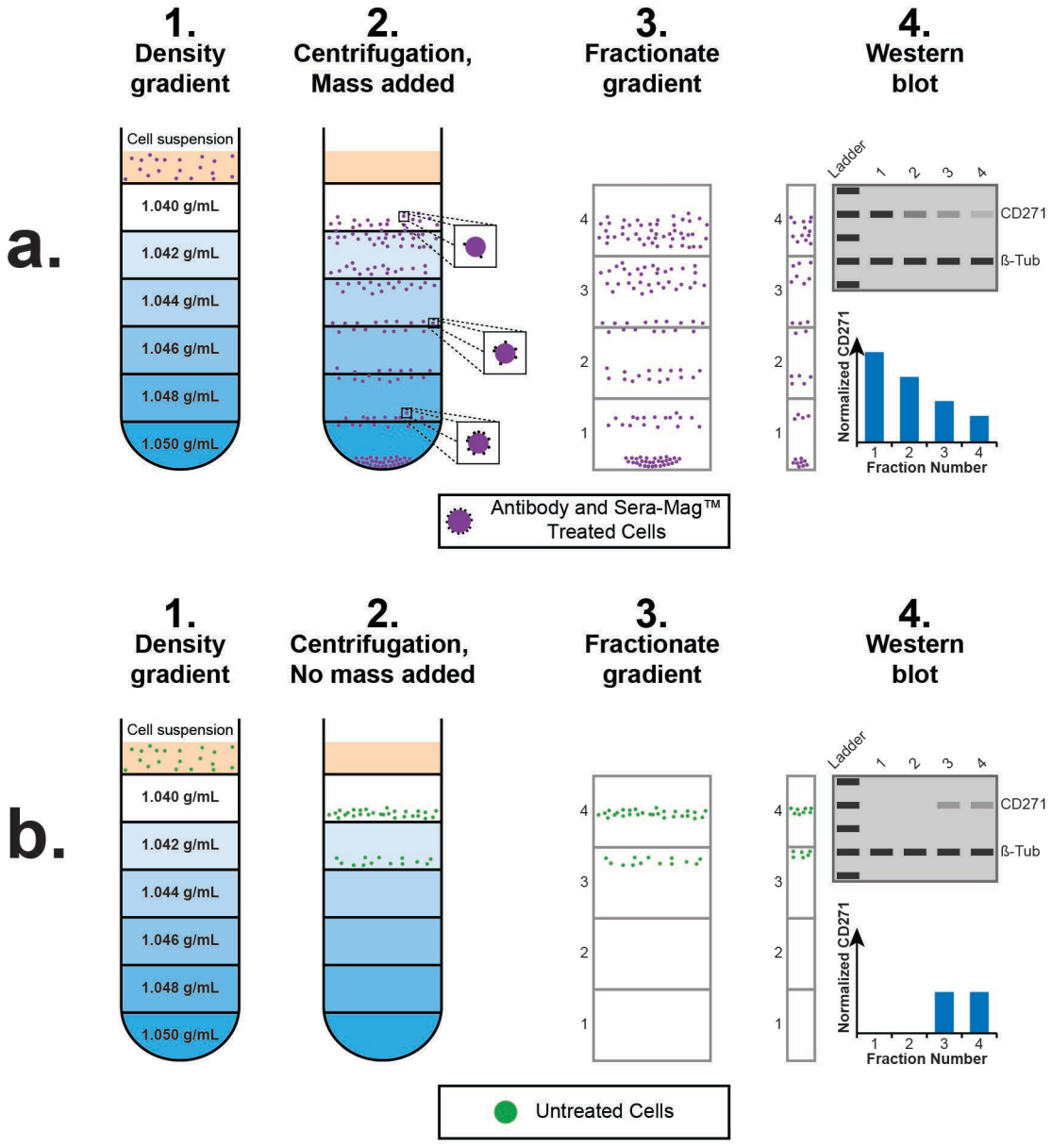

Figure 3-3. Schematics of MADC separation and density gradient centrifugation using discontinuous gradients. a.) MADC-separation of anti-CD271-biotin/Sera-Mag™-treated $MeWo_{30}$ cells. b.) density gradient centrifugation of untreated $MeWo_{30}$ cells.

3.2.9 Cellular Density Estimation

A375 and MeWo cell densities were estimated by subjecting them to density gradient centrifugation. Briefly, unstained A375 and MeWo cells were centrifuged on the top of pre-established, continuous 1.064 g/mL Percoll gradients as previously described,

and compared to a control gradient with density marker beads. Estimated cellular density was determined by comparing the distances from the menisci of the cell bands to those of beads of known density.

3.2.10 Flow Cytometry

To determine the population heterogeneity in CD271 expression, untreated and cisplatin-treated MeWo cells were subjected to a single-color flow experiment using a Guava EasyCyte cytometer (Millipore Sigma) equipped with 488 nm and 642 nm excitation lasers. 1 x 10^6 $MeWo_{NT}$, $MeWo_{15}$, and $MeWo_{30}$ cell pellets were first treated with 1:5 dilutions of anti-CD271-biotin for 10 min at room temperature. After 10 min, the cells were washed twice in 1 mL HBSS, and pelleted. Pellets were resuspended in 1:200 dilutions of Alexa Fluor™ 488-conjugated, goat anti-mouse secondary antibody (Catlogue Number: A-21121, Invitrogen) for 15 min covered at room temperature. After the secondary antibody incubation, the cell pellets were again washed twice in 1 mL HBSS prior to flow assessment. Forward and side scatter (FSC and SSC, respectively) gates and 488 nm laser gains were set using unstained $MeWo_{NT}$, $MeWo_{15}$, and $MeWo_{30}$ cells. Secondary-only controls were included to assess non-specific binding of the secondary antibody.

For the experiment using InnovaCoat® beads, FSC and SSC gates and laser gains were set using unstained A375 cells. A 200,000 event count target was set for each control and isolated fraction. Green fluorescence histograms were plotted for each fraction, and gates were drawn to quantify the relative fraction of non-fluorescent to fluorescent cells (i.e. bead-treated to non-bead treated).

For experiments using Sera-Mag™ beads, FSC and SSC gates and laser gains were set using WGA488-stained cells, WGA647-stained cells (no antibody or microbead treatment), and WGA647-stained cells treated with antibodies and beads. 10,000 event count targets were set for each control and isolated fraction, and samples were diluted to ensure a cell concentration less than 500 cells/μL. Green and red fluorescence signals were plotted on a log/log scale and gates were drawn to determine the relative ratio between green and red fluorescent cells in each fraction.

3.2.11 Cell Lysis and Western Blot

Cell lysis and antigen retrieval was performed in accordance with established protocols.[33,34] Briefly, cell pellets were resuspended in a buffer containing 300 mM Tris-HCl (Fisher Scientific), 10% sodium dodecyl sulfate (SDS, Fisher Scientific), and 2x protease/phosphatase inhibitor cocktail (Pierce, Thermo Fisher Scientific), incubated at 100°C in a boiling water bath for 30 min, and subsequently incubated for an additional 2 hrs in a 60°C water bath. Cell lysates were then centrifuged for 10 min at 14,000 g and 4°C. The supernatant was decanted, and protein content quantified using a BCA assay kit. Protein lysates were stored at -80°C until subjected to Western blot.

Using Any kD™ Mini-Protean TGX pre-cast gels (Catalogue Number: 456-9033, Bio-Rad, Hercules, CA) , 10 μL of Chameleon™ Duo protein ladder (Catalogue Number: 928-60000, LI-COR, Lincoln, NE) and 5 μg of protein per sample were separated for 75 min at 120 V. Proteins were transferred onto Immobilon®-FL membranes (Catalogue Number: IPFL10100, Millipore Sigma) for 70 min at 120V. Prior to primary antibody incubation, membranes were blocked in Odyssey® Blocking Buffer (Catalogue Number:

927-40100, LI-COR) for 1 hr at room temperature while shaking. After blocking, the membrane was incubated overnight at 4°C while shaking with both rabbit anti-human CD271 antibody [p75NTR (D4B3) XP® Rabbit mAb, Catalogue Number: 8238S, Cell Signaling Technology, Danvers, MA) and mouse anti-human β-tubulin antibody (Catalogue Number: E7-S, Developmental Studies Hybridoma Bank at the University of Iowa, Iowa City, IA) each diluted 1:1000 in 1:1 Odyssey® Blocking Buffer:Tris-buffered saline tween (1x TBST). Next, the membrane was incubated separately in 1:5000 IRDye® 800CW goat anti-mouse and IRDye® 680RD donkey anti-rabbit secondary antibody dilutions (Catalogue Numbers: 925-32210 and 925-68073, respectively, LI-COR) for 1 hr at room temperature while shaking. Finally, the membranes were imaged on an Odyssey CLx infrared gel imaging system (LI-COR). CD271/β-tubulin relative protein expression was computed using grayscale densitometry values obtained from ImageJ.

3.2.12 Statistical Analysis

Pearson's correlation coefficients were computed to determine whether relationships existed between per-fraction relative percentage of bead-treated cells and fraction number for both InnovaCoat®- and Sera-Mag™-MADC separations of A375 and $MeWo_{30}$ cells, respectively. Similarly, Pearson's correlation coefficients were calculated to determine whether relationships existed between fraction number and per-fraction CD271/β-tubulin relative expression for both continuous and discontinuous MADC separation of MeWo30 cells using anti-CD271-biotin antibodies and Sera-Mag™ beads.

3.3 Results

3.3.1 Cell Density, Maximum Particles Per Cell, and Simulated Composite Density

Simulated A375 and MeWo per-cell composite densities indicated both InnovaCoat® and Sera-Mag™ beads were theoretically capable of adding sufficient mass to enable successful MADC separation. To determine the simulated per-cell densities of cell/particle composites, the densities of A375 and MeWo cells were empirically determined and the estimated maximum added particles computed for InnovaCoat® and Sera-Mag™ beads. The estimated maximum number of particles added per cell for 80 nm InnovaCoat® gold and 1 μm Sera-Mag™ particles were 250,000 and 1,600, respectively. Estimated A375 and MeWo cell densities were both ~ 1.04 g/mL. Simulated densities of cell/particle composites were computed (**Equation 3-3**) and plotted versus the number of particles bound (**Figure 3-4**) using the empirically determined A375/MeWo cell densities. The predicted range of cell/particle composite densities ranged from 1.04 g/mL to 1.33 g/mL for InnovaCoat®-treated cells and 1.04 g/mL and 1.20 g/mL for Sera-Mag™-treated cells.

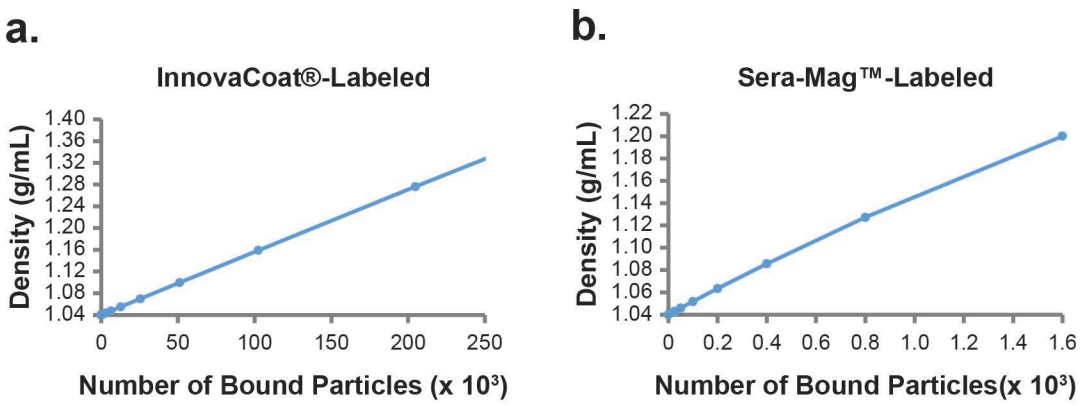

Figure 3-4. Simulated density of cell/particle composites as a function of the number of particles added. Cell labeled with a.) 80 nm, ~ 19.3 g/mL InnovaCoat® beads or b.) 1µm, ~ 2.0 g/mL Sera-Mag™ beads.

3.3.2 MeWo Expression of CD271 in Response to 0 µM, 15 µM, and 30 µM Cisplatin

Western blot and flow cytometry evaluation of MeWo cells exposed to 24 hr treatments of 0 µM, 15 µM, and 30 µM Cisplatin ($MeWo_{NT}$, $MeWo_{15}$, and $MeWo_{30}$, respectively) indicated a dose-dependent upregulation of CD271. Fluorescence histograms of $MeWo_{NT}$, $MeWo_{15}$, and $MeWo_{30}$ populations treated with primary (1°) and fluorescent secondary (2°) antibodies indicated greater proportions of cells expressing high levels of CD271 with increasing cisplatin treatment concentration (**Figure 3-5a-d**). All untreated and 2°-only controls indicated low cellular autofluorescence and non-specific 2° antibody binding, respectively, for $MeWo_{NT}$, $MeWo_{15}$, and $MeWo_{30}$. Western blot confirmed the ensemble average relative upregulation compared to reference gene β-tubulin (**Figure 3-5e**). All subsequent MADC experiments using Sera-Mag™ beads were performed with $MeWo_{30}$ cells, as that population displayed the highest frequency of cells with high CD271 expression, thereby maximizing potential for mass-adding particle binding.

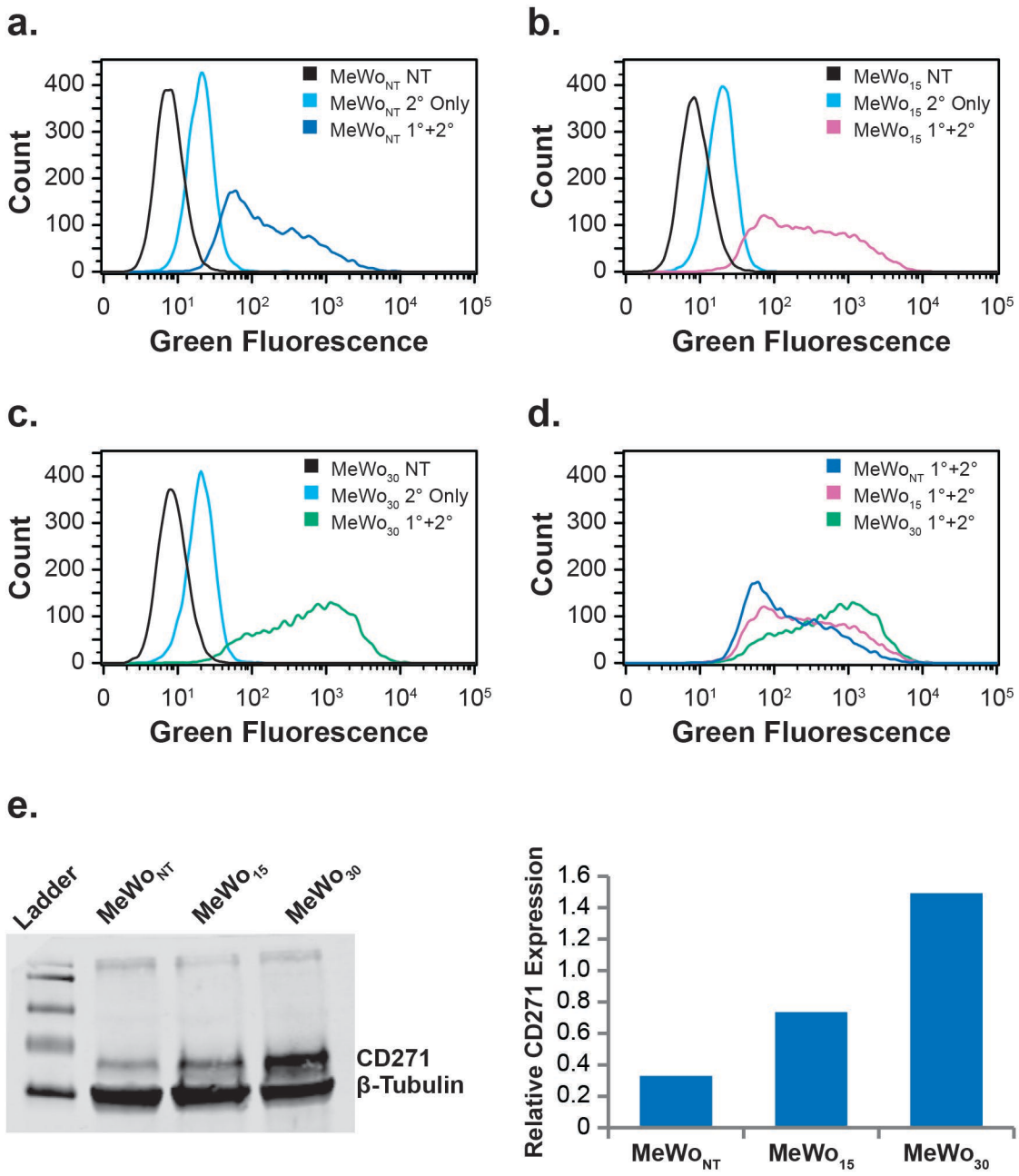

Figure 3-5. Flow cytometry and Western blot evaluation of MeWo cells exposed to 24 hr treatments of 0 µM, 15 µM, and 30 µM cisplatin ($MeWo_{NT}$, $MeWo_{15}$, $MeWo_{30}$, respectively). a.) $MeWo_{NT}$, b.) $MeWo_{15}$, and c.) $MeWo_{30}$ samples treated with both primary and secondary antibodies (1°+2°) were compared to unstained (NT) and secondary only controls (2° Only) within each population, to determine cell autofluorescence and non-specific secondary antibody binding, respectively. d.) 1°+2°-treated conditions of each cell type were compared to assess differences in CD271 expression distribution. e.) Semi-quantitative densitometry analysis of Western blot

bands was performed to assess the ensemble average, relative CD271/β-tubulin expression for each cell population.

3.3.3 Continuous Gradient MADC using InnovaCoat® and Sera-Mag™ Beads

Flow cytometry evaluation of post-continuous gradient MADC fractions indicated successful separation of A375s using anti-CD51/61-functionalized InnovaCoat® beads. Two, distinct cell bands (one colorless, one red) were identified after centrifugation on a pre-established 1.064 g/mL Percoll density gradient (**Figure 3-6a**). Upon fractionation and flow cytometry analysis, a moderately strong negative correlation (r = -0.74) was observed between fraction number and relative, per-fraction InnovaCoat®-treated cell percentage. Furthermore, a distinct shift in the per-fraction WGA488-stained (no bead treatment) and unstained (anti-CD51/61-functionalized InnovaCoat®-treated) split was observed between Fractions 8 and 9. Fractions 1 – 8 displayed relatively more unstained (anti-CD51/61-functionalized InnovaCoat®-treated) A375s than WGA488-stained cells (no bead treatement), while Fractions 9 – 11 displayed the opposite trend, indicating successful separation. Likewise, the concentration profile of unstained (anti-CD51/61-functionalized InnovaCoat®-treated) A375s peaked in a lower fraction than unstained (no bead treatment) A375s (**Figure 3-7**).

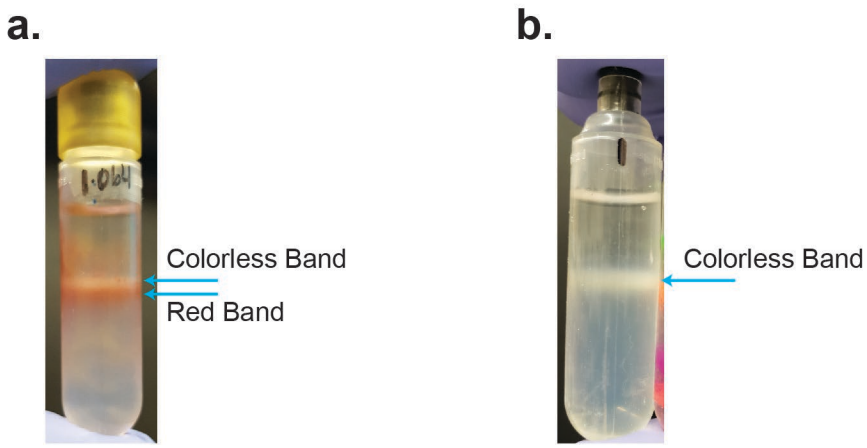

Figure 3-6. Pictures of continuous MADC gradients after secondary centrifugation and before fractionation. a.) anti-CD51/61-functionalized InnovaCoat®-treated + untreated A375 cells. b.) $MeWo_{30}$ cells treated with anti-CD271-biotin and Sera-Mag™ beads + untreated $MeWo_{30}$ cells.

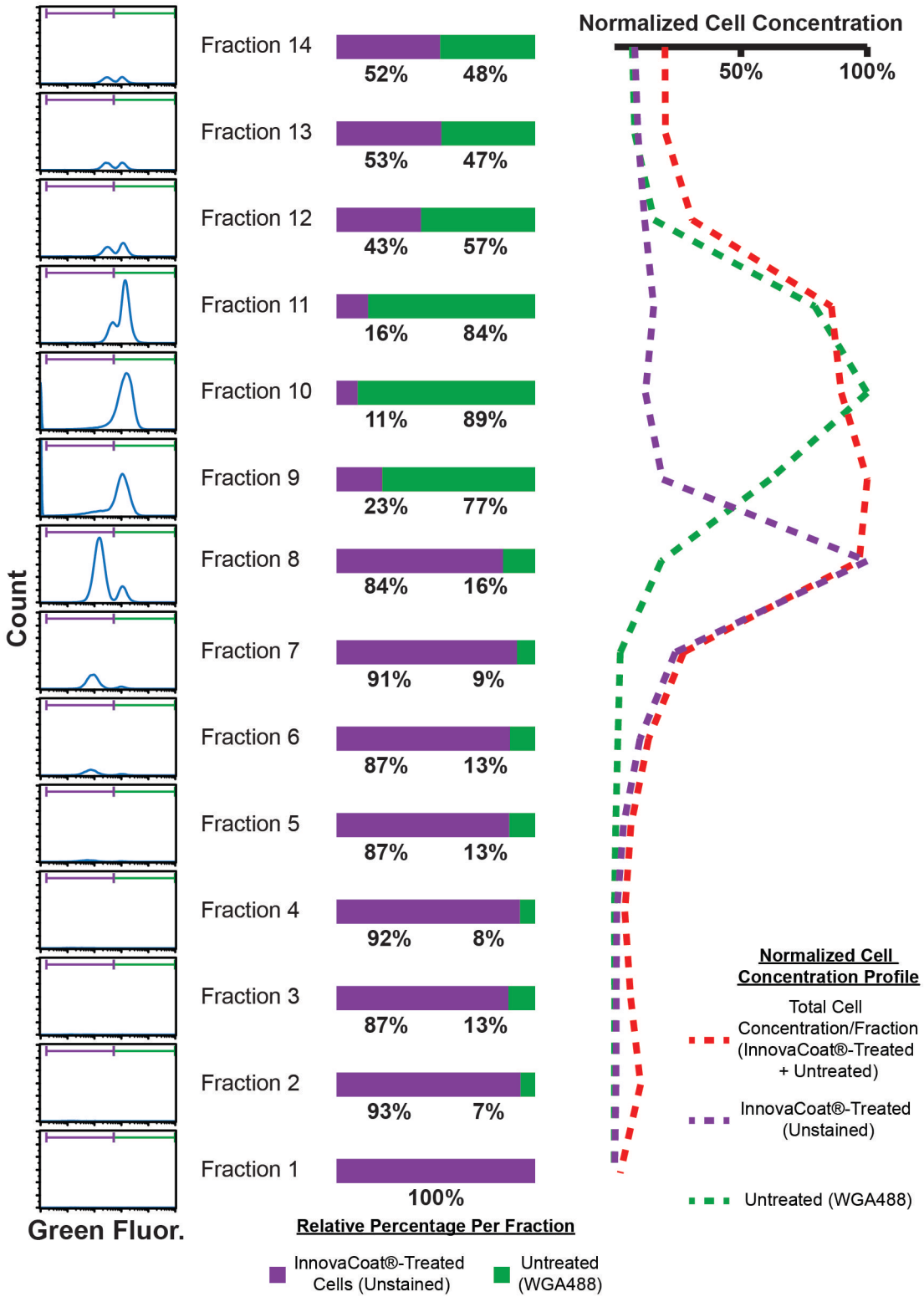

Figure 3-7. Flow cytometry evaluation of post-continuous MADC fractions using anti-CD271-functionalized InnovaCoat® beads and A375 cells. Line gates in per-fraction fluorescence histograms (left) define relative percentage (middle) of InnovaCoat®-

treated to untreated cells. Total, treated, and untreated cell concentration profiles are also plotted (right).

In contrast to continuous gradient MADC separations of A375 cells using antibody functionalized InnovaCoat® beads, flow cytometry evaluation of post-continuous gradient MADC fractions indicated unsuccessful separation of $MeWo_{30}$ cells using anti-CD271-biotin/Sera-Mag™ beads. After centrifugation on pre-established, continuous 1.064 g/mL Percoll gradients, a single band was visible in the centrifuge tube (**Figure 3-6b**). While per-fraction relative percentage of WGA647-stained (antibody/bead-treated) cells displayed a strong negative correlation with fraction number (r = -0.92), the concentration profiles indicated no separation (**Figure 3-8**).

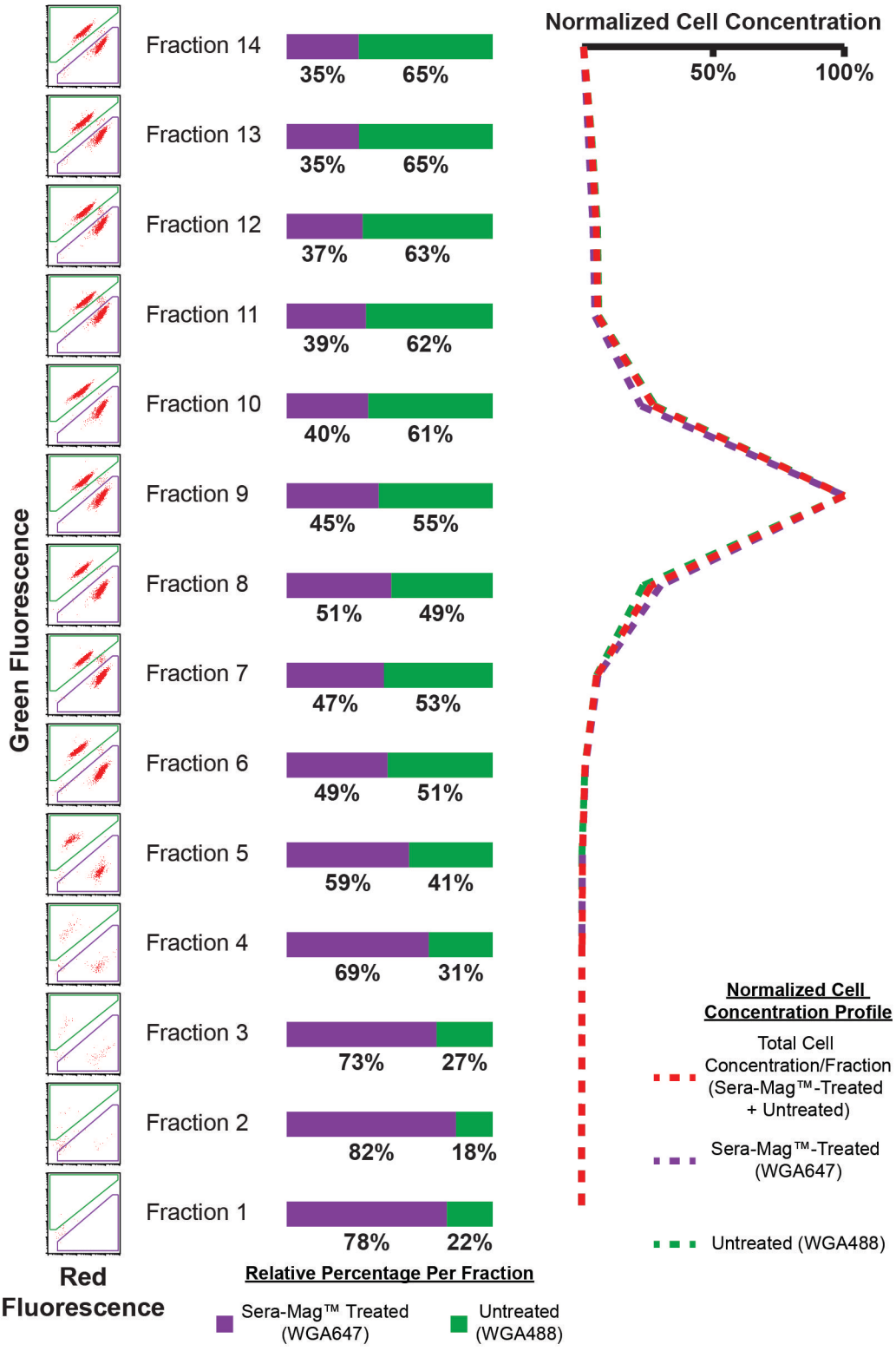

Figure 3-8. Flow cytometry evaluation of post-continuous MADC fractions using anti-CD271-biotin antibodies, Sera-Mag™ beads, and $MeWo_{30}$ cells. Gates in the red vs. green fluorescence scatter plots (left) define the relative percentage (middle) of Sera-

Mag™-treated cells to untreated cells per fraction. Total, treated, and untreated cell concentration profiles are also plotted (right).

Comparisons of post-separation Western blots of continuous gradient MADC fractions versus simple density gradient centrifugation fractions also indicated unsuccessful separation of anti-CD271-biotin/Sera-Mag™-treated $MeWo_{30}$ cells. CD271/β-tubulin relative expression displayed a weak negative correlation (r = -0.42) with fraction number for anti-CD271-biotin/Sera-Mag™-treated $MeWo_{30}$ (**Figure 3-9a**). Untreated $MeWo_{30}$ cells subjected to simple density gradient centrifugation displayed similar behavior with per-fraction CD271/β-tubulin relative expression exhibiting a moderate negative correlation with fraction number (r = -0.73, **Figure 3-9b**).

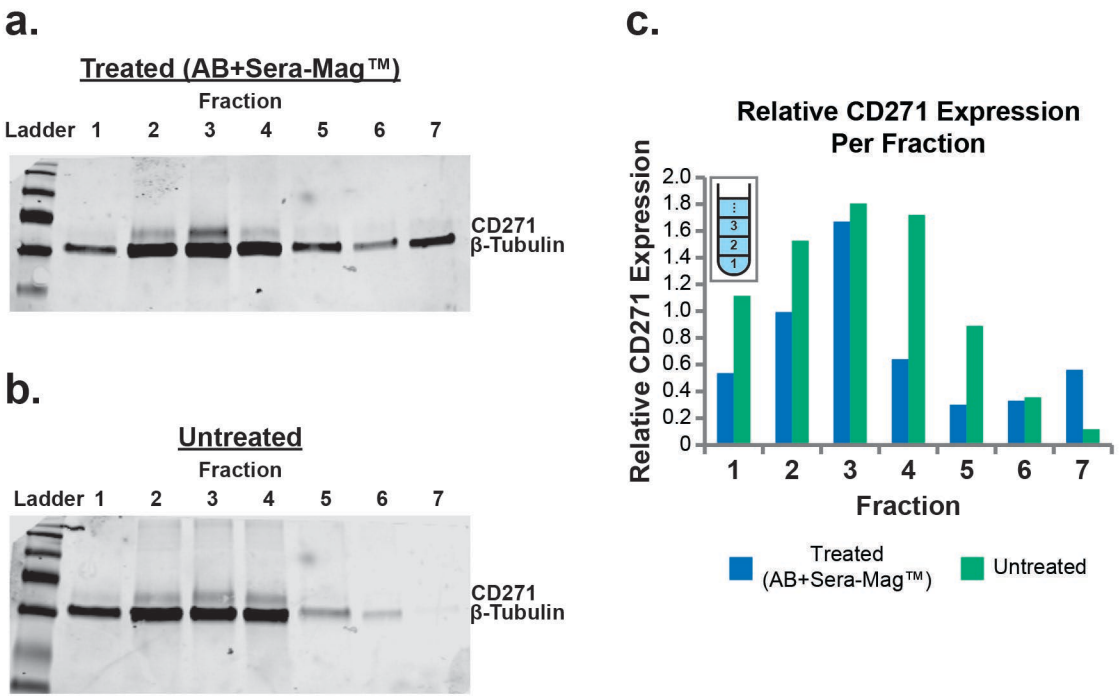

Figure 3-9. Per-fraction quantification of CD271/β-tubulin relative expression post continuous gradient MADC and density gradient centrifugation. a.) Western blots of fractions isolated from continuous gradient MADC (using anti-CD271-biotin/Sera-Mag™-treated $MeWo_{30}$ cells). b.) Western blots of fractions isolated from post-density gradient centrifugation (using untreated $MeWo_{30}$ cells) c.)Per-fraction, semi-quantitative densitometry analysis of CD271/β-tubulin relative expression.

The non-specific binding rate when 10 µL of Sera-Mag™ particles were incubated with 10 x 10^6 A375 cells was ~ 13 - 21%. However, when subjected to additional washes and magnetic separations, the non-specific binding rate could be reduced to ~ 8%. The non-specific binding rate when 50 µL of Sera-Mag™ particles were incubated with 8 x 10^6 $MeWo_{30}$ cells was ~ 44%.

3.3.4 Discontinuous Gradient MADC using Sera-Mag™ Beads

Much like continuous gradient Sera-Mag™-MADC, similar trends were observed between CD271/β-tubulin relative expression and fraction number, indicating unsuccessful MADC separation. Both Sera-Mag™-MADC and simple density gradient centrifugation separations of $MeWo_{30}$ cells displayed strong negative correlations (r = -0.96 and r = -0.98, respectively) between CD271/β-tubulin expression and fraction number (**Figure 3-10**). Despite the strong negative correlations, the apparent differences between per-fraction CD271/β-tubulin were small.

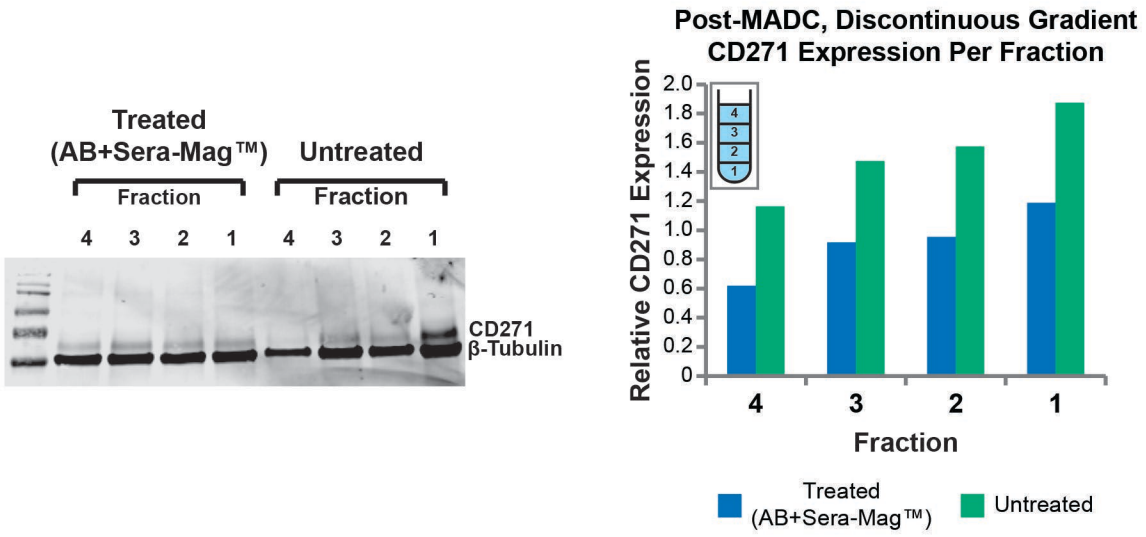

Figure 3-10. Per-fraction quantification of CD271/β-tubulin relative expression post discontinuous gradient MADC and density gradient centrifugation. a.) Western blots of post-discontinuous gradient MADC (anti-CD271-biotin/Sera-Mag™-treated $MeWo_{30}$ cells) and post-density gradient centrifugation (Untreated $MeWo_{30}$ cells) fractions. b.)Per-fraction, semi-quantitative densitometry analysis of CD271/β-tubulin relative expression.

3.4 Discussion

The objective of this study was to develop a novel cell sorting method that combined the gentle, high-throughput characteristics of a particle-based sorting method like MACS, and enabled non-binary separation like FACS. We hypothesized that separation could be accomplished by altering the density of cells with small, massive nano/microparticles, and subsequently subjecting them to density gradient centrifugation. Furthermore, we postulated that targeting the micro/nanoparticles to surface markers would enable cellular density alterations directly proportional to protein expression, thereby enabling non-binary separations. To test this hypothesis, we labeled two different cell types (A375 and MeWo) with antibody-functionalized particles (InnovaCoat® beads) or with a primary, biotinylated antibody followed by NeutrAvidin-coated beads (anti-CD271-biotin/Sera-Mag™), and subjected them to density gradient centrifugation using continuous or discontinuous Percoll gradients. Post-sort flow cytometry analysis indicated that mixtures of untreated A375 and anti-CD51/61-functionalized InnovaCoat® bead-treated A375s were able to be separated by our hypothesized MADC process. However, in attempted MADC separations of $MeWo_{30}$ cells using a combined anti-CD271-biotin/Sera-Mag™ approach with both continuous and discontinuous gradients, flow cytometry and Western blot analyses indicated no separation. Though binary separation of cells by altered density has been proposed and demonstrated using particles larger than the size of the cell, to our knowledge, our successful binary MADC separation of A375 cells is the first demonstration of altered density sorting using non-magnetic, subcellular-sized particles.[16-18]

Anti-CD51/61-functionalized InnovaCoat® gold beads enabled binary separation of treated A375 cells from untreated. Gold was selected as a candidate for particle composition due to its high density, and the commercial availability of a wide range of gold nanoparticles. Though we did attempt to antibody-functionalize other gold nanoparticle sizes and shapes in-house, the conjugation protocols were non-trivial and often suffered from significant particle aggregation or failed antibody attachment (data not shown). The InnovaCoat® system enabled easy functionalization with a commonly used anti-CD51/61 antibody. Initial A375 MADC separations were successful, as two clear bands were visible in the gradient after secondary centrifugation and post-separation per-fraction flow cytometry indicated stark differences in the treated and untreated A375 cell concentration profiles. However, the observed density changes were much less than those predicted when the number of bound particles per cell was maximized (~250,000 InnovaCoat® beads).

There are several possible explanations as to why observed cellular density changes were less than those predicted by simulation in the InnovaCoat®-MADC trials. One possible explanation for this observation is that we simply did not treat the cells with enough of the antibody-functionalized beads. If all 2×10^6 treated A375s expressed $\geq$ 250,000 CD51/61 protein complexes, it would require 5×10^{11} antibody-functionalized InnovaCoat® beads to saturate their surfaces. However, each vial of InnovaCoat® beads is estimated to have 1×10^{11} particles, which would provide ~ 22% coverage per cell. Despite this, the anticipated per-cell density of an A375 cell with ~ 22% maximum predicted bead coverage (~ 55,000 beads/cell) would still be large (~ 1.104 g/mL)

compared to an untreated cell (~ 1.04 g/mL). As such, sub-saturating bead treatment numbers is not the most likely explanation for our lower-than-expected density changes.

Another possible explanation is that fewer than 250,000 CD51/61 protein complexes were expressed per A375 cell. While it has been established that A375 cells highly express CD51/61, the exact number of surface proteins is unknown, and would require complex quantitative proteomic analyses outside the scope of this study to determine.[19,35,36] Additionally, non-specific binding of the antibody-functionalized beads may have decreased the effective density difference between treated and untreated cells. If CD51/61 protein levels in the treated A375 cells were insufficient to bind all antibody-functionalized microbeads during the treatment step, unbound beads could have bound the untreated A375 cells during the centrifugation process. As such, the density of the untreated cells would have been increased, thereby decreasing the effective density difference compared to the treated cells. Similarly, it is possible CD51/61 was not expressed at sufficient levels to bind enough of the InnovaCoat® beads to add sufficient mass to yield a larger physical separation within the density gradient.

Though they enabled successful binary separation, the InnovaCoat®-A375 pairing was unsuitable for further, more thorough studies. Initial flow cytometry experiments indicated that A375s expressed CD51/61 at a high, consistent level throughout the population (data not shown). This made the cell type/marker combination suitable for binary separation proof-of-concept experiments, but precluded non-binary separations. Additionally, the price of the InnovaCoat® gold nanoparticles made significant optimization impractical, as each separation required an entire InnovaCoat® vial (~ $570). Finally, while the InnovaCoat® particle enabled easy antibody

functionalization, it would have necessitated the purchase of entirely new batches of particles for each candidate antibody/protein target. To address these limitations, we identified a new candidate cell line, a different surface protein target, and alternative mass-adding particle. Cisplatin pre-treated MeWo, whose expression of CD271 spanned a wide range, was identified as a candidate cell line/protein target in which to test non-binary MADC separations. Next, we identified a less expensive, physically larger particle (~ 1.0 μm, ~ 2.0 g/mL), in Sera-Mag™ NeutrAvidin coated beads, in an effort to add more mass per CD271 protein bound. Sera-Mag™ NeutrAvidin particles also offered the flexibility to change candidate protein markers, as the same particles could be used with any biotinylated antibody.

Even with the potential advantages Sera-Mag™ NeutrAvidin beads possessed over InnovaCoat® particles, attempted continuous gradient MADC separations of $MeWo_{30}$ cells were unsuccessful. Two of the same potential explanations that prevented InnovaCoat® beads from generating a large physical separation between treated and untreated A375s can be extended to the attempted Sera-Mag™ separations of $MeWo_{30}$ cells: non-specific bead binding and insufficient protein expression. Effort was made to optimize the initial Sera-Mag™ bead treatment volumes to ensure minimal excess Sera-Mag™ particles during the centrifugation step, thereby minimizing the possibility of non-specific binding. The lack of numerous unbound beads after Sera-Mag™ treatment was confirmed using phase contrast microscopy (data not shown), making non-specific binding an unlikely culprit. Similarly, $MeWo_{30}$ cells were specifically selected due to the increased frequency of CD271 high expressers as confirmed by flow cytometry, making insufficient protein expression a less likely explanation. Somewhat surprisingly, though

initially identified as an attractive characteristic imparting flexibility, the Sera-Mag™ beads' NeutrAvidin coating may be the most likely explanation for the unsuccessful separation. As NeutrAvidin possesses four binding domains for biotin molecules, it is possible that only a quarter of the possible particles were bound per cell, limiting the effective mass added. Still, simulations indicated a quarter of the maximum number of particles (~ 400 beads) would result in an estimated per-cell density of ~1.09 g/mL; a density difference still generating considerable movement on the continuous 1.064 g/mL density gradient. As such, we hypothesized that much fewer than the anticipated number of particles bound the $MeWo_{30}$ cells, resulting in a vastly smaller than anticipated density difference. Subsequently, we revised our experimental design in an effort to reduce the possibility of a single Sera-Mag™ bead binding multiple biotinylated antibodies, and to increase the physical separation within a narrow density range.

Despite using five times the number of Sera-Mag™ beads and a lower cell treatment concentration, discontinuous-MADC separations of $MeWo_{30}$ cells were likely unsuccessful due to cell aggregation. Initial discontinuous gradient tests using the same Sera-Mag™ bead treatment volumes (10 µL of 10 mg/mL Sera-Mag™ beads + 90 µL of autoMACS Rinsing Solution + 0.5% BSA) used in continuous trials displayed significant cell aggregation when subjected to secondary centrifugation (data not shown). Both Sera-Mag™ bead number and treatment volume were increased in an effort to minimize the possibility of a single bead binding multiple biotinylated antibodies, and to decrease the chance of cell-to-cell contact, respectively. After antibody and Sera-Mag™ bead treatment steps, the cell pellet looked much darker (as the Sera-Mag™ beads were brown in color) than continuous gradient MADC trials, suggesting more beads were bound per

cell. However, when placed on top of the discontinuous Percoll gradients and centrifuged, large cell aggregates were still visible in the gradient. Upon examination under phase contrast microscopy, the presence of cell-cell aggregates heavily labeled with microbeads was confirmed. It is likely that the NeutrAvidin-coated Sera-Mag™ beads were acting as crosslinkers, connecting the biotinylated antibody-bound CD271 molecules from one cell to that of another. Furthermore, it is possible that the large size of the Sera-Mag™ beads exacerbated the crosslinking problem, as it provided increased surface area for potential NeutrAvidin interaction with nearby biotinylated antibody-bound CD271 proteins on adjacent cells.

Cellular aggregation effectively spreads the mass change as a result of bead binding over a much larger volume (i.e. the collective volume of all the cells and beads in the aggregate), reducing the effective density change. According to our cell/particle density simulation, a single fully labeled MeWo cell (i.e. with 1,600 Sera-Mag™ beads bound, predicted density ~ 1.20 g/mL) need only aggregate with three additional unlabeled MeWo cells before the collective aggregate density is ~ 1.043 g/mL. This aggregate density value continues to decrease as additional cells are added, approaching the initial density of a single cell (~ 1.04 g/mL). In fact, it is possible that cellular aggregation was present in both the InnovaCoat®- and Sera-Mag™- MADC separations using continuous gradients and contributed to the less-than-anticipated physical separation between bands and failure to separate, respectively. However, due to the smaller physical dimensions of the centrifuge tubes used in the continuous gradient experiments coupled with the smaller physical separations between narrow density ranges, it is likely cellular aggregation escaped detection in these trials.

Future work will focus on refining treatment protocols and reagent choices to minimize cellular aggregation and non-specific nano/microparticle binding, and to enable post-separation particle removal. While sufficient to illustrate binary separation in the InnovaCoat® trials, our fractionation methodology was rudimentary and may have resulted in slight mixing of adjacent gradient layers.[13] In future work, more controlled gradient fractionators will be implemented. Per the success of the smaller, denser InnovaCoat® gold beads in the current study, smaller nanoparticles (~ 80 - 100 nm) made of more affordable metals like iron oxide, iron, or silver (5.24 g/mL, 7.87 g/mL, an 10.50 g/mL, respectively) will be considered. Additionally, these smaller nanoparticles may reduce the possibility of nanoparticle-mediated cell-to-cell crosslinks. Similarly, alternative nanoparticle avidin coating densities will be investigated in an effort to minimize cell crosslinking potential. Various nanoparticle modifications (i.e. PEGylation) will be also be investigated in an effort to diminish the potential for non-specific binding. Finally, desthiobiotinylated antibodies, which enable dissociation from avidin without harsh chemical treatments, will be investigated so that particle labeling can be removed post-separation.[37]

In summary, the study presented herein illustrates the feasibility of MADC for performing binary separations of A375 treated and untreated cell mixtures using anti-CD51/61-functionalized 80 nm InnovaCoat® gold beads and continuous 1.064 g/mL Percoll density gradients. However, widespread cellular aggregation likely hampered the predicted physical separation of treated and untreated A375 bands in these trials. Likewise, cellular aggregation prevented successful separation of anti-CD271-biotin/Sera-Mag-treated $MeWo_{30}$ cells using both continuous and discontinuous

gradients. Future work will focus on protocol and particle modifications in order to prevent non-specific particle binding and nanoparticle-mediated cell aggregation, and to enable post-separation nanoparticle removal. These refinements will facilitate bulk, non-binary separation of billions of cells without expensive equipment, and expand the usefulness of our already powerful, novel separation technique.

3.5 Acknowledgements

The author would like to thank Vera Fonseca, M.S. for performing the Western blots in this study. This work was funded by National Institutes of Health (R01 AR063642) and National Science Foundation (EAGER CBET 1547819 and CAREER CBET 1253189).

3.6 References

1 Herzenberg, L. A. *et al.* The history and future of the fluorescence activated cell sorter and flow cytometry: a view from Stanford. *Clin Chem* **48**, 1819-1827 (2002).

2 Shields, C. W. t., Reyes, C. D. & Lopez, G. P. Microfluidic cell sorting: a review of the advances in the separation of cells from debulking to rare cell isolation. *Lab Chip* **15**, 1230-1249, doi:10.1039/c4lc01246a (2015).

3 Plouffe, B. D., Murthy, S. K. & Lewis, L. H. Fundamentals and application of magnetic particles in cell isolation and enrichment: a review. *Rep Prog Phys* **78**, 016601, doi:10.1088/0034-4885/78/1/016601 (2015).

4 Bonner, W. A., Hulett, H. R., Sweet, R. G. & Herzenberg, L. A. Fluorescence activated cell sorting. *Rev Sci Instrum* **43**, 404-409 (1972).

5 Miltenyi, S., Muller, W., Weichel, W. & Radbruch, A. High gradient magnetic cell separation with MACS. *Cytometry* **11**, 231-238, doi:10.1002/cyto.990110203 (1990).

6 Hulett, H. R., Bonner, W. A., Barrett, J. & Herzenbe.La. Cell Sorting - Automated Separation of Mammalian Cells as a Function of Intracellular Fluorescence. *Science* **166**, 747-&, doi:DOI 10.1126/science.166.3906.747 (1969).

7 Durack, G. & Robinson, J. P. *Emerging tools for single-cell analysis : advances in optical measurement technologies*. (Wiley-Liss, 2000).

8 Li, Q. *et al.* Comparison of the sorting efficiency and influence on cell function between the sterile flow cytometry and immunomagnetic bead purification

methods. *Prep Biochem Biotechnol* **43**, 197-206, doi:10.1080/10826068.2012.719846 (2013).

9 Brakke, M. K. Density Gradient Centrifugation - a New Separation Technique. *J Am Chem Soc* **73**, 1847-1848, doi:DOI 10.1021/ja01148a508 (1951).

10 Brakke, M. K. Zonal separations by density-gradient centrifugation. *Arch Biochem Biophys* **45**, 275-290 (1953).

11 Gartner, I. Separation of human eosinophils in density gradients of polyvinylpyrrolidone-coated silica gel (Percoll). *Immunology* **40**, 133-136 (1980).

12 Meselson, M., Stahl, F. W. & Vinograd, J. Equilibrium Sedimentation of Macromolecules in Density Gradients. *Proceedings of the National Academy of Sciences of the United States of America* **43**, 581-588 (1957).

13 Pertoft, H. Fractionation of cells and subcellular particles with Percoll. *J Biochem Biophys Methods* **44**, 1-30 (2000).

14 Pertoft, H., Laurent, T. C., Laas, T. & Kagedal, L. Density gradients prepared from colloidal silica particles coated by polyvinylpyrrolidone (Percoll). *Anal Biochem* **88**, 271-282 (1978).

15 Pertoft, H., Rubin, K., Kjellen, L., Laurent, T. C. & Klingeborn, B. The viability of cells grown or centrifuged in a new density gradient medium, Percoll(TM). *Exp Cell Res* **110**, 449-457 (1977).

16 Van Vlasselaer, P., Palathumpat, V., Strang, G. & Shapero, M. in *Cell Separation Methods and Applications* (ed D Recktenwald) Ch. 2: New Approaches in Density Gradient Separation Using Colloidal Silica Gradients in the Processing of Human Hematopoietic Progenitor Cells, (Taylor and Francis, 1997).

17 Van Vlasselaer, P. Methods for enriching specific cell-types by density gradient centrifugation. USA patent (1998).

18 Wei, X. *et al.* Highly sensitive and rapid isolation of fetal nucleated red blood cells with microbead-based selective sedimentation for non-invasive prenatal diagnostics. *Nanotechnology* **29**, 434001, doi:10.1088/1361-6528/aad8c4 (2018).

19 Marshall, J. F. *et al.* Integrin expression in human melanoma cell lines: heterogeneity of vitronectin receptor composition and function. *Int J Cancer* **49**, 924-931 (1991).

20 Albelda, S. M. *et al.* Integrin distribution in malignant melanoma: association of the beta 3 subunit with tumor progression. *Cancer research* **50**, 6757-6764 (1990).

21 Felding-Habermann, B., Mueller, B. M., Romerdahl, C. A. & Cheresh, D. A. Involvement of integrin alpha V gene expression in human melanoma tumorigenicity. *J Clin Invest* **89**, 2018-2022, doi:10.1172/JCI115811 (1992).

22 Cheresh, D. A. & Spiro, R. C. Biosynthetic and functional properties of an Arg-Gly-Asp-directed receptor involved in human melanoma cell attachment to vitronectin, fibrinogen, and von Willebrand factor. *J Biol Chem* **262**, 17703-17711 (1987).

23 Petitclerc, E. *et al.* Integrin alpha(v)beta3 promotes M21 melanoma growth in human skin by regulating tumor cell survival. *Cancer research* **59**, 2724-2730 (1999).

24 Redmer, T. *et al.* The role of the cancer stem cell marker CD271 in DNA damage response and drug resistance of melanoma cells. *Oncogenesis* **6**, e291, doi:10.1038/oncsis.2016.88 (2017).

25 Guo, R. *et al.* Increased expression of melanoma stem cell marker CD271 in metastatic melanoma to the brain. *Int J Clin Exp Pathol* **7**, 8947-8951 (2014).

26 Lehraiki, A. *et al.* Increased CD271 expression by the NF-kB pathway promotes melanoma cell survival and drives acquired resistance to BRAF inhibitor vemurafenib. *Cell Discov* **1**, 15030, doi:10.1038/celldisc.2015.30 (2015).

27 Valyi-Nagy, K., Kormos, B., Ali, M., Shukla, D. & Valyi-Nagy, T. Stem cell marker CD271 is expressed by vasculogenic mimicry-forming uveal melanoma cells in three-dimensional cultures. *Mol Vis* **18**, 588-592 (2012).

28 Boiko, A. D. *et al.* Human melanoma-initiating cells express neural crest nerve growth factor receptor CD271. *Nature* **466**, 133-U155, doi:10.1038/nature09161 (2010).

29 Civenni, G. *et al.* Human CD271-Positive Melanoma Stem Cells Associated with Metastasis Establish Tumor Heterogeneity and Long-term Growth. *Cancer research* **71**, 3098-3109, doi:10.1158/0008-5472.Can-10-3997 (2011).

30 Redmer, T. *et al.* The Nerve Growth Factor Receptor CD271 Is Crucial to Maintain Tumorigenicity and Stem-Like Properties of Melanoma Cells. *Plos One* **9**, doi:ARTN e9259610.1371/journal.pone.0092596 (2014).

31 Furuta, J., Inozume, T., Harada, K. & Shimada, S. CD271 on Melanoma Cell Is an IFN-gamma-Inducible Immunosuppressive Factor that Mediates

Downregulation of Melanoma Antigens. *Journal of Investigative Dermatology* **134**, 1369-1377, doi:10.1038/jid.2013.490 (2014).

32 in *Cell Separation Media: Methodology and Applications* (GE Healthcare Bio-Sciences AB, Uppsala, Sweden, 1985).

33 Sadick, J. S., Boutin, M. E., Hoffman-Kim, D. & Darling, E. M. Protein characterization of intracellular target-sorted, formalin-fixed cell subpopulations. *Sci Rep* **6**, 33999, doi:10.1038/srep33999 (2016).

34 Sadick, J. S. & Darling, E. M. Processing fixed and stored adipose-derived stem cells for quantitative protein array assays. *Biotechniques* **63**, 275-280, doi:10.2144/000114620 (2017).

35 Kito, K. & Ito, T. Mass spectrometry-based approaches toward absolute quantitative proteomics. *Curr Genomics* **9**, 263-274, doi:10.2174/138920208784533647 (2008).

36 Shuford, C. M. *et al.* Absolute Protein Quantification by Mass Spectrometry: Not as Simple as Advertised. *Analytical chemistry* **89**, 7406-7415, doi:10.1021/acs.analchem.7b00858 (2017).

37 Hirsch, J. D. *et al.* Easily reversible desthiobiotin binding to streptavidin, avidin, and other biotin-binding proteins: uses for protein labeling, detection, and isolation. *Analytical Biochemistry* **308**, 343-357, doi:Pii S0003-2697(02)00201-4 Doi 10.1016/S0003-2697(02)00201-4 (2002).

3.7 Supplemental Information

3.7.1 Determination of Percoll Gradient Parameters

Percoll gradients of varied starting density (1.016 g/mL, 1.028 g/mL, 1.040 g/mL, 1.052 g/mL, 1.064 g/mL, 1.076 g/mL, and 1.087 g/mL) were mixed with density marker beads and centrifuged for 15 min at 4°C at various centrifugation rates (15,000 g, 30,000 g, 45,000 g, 60,000 g, 75,000 g, and 90,000 g). After centrifugation, the distances of the marker bead bands to the meniscus were measured and plotted (**Figure S 3-1**). 1.064 g/mL gradients centrifuged at 45,000 g offered large, linear physical separation in the predicted cell density range (1.04 g/mL – 1.06 g/mL). All subsequent continuous density gradient centrifugations were performed with gradients formed as such.

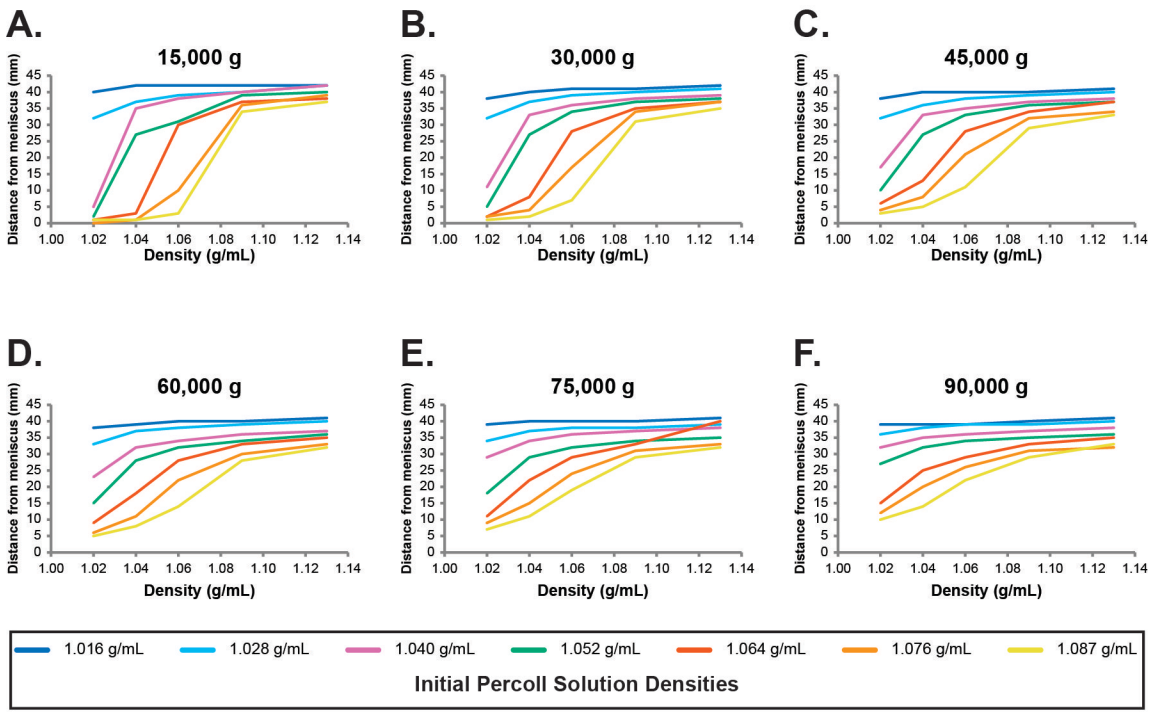

Figure S 3-1. Preliminary experiments to determine candidate Percoll gradient parameters. Percoll solutions of 1.016 g/mL, 1.028 g/mL, 1.040 g/mL, 1.052 g/mL, 1.064 g/mL, 1.076 g/mL, and 1.087 g/mL starting density containing calibration beads were centrifuged at A.) 15,000 g, B.) 30,000 g, C.) 45,000 g, D.) 60,000 g, E.) 75,000 g, and F.) 90,000 g for 15 min at 4°C. After centrifugation, distances from the meniscus to the bead bands of known density were measured and plotted. Calibration bead densities: 1.02 g/mL, 1.04 g/mL, 1.06 g/mL, 1.08 g/mL, and 1.13 g/mL.

Chapter 4

Conclusions and Future Work

Sorting technologies are critical tools enabling investigations into the functional implications of cellular heterogeneity. While purity is a particularly important and often discussed sorting parameter, yield and throughput are rarely considered thoroughly. Furthermore, it is imperative to have a holistic understanding of the strengths and weaknesses of each sorting method in order to make appropriate sorting decisions. As such, the first goal of this thesis was to provide researchers with a thorough, quantitative characterization of the two most common sorting methods, FACS and MACS. Next, having witnessed the weaknesses of FACS and MACS firsthand, we set out to design a novel sorting technique aimed at addressing the shortcomings of the two popular sorting methods. This thesis will serve as a resource for researchers currently utilizing conventional cell sorting methods, and provides a detailed description of the fundamentals of MADC, our new and exciting, alternative sorting method. In the future, we will continue to work on thorough characterization of existing, conventional sorting technologies as improvements are made, as well as further MADC refinements.

4.1 Chapter 2

In Chapter 2, we thoroughly characterized the ability of FACS and MACS to separate known mixtures of osteogenically primed SVF cells and A375 human melanoma cells.

We found our preconceptions of FACS sorting to be mostly accurate: FACS produced accurate separations of our ALPL+ and ALPL- cells, but with considerable cell loss. In comparison, MACS performed using the manufacturer's protocol antibody and microbead concentrations resulted in high cell yields, but produced divergent ALPL+:ALPL- splits. Flow cytometry analysis of the retained and flow-through fractions confirmed an inefficient separation, and a high false-negative rate. Reports from studies evaluating both FACS and MACS in the course of their separations indicated similarly high false-negative rates of 40-60%.[1,2] In contrast to previous studies, we rigorously optimized antibody and microbead concentrations and found MACS was capable of recapitulating the accurate separations of FACS, while maintaining high yield.

While our study examined established FACS sorting methods and machinery, future evaluations should include new, commercially available FACS technologies. The Influx™ cell sorter (Becton Dickinson, Franklin Lakes, NJ) used in the study presented in Chapter 2 belongs to the "jacket-in-air" type of FACS machines. These devices require a careful calibration and expert operation to maximize yields and ensure accurate sorting. To ensure maximum accuracy, a single operator with 20+ years of experience was employed to calibrate and perform the sorts in our study, however new technologies exist to automate the calibration process. Specifically, the S3e™, a new desktop cell sorter manufactured by Bio-Rad (Hercules, CA), is marketed as capable of performing "lossless sorting."[3,4] It is equipped with ProDrop™ technology, that functions to automatically calculate the optimal droplet delay time, a parameter critical to sorting yield.[5] However, we recently conducted demo experiments analogous to those presented in Chapter 2 using the S3e™ and observed no benefit to cell yields, and considerable decreases in

throughput. In reality, the innovation provided by the S3e™ may be its lowering the barrier-of-entry to cell sorting compared to more manual sorters like the Influx™. Additionally, two new sorting products based on microfluidic technologies, the WOLF® (NanoCellect Biomedical, Inc., San Diego, CA) and the MA900 (Sony Biotechnology, San Jose, CA) cell sorters, would be interesting systems to evaluate. The low flow/event rates of these sorters likely reduce potential throughput, but may result in increased viability and yield.[6,7] As such, these sorters may be most appropriate for low cell-number applications that require high cell recovery. Finally, like the S3e™, the accessibility of these machines may ultimately be their most attractive features.

Though increased antibody and microbead concentrations enabled our MACS optimized protocol sorts to accurately sort highly viable subpopulations, their long-term effects on the cells were not thoroughly investigated. To establish the effects of high antibody and microbead concentrations on growth rate and long-term viability, cells sorted using the optimized MACS protocol will have to be subjected to proliferation assays, like MTT, and prolonged viability assessment. Though the low concentrations of antibodies and beads suggested by the manufacturer's protocols have been reported to not affect cell function, additional functional assays (differentiation, motility, etc…) should be performed, as well. If increased magnetic bead concentration is found to adversely influence separated cells, it may be beneficial to develop novel magnetic beads capable of being removed post-sort. A desthiobiotinylated primary antibody coupled with an avidin-coated magnetic particle may provide a method for achieving this goal.[8]

4.2 Chapter 3

Chapter 3 detailed our development of a novel, particle-based sorting method, MADC. We found that by treating A375 cells with anti-CD51/61-functionalized, InnovaCoat® beads and subsequently subjecting them to continuous density gradient centrifugation, we could separate the cells in a binary manner. However, attempts to separate $MeWo_{30}$ cells with a combination of anti-CD271-biotin antibodies, Sera-Mag™ NeutrAvidin beads, and either continuous or discontinuous density gradient centrifugation were unsuccessful. Close post-centrifugation inspection of discontinuous SeraMag™-treated $MeWo_{30}$ gradients revealed significant cellular aggregation. Composite cell/bead density estimates given by our simulations indicated that a fully labeled $MeWo_{30}$ cell need only aggregate to three other unlabeled cells to effectively negate density changes. In hindsight, it is likely that cellular aggregation played a role in limiting the physical separation between InnovaCoat®-labeled and unlabeled A375s, and is the most likely culprit for failed continuous and discontinuous gradient Sera-Mag™ separations of $MeWo_{30}$ cells.

The first issue to address in MADC development is to reduce cellular aggregation. Initial tests of MADC utilized commercially available resources in an effort to maximize the accessibility of the technology. However, going forward, it may be necessary to synthesize our own particles, or modify existing ones, to enable more control over multiple variables. If the technique is to proceed using the primary biotinylated antibody/secondary avidin-coated bead strategy, we will likely have to experiment with the density of avidin surface coating in an order to minimize crosslinking potential.

Similarly, the size of the beads will likely have to be optimized to minimize the exposed, avidin-coated surfaces of bound beads available for crosslinking to nearby cells.

Various surface modifications and functionalizations of mass-adding particles may be helpful in combatting cellular aggregation, as well. Mass-adding particles with two distinctly functionalized hemispheres, or "Janus" particles, could potentially be synthesized as described by Sulchek and colleagues in 2012.[9] In their study, the researchers sputter-coated gold onto a single side of either polystyrene or silica microparticles, resulting in two unique hemispheres with different reaction chemistries. Though we would likely use a more massive, iron/iron oxide/silver starting particle, we could conceivably functionalize the sputter-coated gold hemisphere with avidin molecules, as described in the aforementioned study, and the other hemisphere with a simple polyethylene glycol (PEG). By confining avidin functionalization to a single side of the particle, we could minimize the effective surface area available for particle-mediated crosslinking to nearby cells. Furthermore, the opposing, PEGylated face can act as an anti-fouling agent, preventing non-specific binding.

Future work may include investigating alternatives to Percoll for density-mediated separation. Accurate fractionation of density gradients can be difficult without specialized, and potentially expensive, equipment. However, microfluidic acoustophoresis devices that enable separations based on a combination of cell size and density may enable an alternative method for mass-added sorting.[10,11]

Finally, further refinement of MADC may expand its usefulness beyond cell separations. Operating ideally, the single-cell density modulation of MADC directly correlates to expression of a protein target. As such, the gradient position of the cell/bead

composite can be translated into the approximate protein level on the surface. In this way MADC could potentially serve as a proteomic quantification method.

4.3 Closing Remarks

The importance of cellular heterogeneity is becoming more and more apparent. Performing a simple *Web of Science* search for publications in which "cell heterogeneity" appears in the title returns 117 manuscripts in 2012 (my first year at Brown) and 362 in 2017 (the last *full* year for which data is available); a staggering 209% increase. Sorting technologies are a necessary tool for isolating cells based on their individual characteristics so that we may gain understanding of the ramifications of heterogeneity. It is therefore imperative that we both characterize existing sorting technologies, and develop new ones, so that we may most effectively study single-cell differences. In conclusion, this thesis contributes to the advancement of single-cell isolations by calling attention to two oft-forgotten sorting parameters, yield and throughput, which will become increasingly important as basic science and clinical applications require larger cell numbers. Additionally, we have developed a new and exciting sorting method that will prove useful as a high-throughput, high-yield alternative to current technologies.

4.4 References

1 Fong, C. Y., Peh, G. S., Gauthaman, K. & Bongso, A. Separation of SSEA-4 and TRA-1-60 labelled undifferentiated human embryonic stem cells from a heterogeneous cell population using magnetic-activated cell sorting (MACS) and fluorescence-activated cell sorting (FACS). *Stem Cell Rev* **5**, 72-80, doi:10.1007/s12015-009-9054-4 (2009).

2 Li, Q. *et al.* Comparison of the sorting efficiency and influence on cell function between the sterile flow cytometry and immunomagnetic bead purification methods. *Prep Biochem Biotechnol* **43**, 197-206, doi:10.1080/10826068.2012.719846 (2013).

3 Laboratories, B.-R. *Lossless Cell Sorting on the S3e™ Cell Sorter*, <https://www.youtube.com/watch?v=S4yED3FyejA> (2017).

4 Laboratories, B. R. *S3e™ Cell sorter*, <http://www.bio-rad.com/en-us/product/s3e-cell-sorter?ID=OK1GROIVK> (2018).

5 Oxford, C. *et al. ProDrop™ Technology — A Novel Approach to Automated Drop Delay Measurement and Monitoring*, <http://www.bio-rad.com/webroot/web/pdf/lsr/literature/Bulletin_6397.pdf> (

6 NanoCellect Biomedical, I. *WOLF Cell Sorter*, <http://www.nanocellect.com/wolf-cell-sorter> (

7 Biotechnology, S. *Sony MA900 Multi Application Cell Sorter*, <https://www.sonybiotechnology.com/us/instruments/ma900-multi-application-cell-sorter/sorting/> (

8 Hirsch, J. D. *et al.* Easily reversible desthiobiotin binding to streptavidin, avidin, and other biotin-binding proteins: uses for protein labeling, detection, and isolation. *Analytical Biochemistry* **308**, 343-357, doi:Pii S0003-2697(02)00201-4 Doi 10.1016/S0003-2697(02)00201-4 (2002).

9 Tang, J. L., Schoenwald, K., Potter, D., White, D. & Sulchek, T. Bifunctional Janus microparticles with spatially segregated proteins. *Langmuir* **28**, 10033-10039, doi:10.1021/la3010079 (2012).

10 Petersson, F., Aberg, L., Sward-Nilsson, A. M. & Laurell, T. Free flow acoustophoresis: microfluidic-based mode of particle and cell separation. *Analytical chemistry* **79**, 5117-5123, doi:10.1021/ac070444e (2007).

11 Shi, J., Huang, H., Stratton, Z., Huang, Y. & Huang, T. J. Continuous particle separation in a microfluidic channel via standing surface acoustic waves (SSAW). *Lab Chip* **9**, 3354-3359, doi:10.1039/b915113c (2009).